IN VITRO DETECTION OF DISEASE BIOMARKERS AND DRUG CONTAMINANTS

A Dissertation
Submitted to the Graduate Faculty
of the
North Dakota State University
of Agriculture and Applied Sciences

By

Erin Kathryn Nyren-Erickson

In Partial Fulfillment
For the Degree of
DOCTOR OF PHILOSOPHY

Major Department:
Pharmaceutical Sciences

August 2013

Fargo, North Dakota

North Dakota State University
Graduate School

Title

IN VITRO DETECTION OF DISEASE BIOMARKERS AND DRUG CONTAMINANTS

By

Erin Kathryn Nyren-Erickson

The Supervisory Committee certifies that this ***disquisition*** complies with North Dakota State University's regulations and meets the accepted standards for the degree of

DOCTOR OF PHILOSOPHY

SUPERVISORY COMMITTEE:

Dr. Sanku Mallik
Chair

Dr. Estelle Leclerc

Dr. Benedict Law

Dr. D. K. Srivastava

Approved:

8/14/13
Date

Jagdish Singh
Department Chair

ABSTRACT

In recent years the rising cost and increased regulation within the U.S. healthcare system have caused medical laboratory tests to become more costly and more frequently required. As a result, insurance premiums are rising, and small independent laboratories are threatened with closure as their already narrow margins dwindle. Concurrently, there have been several incidents of contaminants and impurities in pharmaceutical drugs causing hundreds of deaths and thousands of illnesses. These challenges substantiate the need for simple and cost-effective screening tests for the presence of disease biomarkers, as well as for contaminants and impurities present in pharmaceutical drugs.

The following disquisition reports three independent studies, each with the development of simple screening tools as its objective. Paper 1 reports the use of fluorescent lipid nanoparticles (liposomes) to detect changes in the species and concentrations of glycosaminoglycans (GAGs) in solution. We conclude that the emission intensity from the present fluorophores changes in response to increasing concentrations of GAGs, and can distinguish between serum from a healthy patient and serum having the same GAG concentrations as an Alzheimer's disease patient (simulated).

Paper 2 reports the use of lipid nanoparticles to detect dangerous over-sulfated contaminants in pharmaceutical heparin. We report that liposomes in the presence of heparin or over-sulfated contaminants and Mg^{2+} ions form aggregates, and the size and zeta potential of these aggregates is dependent on the heparin/contaminant present. Further, the variation in aggregate zeta potential varies significantly upon heparin contamination, and may be used to detect 0.5% contaminant by weight.

Paper 3 reports a clinical study to validate the presence of ADAM 12 (a disintegrin and metalloproteinase) enzyme in urine as a biomarker for breast cancer detection and diagnosis, as well as to monitor the effects of tumor removal on the urinary levels of this enzyme. We find no significant differences between recently diagnosed cancer patients (having undergone no treatment for cancer) and age-matched controls having no cancer present. Significant increases in urinary ADAM 12 only occur following surgery. Overall, we conclude that it is unlikely that a screen for urinary ADAM 12 will be useful for the diagnosis of breast cancer.

ACKNOWLEDGEMENTS

I would like to convey my sincere thanks to the Department of Pharmaceutical Sciences, the College of Pharmacy, Nursing, and Allied Sciences, the Graduate School, and North Dakota State University for providing the support and infrastructure to make my studies possible.

Thanks to my advisor, Dr. Sanku Mallik, and my committee members Dr. Ben Law, Dr. Estelle Leclerc, and Dr. D. K. Srivastava for their guidance and support; the department chair, Dr. Jagdish Singh, and the dean of the college, Dr. Charles Peterson, for their brilliant leadership; my labmates past and present, Dr. Jayati Banerjee, Dr. Rajesh Subramaniam, Dr. Rinku Dutta, Dr. Michael D. Scott, Dr. Manas K. Haldar, Rahul Nahire, Prajakta Kulkarni, Tapas Nandy, and Ryne Hendrickson for their support, ideas, and enthusiasm.

Thanks to the faculty, staff, and students of the department and the college for their friendship and generous encouragement.

Thanks to my former students, Brendan O'Gorman, Delveen Amedi, Siar Khaleel, Brett Johnson, Dilip Patel, Riley Ceglowski, Justin Jones, and Jessica Totzauer for making me a better teacher and mentor.

Thanks to the NDSU Research and Technology Park, the NDSU Office of Technology Transfer, and the NDSU Research Foundation for their support of my ideas and future plans.

Thanks to Dr. Neville Alberto for making our collaboration with Sanford Health possible, and to Dr. Mihir Raval, Dr. Michael Bouton, Kim Wold, and Abby Zimmerman for supporting this collaboration.

Thanks to the National Institutes of Health, the Department of Pharmaceutical Sciences at NDSU, Sanford Health, and the American Foundation for Pharmaceutical Education for providing funding for these projects.

Thanks to Dr. Edward Deckard, Dr. Robert Stack, Dr. Steven Meinhardt, Dr. Robert Sparks, Mr. Leonard Cook, and Mr. Peter Gregoire for supporting my research from the beginning, and helping me get an early start to my academic career.

Finally, thanks to my mother and father, Anne and Paul Nyren, my husband, Mark Erickson, and my friends and family for their encouragement and faith in me.

DEDICATION

To my mother and father, Anne and Paul, for supporting, encouraging, and believing in me from the very beginning.

And to my husband Mark, for filling my hours outside the lab with happiness.

TABLE OF CONTENTS

LIST OF TABLES

Table Page

LIST OF FIGURES

LIST OF ABBREVIATIONS

ADAM.....a disintegrin and metalloproteinase

aPTT……..activated partial thromboplastin time

CA15-3…….cancer antigen 15-3 and

CA27.29……...cancer antigen 27.29

CEA…..…….carcinoembryonic antigen

DCIS.....ductal carcinoma *in situ*

DLS…….…dynamic light scattering

DSPC……..……...……..1,2-distearoyl-*sn*-glycero-3-phosphocholine

ELISA…….…….enzyme-linked immunosorbent assay

GAG…….……glycosaminoglycan

HEPES.....2-[4-(2-hydroxyethyl)piperazin-1-yl]ethanesulfonic acid

HER2/neu.....human epidermal growth factor receptor 2

HIPAA.....health insurance portability and accountability act

HPLC……...…….high performance liquid chromatography

IBC……...…invasive breast cancer

ICF……..…..informed consent form

kDa……...….kilodaltons

LDA……..……linear discriminant analysis

MS……....…….....…..mass spectrophotometry

MMP…….……matrix metalloproteinase

NCCN……..…….national cancer cooperative network

NMR…….nuclear magnetic resonance

OSCS…….……over-sulfated chondroitin sulfate

OSD……..…….over-sulfated dermatan sulfate

OSH……...over-sulfated heparin

POPC……1-palmitoyl-2-oleoyl-*sn*-glycero-3-phosphocholine

PT……..prothrombin time

TEM……..transmission electron microscopy

LIST OF APPENDIX TABLES

LIST OF APPENDIX FIGURES

INTRODUCTION

Rising cost of medical care and the need for simple tests

Recent and ongoing changes to the laws and policies governing health care have produced numerous concerns and queries, particularly concerning how much medical care will cost. While it is not the goal of this disquisition to make political or macro-economic statements or predictions on this subject, the general consensus is that costs are increasing! A recent article in Forbes magazine predicts that individual health care insurance policy premiums will increase 64%-146% in California (a market that traditionally has very competitive rates for individuals)[1]. Concurrent to these purported increases in insurance premiums is an increased need for laboratory tests, as reported in Dark Daily, a web-based periodical providing alerts on laboratory and pathology news and trends. They point out that 27+ preventative medical services listed that must be covered under the new law all require laboratory tests as part of the protocol[2]. However, Dark Daily also reported on May 22, 2013, that many independent medical laboratory testing facilities may be forced into bankruptcy by recent cuts to the Medicare Part B Clinical Laboratory Price Schedule and Federal funding sequester[3]. Many of these laboratories—often the only clinical laboratory serving their area—must operate on a profit margin of only 3-6% per annum; add the 2% fee reduction specified in the sequester, and these companies can no longer make a profit[3].

To complicate matters further, a recent Laboratory National Status report sponsored by the Center for Disease Control and Prevention indicates high rates of laboratory error. The report cites a number of quality challenges, such as lack of standardization of test values, poor quality control, and poor test reproducibility as some of the challenges to be addressed[4]. The

development of simple, inexpensive, and easily interpreted clinical laboratory tests would go a long way toward providing a solution for many of these issues.

Increasing concerns about drug quality

The last decade has seen a significant number of pharmaceutical drugs contaminated before reaching the patient, and has witnessed considerable resulting illness. In 2007-08, lots of heparin were contaminated with over-sulfated chondroitin sulfate, leading to illness and death in 10 countries globally[5] (this contamination will be discussed further in the section entitled "PAPER 2: An inexpensive, rapid, accurate screen for the presence of dangerous over-sulfated heparin contaminants"). In 2012, steroidal injections contaminated with fungal meningitis caused a total of 745 reported meningitis cases, and 58 deaths[*], according to the Center for Disease Control and Prevention[6]. Also in 2012, cardiac drugs administered to patients in Lahore, Pakistan, were contaminated with pyrimethamine, an antimalarial drug. This contamination resulted in 107 confirmed deaths, with over 450 others becoming ill[7]. Whether such contaminations occur by accident or deliberately, there is clearly a need for simple, accurate tests to confirm drug quality at all stages of the pharmaceutical supply chain.

Research significance

The chapters presented in this disquisition represent three independent studies with three corresponding papers either published previously, or currently submitted for publication. Throughout the studies presented, the common thread is that of simple and clinically relevant detection methods for significant biological compounds; we explore various biochemical methods for detection of disease biomarkers, as well as over-sulfated contaminants in heparin.

[*] These numbers reflect death from all causes. All were confirmed cases of meningitis caused by contaminated drug.

The compounds or proteins we wish to detect during the presented studies are either potentially indicative of a patient's disease state (i.e. a disease biomarker, as in the chapters entitled PAPER 1 and PAPER 3), or potentially dangerous over-sulfated heparin contaminants (as in the chapter entitled PAPER 2). For each of these target compounds, a simple detection method could prove both medically and economically beneficial. In order to best consider the potential benefits of the presented studies, we will now discuss the goals of these as individual chapters.

Paper 1: A new method for detection and diagnosis of Alzheimer's disease

In this chapter, we develop a method to discriminate between different glycosaminoglycans in solution using lipid nanoparticles (liposomes) labeled with a fluorescent reporter molecule. Glycosaminoglycans (GAGs) are carbohydrate polymers composed of repeating uronic acid-amino sugar disaccharides[8] and have numerous physiological functions in their various forms, which include chondroitin sulfate[9], heparin sulfate[10,11], heparan sulfate[10,12], and hyaluronic acid[13]. There are a number of disease conditions in which the patient's serum or urine GAG concentrations begin to change, such as Schizophrenia[14], some metastatic cancers[15,16], and Alzheimer's disease[17]. Of particular interest is the potential to monitor these changes in patients' to detect and accurately diagnose Alzheimer's disease.

Currently Alzheimer's disease affects 5.3 million people in the United States alone, making it the most common neurodegenerative disease associated with advanced age[18]. Current methods for diagnosis of Alzheimer's include cognitive and behavioral evaluations, as well as brain scans[19], but the predictive factors for individuals' risk of developing the disease remain largely unknown[20]. We show in our study presented in PAPER 1 that changes in emission intensity from fluorescently labeled liposomes in the presence of different GAGs can discriminate between these GAGs in a concentration dependent fashion. As such, the presence

of elevated GAGs in the serum of Alzheimer's patients could also be detected by these liposomes. We demonstrate that liposomes labeled with pyranine fluorophore show marked differences in their fluorescence emission intensities in the presence of dilute serum from a healthy individual as compared with dilute simulated serum from an individual with Alzheimer's disease[21]. As such, we believe that with further development this method may be able to aid in the accurate diagnosis of Alzheimer's disease, as well as monitoring patient risk and prognosis.

Paper 2: A simple screen for the presence of heparin contaminants

In this chapter we develop a new screening tool for the presence of dangerous heparin contaminants, particularly over-sulfated chondroitin sulfate, using liposomes composed of 99 mol% 1-palmitoyl-2-oleoyl-*sn*-glycero-3-phosphocholine (POPC) and 1 mol% of a lissamine-rhodamine labeled lipid. In 2007-08, lots of heparin exported from China were contaminated with over-sulfated chondroitin sulfate (OSCS)[22,23]. Use of this heparin was associated with numerous illnesses and deaths in the United States alone[5], with a total of ten countries worldwide affected by the contamination. The United States Food and Drug Administration now mandates that heparin be screened for the presence of this compound.

Current screening methods for OSCS—such as ^{1}H NMR and strong anion exchange HPLC—are effective, but not without drawbacks: they are expensive, time consuming, and require considerable training for their proper interpretation. A rapid, easily interpreted method of screening heparin would thus have considerable economic advantages.

The method we have developed uses the particular tendency of phosphocholine liposomes to aggregate in the presence of sulfated glycosaminoglycans (such as heparin) and divalent cations such as Mg^{2+}.[24,25] The aggregates formed by these liposomes in the presence of heparin only have a consistent average aggregate diameter and zeta potential, as measured by

dynamic light scattering. As the heparin becomes contaminated with small quantities of OSCS, the size and zeta potential of these aggregates begin to change, reflecting the greater degree of sulfation and thus the greater negative charge of this contaminant[26]. These changes may be detected by statistical analysis. This method presents considerable potential as a screening method for pharmaceutical heparin, and with minimal further optimization could be produced as a mass-produced product for this purpose.

Paper 3: ADAM 12 as a potential urinary biomarker for breast cancer

In this chapter we examine the efficacy of urinary ADAM 12 (A Disintegrin and Metalloproteinase enzyme-12) as a viable biomarker for the diagnosis of breast cancer. As the leading cause of cancer deaths in the United States in women from the ages of 40 to 59.5 years, breast cancer kills one woman every 13 minutes in the US alone[27]. However, if breast cancer is detected and treated before it becomes metastatic (spreads beyond the breast), the 5-year survival rate may be as high as 93%[†], and as such early detection of breast cancer is critical to patient prognosis. Currently, breast cancer is detected primarily through mammograms and self-exams, as well as blood-based biomarkers (e.g. cancer antigen 15-3 and 27.29, carcinoembryonic antigen, and HER2/neu)[28,29]. Unfortunately these biomarkers show little promise regarding early detection[30], and the rising costs of healthcare are making mammograms less available[31]. The use of a urinary biomarker for breast cancer diagnosis could therefore provide a significant advantage, both for reduction of medical costs and patient convenience.

A disintegrin and metalloproteinase (ADAMs) enzymes are a family of 35 multi-domain, zinc-dependent metalloproteinase enzymes. These enzymes have a variety of physiological roles

[†] This number reflects death from all causes.

in healthy tissues[32]; however dysregulation of their transcription or translation has been associated with a number of disease conditions, including breast cancer[32].

A study published in 2004 by Roopali Roy, *et al*., concludes that there is a strong correlation between the amount of urinary ADAM 12 in a patient's urine and their breast cancer status and stage[33]. The authors claim that the elevation in urinary ADAM 12 was significant for patients with ductal carcinoma *in situ* (DCIS), invasive breast cancer (IBC), and metastatic cancer. They further state that all patients diagnosed with cancer tested positive for the presence of urinary ADAM 12 at a significantly greater rate compared with controls—15% positive for controls, 78% positive for atypical ductal hyperplasia/lobular carcinoma *in situ*, 82% for ductal carcinoma *in situ*, 86% for invasive breast cancer, and 85% for metastatic breast cancer. These results strongly suggest that a screen for the presence of urinary ADAM 12 could be valuable in the diagnosis of breast cancer.

Patients diagnosed with breast cancer and their age matched controls were recruited as participants for this study from the Sanford Medical Center and Rodger Maris Cancer Center in Fargo, North Dakota in collaboration with Sanford Health (all procedures for this study were reviewed and approved by the Sanford Health Institutional Review Board). Urine was collected from the breast cancer patients both prior to any treatment, as well as 2-4 weeks following surgery, and subjected to commercially available ELISA (Enzyme Linked Immuno Sorbent Assay) tests to quantify the amount of urinary ADAM 12 present. These quantities were compared with age-matched controls. Interestingly, we find no significant differences between the urinary ADAM 12 levels of cancer patients prior to treatment and age-matched controls. ADAM 12 levels do become significantly elevated following surgery, and this elevation is more significant for patients having undergone more severe surgeries (patients having undergone a

mastectomy have more significant elevations than those who underwent a lumpectomy). Based on these data, we must conclude that urinary ADAM 12 is unlikely to be a viable biomarker for breast cancer diagnosis.

References

(1) Roy, A.; Rate shock: In California, Obamacare to increase individual health insurance premiums by 64-146%; Forbes, May 30, 2013.

(2) New Obamacare mandate on screening and preventative care may benefit clinical pathology laboratories., Dark Daily, October 6, 2010, www.darkdaily.com.

(3) Community clinical lab companies hard hit by Medicare lab test fee cuts and owners fear negative financial consequences of coming price cuts, Dark Daily, May 22, 2013,www.darkdaily.com.

(4) The Lewin Group; Laboratory medicine: a national status report, Center for Disease Control and Prevention, 2008.

(5) Pan, J.; Qian, Y.; Zhou, X.; Pazandak, A.; Frazier, S. B.; Weiser, P.; Lu, H.; Zhang, L. Nature Biotechnology **2010**, 28, 203-207.

(6) Multi-state meningitis outbreak - current case count, Center for Disease Control and Prevention, June 3, 2013, www.cdc.gov.

(7) Cardiac drug contamination warning in Pakistan, National Travel Health Network and Centre, February 17, 2012, www.nathnac.org.

(8) Zhang, F.; Zhang, Z.; Linhardt, R. J. The Handbook of Glycomics; Elsevier: London, UK, 2009.

(9) Numakura, M.; Kusakabe, N.; Ishige, K.; Ohtake-Niimi, S.; Habuchi, H.; Habuchi, O. Glycoconj J **2010**, 27, 479-489.

(10) Ori, A.; Wilkinson, M. C.; Fernig, D. G. J Biol Chem **2011**, 286, 19892-19904.

(11) Engelberg, H. Pharmacol Rev **1996**, 48, 327-352.

(12) Ihrcke, N. S.; Wrenshall, L. E.; Lindman, B. J.; Platt, J. L. Immunol Today **1993**, 14, 500-505.

(13) Ogston, A. G.; Stanier, J. E. J Physiol **1953**, 119, 244-252.

(14) Varma, R.; Hoshino, A. Y.; Vercellotti, J. R. Carbohydrate Research **1980**, 82, 343-351.

(15) Corte, M. D.; Gonzalez, L. O.; Junquera, S.; Bongera, M.; Allende, M. T.; Vizoso, F. J. Journal of Cancer Research and Clinical Oncology **2010**, 136, 745-750.

(16) Masahiro, M.; Akiko, Y.; Yokohama, K. Y.; Kokuryo, T.; Tsunoda, N.; Oda, K.; Nagino, M.; Ishimaru, T.; Shimoyama, Y.; Utsunomiya, H.; Iwata, H.; Itoh, Y.; Itoh, J.; Kannagi, R.; Kyogashima, M. Glycoconjugate Journal **2010**, 27, 661-672.

(17) Kurup, R. K.; Kurup, P. A. International Journal of Neuroscience **2003**, 113, 361-381.

(18) Niedowicz, D. M.; Studzinski, C. M.; Weidner, A. M.; Platt, T. L.; Kingry, K. N.; Beckett, T. L.; Bruce-Keller, A. J.; Keller, J. N.; Murphy, M. P. Biochim Biophys Acta **2013**, 1832, 439-444.

(19) Matoug, S.; Abdel-Dayem, A. Journal of Physics: Conference Series **2012**, 341.

(20) Rodriguez-Rodriguez, E.; Sanchez-Juan, P.; Vazquez-Higuera, J. L.; Mateo, I.; Pozueta, A.; Berciano, J.; Cervantes, S.; Alcolea, D.; Martinez-Lage, P.; Clarimon, J.; Lleo, A.; Pastor, P.; Combarros, O. J Neural Transm **2013**, 120, 807-812.

(21) Nyren-Erickson, E. K.; Haldar, M. K.; Gu, Y.; Qian, S. Y.; Friesner, D. L.; Mallik, S. Analytical Chemistry **2011**, 83, 5989-5995.

(22) Maruyama, T.; Toida, T.; Imanari, T.; Yu, G.; Linhardt, R. Carbohydrate Research **1998**, 306, 35-43.

(23) Beyer, T.; Matz, M.; Brinz, D.; Radler, O.; Wolf, B.; Norwig, J.; Baumann, K.; Alban, S.; Holzgrabe, U. Eur J Pharm Sci **2010**, 40, 297-304.

(24) Krumbiegel, M.; Arnold, K. Chemistry and Physics of Lipids **1990**, 54, 1-7.

(25) Satoh, A.; Toida, T.; Yoshida, K.; Kojima, K.; Matsumoto, I. FEBS Letters **2000**, 477, 249-252.

(26) Nyren-Erickson, E. K.; Haldar, M. K.; Totzauer, J. R.; Ceglowski, R.; Patel, D. S.; Friesner, D. L.; Srivastava, D. K.; Mallik, S. Langmuir **2012**, 28, 16115-16125.

(27) National Breast Cancer Statistics, Northeast Ohio Affiliate of Susan G. Komen, January 2012, www.komenneohio.org.

(28) Sturgeon, C. M.; Duffy, M. J.; Stenman, U. H.; Lilja, H.; Brunner, N.; Chan, D. W.; Babaian, R.; Bast, R. C., Jr.; Dowell, B.; Esteva, F. J.; Haglund, C.; Harbeck, N.; Hayes, D. F.; Holten-Andersen, M.; Klee, G. G.; Lamerz, R.; Looijenga, L. H.; Molina, R.; Nielsen, H. J.; Rittenhouse, H.; Semjonow, A.; Shih Ie, M.; Sibley, P.; Soletormos, G.; Stephan, C.; Sokoll, L.; Hoffman, B. R.; Diamandis, E. P. Clin Chem **2008**, 54, e11-79.

(29) Ludwig, J. A.; Weinstein, J. N. Nat Rev Cancer **2005**, 5, 845-856.

(30) Opstal-van Winden, A. W.; Rodenburg, W.; Pennings, J. L.; van Oostrom, C. T.; Beijnen, J. H.; Peeters, P. H.; van Gils, C. H.; de Vries, A. Int J Mol Sci **2012**, 13, 13587-13604.

(31) Eastern Research Group, I.; Assessment of the availability of mammography services, Food and Drug Administration, 2001.

(32) Nyren-Erickson, E. K.; Jones, J. M.; Srivastava, D. K.; Mallik, S. Biophysica et. Biochimica Acta **2013**, http://dx.doi.org/10.1016/j.bbagen.2013.1005.1011.

(33) Roy, R.; Wewer, U. M.; Zurakowski, D.; Pories, S. E.; Moses, M. A. J Biol Chem **2004**, 279, 51323-51330.

PAPER 1. FLUORESCENT LIPOSOMES FOR DIFFERENTIAL INTERACTIONS WITH GLYCOSAMINOGLYCANS

Abstract

We have successfully synthesized a lipid containing the pyranine dye as the hydrophilic head group. This lipid was incorporated into liposomes with 1-palmitoyl-*sn*-glycero-3-phosphocholine as the major component. The resultant liposomes displayed differential enhancements in fluorescence emission intensity in the presence of nanomolar concentrations of different glycosaminoglycans. Linear discriminant analysis of the fluorescence response data demonstrate that the liposomes are able to distinguish between different GAGs. In addition, we also demonstrate that the liposomes incorporating the pyranine lipid are able to distinguish between dilute serum from healthy individuals and serum containing elevated chondroitin sulfate (simulated serum from an Alzheimer's disease patient).

Introduction

Glycosaminoglycans (mucopolysaccharides) are linear polysaccharides composed of repeating disaccharide units of uronic acid and an amino sugar (Figure 1.1).[1] They may be either sulfated or non-sulfated, and are involved in many physiological functions.[2] In several diseases, the serum or urine levels of glycosaminoglycans (GAGs) change relative to that of healthy individuals. For example, abnormal metabolism of the GAGs and glycoproteins present in the blood-brain barrier and neuron receptors contribute to abnormally high levels of GAGs in the serum of schizophrenics,[3,4] with a concurrent decrease in urine glycosaminoglycan level.[4,5] The serum concentrations of glycosaminoglycans (uronic acids and chondroitin sulfate) increase considerably in Alzheimer's disease patients relative to that of healthy individuals.[6] The urine

GAG concentrations are also elevated for patients with various types of metastatic cancers,[7-9] and for children with acute urinary tract infections.[10]

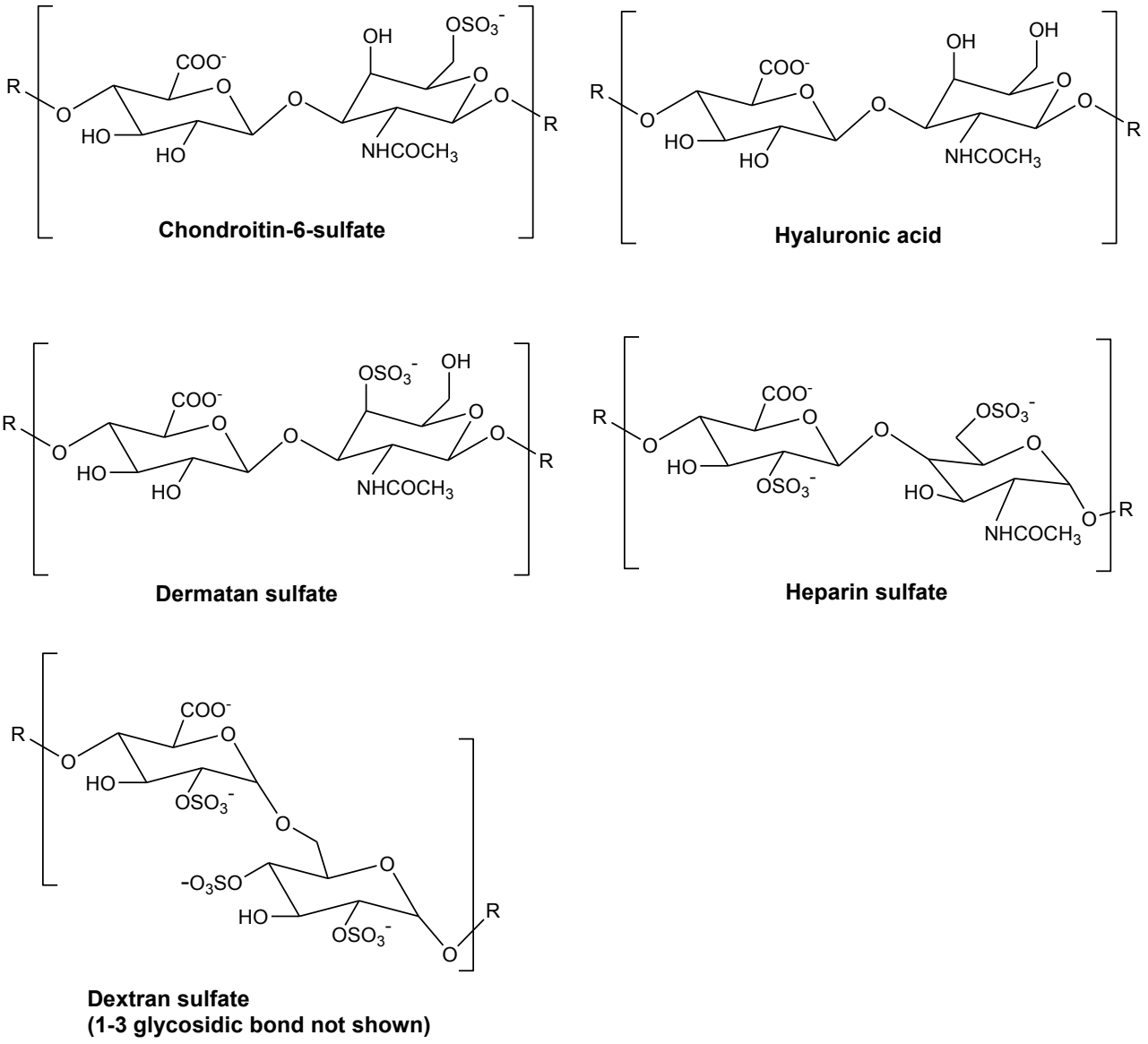

Figure 1.1. **Structures of the glycosaminoglycans (GAGs).**

Usually, the detection of GAGs involves chemical or enzymatic hydrolysis of the polymers to smaller units and subsequent conjugation with suitable dyes for spectrophotometric or spectrofluorometric detection of the hydrolysis products (often by HPLC).[11,12] There are

commercially available GAG detection kits based on these principles.[‡] However, these techniques provide the total concentration of the glycosaminoglycans in the sample, and do not provide the identity of the GAG present. Nuclear magnetic resonance (NMR), capillary electrophoresis (CE) and mass spectrometry (MS) have been used to detect the hydrolysis products and to identify the GAGs present in the original samples.[11] These techniques are involved, require specialized equipment and purified, known samples of the hydrolysis products for calibration. ELISA-like assays and immunoblotting have been developed for selective detection of GAGs.[13,14] Although these methods are successful in detecting the individual GAGs, sensitive biological antibodies are used as the recognition elements.

Herein, we report the synthesis of a lipid containing the pyranine dye as the hydrophilic head group and demonstrate that liposomes incorporating this lipid show differential modulations of the emission intensity in the presence of different glycosaminoglycans. Linear discriminant analysis of the fluorescence response data demonstrate that the liposomes are able to distinguish between different GAGs. In addition, we also demonstrate that these liposomes (containing the pyranine lipid) are able to distinguish between dilute serum from healthy individuals and serum containing elevated chondroitin sulfate (simulated serum from an Alzheimer's disease patient). With further development, we anticipate that this fluorescence-based approach to detect the individual GAGs (without prior chemical or enzymatic hydrolysis or without using biological antibodies) will be invaluable for accurate and early diagnosis of these diseases.

[‡] GAG detection kits are available from several suppliers. For example: Biocolor Ltd (UK); Kamiya Biomedical Company, Seattle, WA (US); ALPCO Diagnostics, Salem, NH (US) etc.

Materials and methods

Materials: All reagents were purchased from either TCI America or Alfa-Aesar and were used as received. Table 1.1 shows the glycosaminoglycans used, and their respective molecular weights.

Table 1.1. **Glycosaminoglycans used and respective molecular weights**

GAG Used	MW (kDa)
Chondroitin Sulfate	35
Dermatan Sulfate	30
Dextran Sulfate	40
Heparin Sulfate	13.5
Hyaluronic Acid	1400

The dansyl, rhodamine and POPC lipids were purchased from Avanti Polar Lipids. Human serum was purchased from Sigma-Aldrich. Probe sonication was carried out using a Misonix Microson Ultrasonic Cell Disruptor, with a VWR digital heatblock for temperature control. Fluorescence spectra were recorded using a *Horiba Jobin Yvonne* FluoroMax-4 spectrofluorometer.

Synthesis of the pyranine lipid: The synthetic details are provided in Appendix A.

Preparation of liposomes: For pyranine-containing liposomes, 1.2 mL of POPC solution in chloroform (2 mg/mL), and 4.2 mL of pyranine lipid solution in chloroform (0.01 mg/mL) were added to a 10 mL round-bottom flask. For lissamine-rhodamine-containing liposomes 1.2 mL of POPC solution in chloroform (2 mg/mL), and 4 mL of lissamine-rhodamine lipid solution in chloroform (0.01 mg/mL) were added to a 10 mL round-bottom flask. For dansyl-containing liposomes, 1 mL of POPC solution in chloroform (2 mg/mL), and 1.74 mL of dansyl lipid solution in chloroform (1 mg/mL) were added to a round-bottom flask. The solutions were evaporated using a rotary evaporator at 50 ^{o}C for 10 minutes. The resulting lipid thin film was

stored in a desiccator for 8 hours or overnight. The lipid thin film was hydrated with 2 mL of 25 mM HEPES buffer (pH 8) for 1 hour at 50 ºC with rotation and then probe-sonicated at 70 ºC for 45 min. The liposomes were stored at room temperature (22 ºC) in darkness for 1 hour and then extruded 15 times through a 100 nm filter at 70 ºC. The extruded liposomes were allowed to come to room temperature (15 min) before use.

Calculation of fluorophore on outer leaflet:

Equation used is as follows:

$$\frac{(60\%\ of\ lipid\ on\ outer\ leaflet)x\ (wt.of\ pyranine\ lipid\ added\ in\ grams)x\ (1{,}000)}{(Molar\ mass\ of\ fluorophore\ lipid\ in\ grams)x\ (final\ volume\ of\ preparation\ in\ mL)}$$

Therefore, for 1.8 mL final volume of pyranine-containing liposomes, the calculation is as such: (0.6) x (0.000044g) x (1000)/(1329.61g) x (1.8mL) = 1.1 x 10^{-5} M, or 11μM stock solution of liposomes. This solution was then diluted for use in the same buffer used for hydration of the thin film (see above). In addition, it is this concentration (that of the fluorophore on the outer liposome leaflet) that was used to express the concentrations of liposomes used during fluorescence emission studies.

Fluorescence spectroscopic studies: To determine the changes in fluorescence emission upon addition of GAGs to each fluorophore-containing liposome, the following sequential additions were made to a quartz fluorimeter cell. Each sample was measured six times for the statistical analysis of the data.

1. 193 μL of 25 mM HEPES buffer, pH 8.
2. 5 μL liposomes solution (200 nM solution for pyranine and rhodamine liposomes, and 8 μM for dansyl liposomes (final concentration of 5 nM for pyranine and rhodamine, 200 nM for dansyl liposomes). Following this addition, the solution was excited six times at a

wavelength corresponding to the excitation wavelength of the fluorophore present, and each excitation was followed by collection of the emission spectrum.

3. 2 μL GAG solution in 25 mM HEPES (100 nM solution added—final concentration 1 nM).
4. 1.8 μL GAG solution (1 μM solution added—final concentration 10 nM).
5. 8 μL GAG solution (1 μM solution added—final concentration 50 nM).
6. 10 uL GAG solution (1 μM solution added—final concentration 100 nM).

The maximum emission wavelength for each fluorophore was recorded; data at this wavelength for all cycles was collected and used for data analysis.

Experiments with human serum: Normal human serum was diluted 10,000 times using 25 mM HEPES buffer at pH 8. Chondroitin sulfate was added to bring the concentration up to 48 nM from 26 nM. This corresponds to 8.1 mg/dL of uronic acid in the serum without dilution (similar to that observed for Alzheimer's disease patients). The serum was diluted so that the concentration of chondroitin sulfate is close to 50 nM (the concentration where the pyranine liposomes has the best discriminating ability). An aliquot (1 mL) of each serum mixture was withdrawn and 5 μL solution of the pyranine liposomes (1 μM pyranine concentration in the outer leaflet of the liposomes) was added to each, resulting in final concentration of 5 nM pyranine in the outer lipid layer liposomes. A portion of the liposome-serum mixture (200 μL) was used in the fluorescence experiments.

Results and discussion

GAGs are known to interact with liposomes and depending on the concentration of the GAG, this leads to liposomal aggregation.[15,16] We reasoned that this interaction can be modulated and monitored by incorporating lipids with charged fluorophores (as head groups) in

the liposomes. With this goal, we synthesized a lipid with the pyranine dye as the hydrophilic head group (Figure 1.2). For comparison, we selected two other commercially-available lipids incorporating the lissamine rhodamine and dansyl moieties as the hydrophilic head groups (Figure 1.2).

The synthesis of the pyranine lipid started with the commercially available pyranine dye (Figure 1.2). The phenolic hydroxyl group was alkylated to produce the compound **4** containing the carboxylic acid moiety. The compound **4** was subsequently conjugated with the synthesized bis-oleoyl lipid **1** to produce the desired pyranine lipid as a yellow waxy solid. We used the racemic 2,3-diaminopropanoic acid in the synthesis, resulting in the racemic form of the pyranine lipid.

We prepared liposomes with 1-palmitoyl-2-oleoyl-*sn*-glycero-3-phosphocholine (POPC) as the major lipid and monitored changes in fluorescence intensity in the presence of varying concentrations of five different GAGs (heparin sulfate, dermatan sulfate, chondroitin sulfate, dextran sulfate, and hyaluronic acid, Figure 1.1). We hypothesized that the presence of different GAGs will cause varying degrees of liposomal aggregation, causing each fluorophore to exhibit different patterns of fluorescence emission intensity changes. This will therefore serve to not only detect GAGs in solution, but also to distinguish between different glycosaminoglycan types.

The liposomes were prepared in 25 mM HEPES buffer (pH = 8.0) by the thin film hydration method.[17] Unilamellar vesicles were generated by probe sonication followed by repeated extrusions through membranes of 100 nm pore sizes at 70 ^{o}C (Appendix A).[17] The average diameter of the extruded liposomes was observed to be 88 $\pm$ 5 nm (by dynamic light scattering). We used 1 mol% of the pyranine lipid or the rhodamine lipid in the liposomes. A significantly higher amount of the dansyl lipid (40 mol%) was required in the liposomes to

compensate for its lower quantum yield.[18] Differential scanning calorimetric studies revealed that the fluorophore lipids were mixed in the lipid bilayer of the liposomes (data not shown).

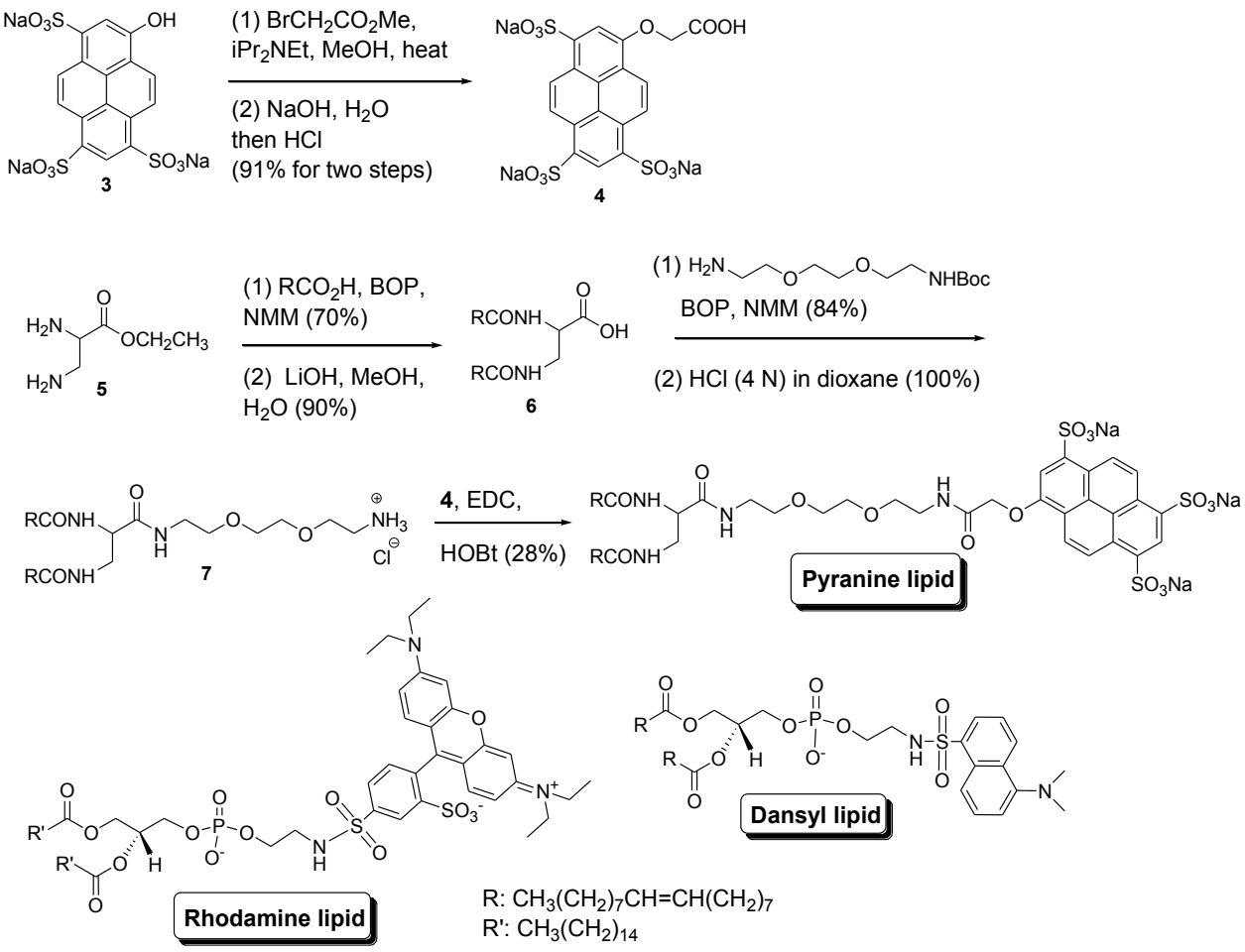

Figure 1.2. **Fluorescent lipid structures**. Structures of the lipids with pyranine, lissamine rhodamine and dansyl as the head groups and the synthesis of the pyranine lipid.

To conduct fluorescence spectroscopic studies, liposomes from each batch were incubated with four different concentrations (1 nM, 10 nM, 50 nM, and 100 nM) of each of the glycosaminoglycans. The low concentrations of the GAGs in 25 mM HEPES buffer (pH = 8.0) ensure that the molecules are completely ionized and the degree of ionization is not influencing the fluorescence spectra from the liposome-incorporated dyes. Six fluorescence emission spectra

were recorded for each concentration of each glycosaminoglycan, and these were compared with the corresponding emission spectra from the liposomes in the absence of GAGs. The ratios of emission intensities from liposomes alone to that in the presence of GAGs (Em_{lip}/Em_{GAG}) were calculated for each spectrum at the peak emission wavelength, and these ratio data were subjected to linear discriminant analysis.[19-21]

We observed that liposomes containing the selected fluorophores respond differently to the presence of the different GAGs tested. Figure 1.3B depicts the ratios of the fluorescence emission intensity of the pyranine liposomes for each GAG at 50 nM concentration (λ_{ex} = 390 nm). Figure 1.3A depicts representative full fluorescence emission spectra for these liposomes in the presence of each GAG.

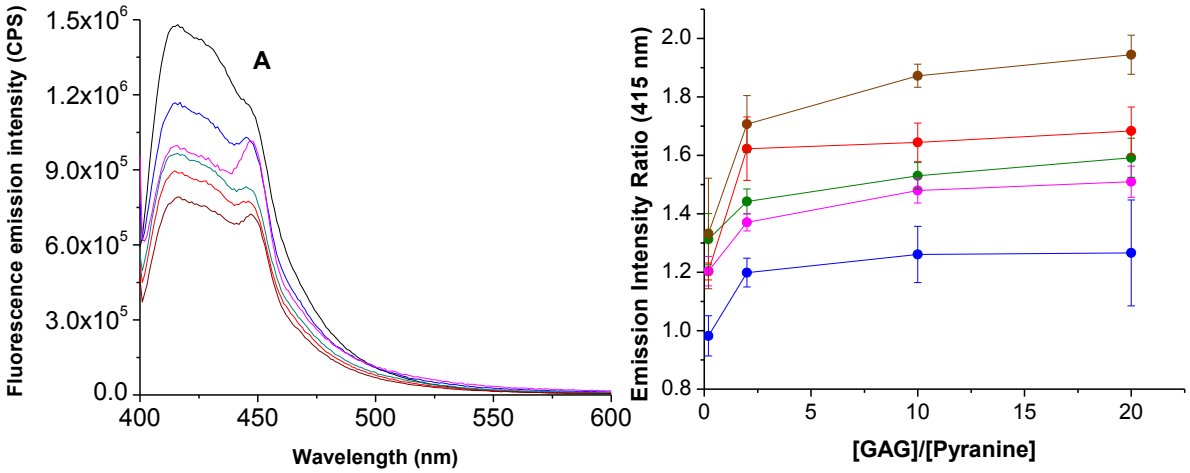

Figure 1.3. **Liposome fluorescence spectra.** The fluorescence spectra (A) of the liposomes incorporating the pyranine lipid (λ_{ex} = 390 nm) in the presence of 50 nM of each of the glycosaminoglycans are shown. The emission intensity ratios in the absence and presence of added GAGs are shown in (B). The GAGs include chondroitin sulfate (olive), dextran sulfate (blue), heparin sulfate (red), hyaluronic acid (magenta), and dermatan sulfate (brown). The black trace in (A) is for the liposomes in the absence of any added GAGs. The data points in (B) are connected by straight lines.

Notable from this figure is that each GAG produces a different Em_{lip}/Em_{GAG} ratio (Figure 1.3B; the plots for the liposomes incorporating the other fluorophores are included in Appendix A). Transmission electron microscopy of the liposomes after the addition of 50 nM GAGs indicated aggregation leading to increase in size (Figure 1.4); however, we did not observe any precipitate formation.

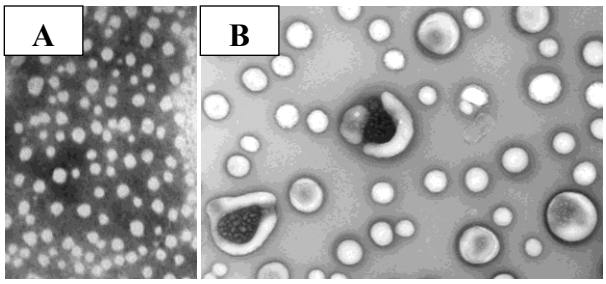

Figure 1.4. **TEM micrographs of pyranine liposomes in buffer only and with chondroitin sulfate**. Transmission electron micrographs of the pyranine liposomes in buffer (2) and in the presence of 50 nM chondroitin sulfate (2) are shown. The magnification was 79,200 (1 cm in the figures corresponds to 250 nm in size).

To determine whether a change in the molecular weight of the glycosaminoglycan would alter the fluorescence intensity change, we repeated the studies with another sample of chondroitin sulfate with a lower molecular weight (20 kDa) and compared the responses with those from the chondroitin sulfate of molecular weight 35 kDa. We observed that the higher molecular weight chondroitin sulfate caused more pronounced decreases in the emission intensity from the pyranine and dansyl-containing liposomes (Appendix A). It is likely that the higher molecular weight GAG leads to a greater degree of liposomal aggregation, and a greater decrease in emission intensity from the liposomes. However, the reverse was observed with lissamine-rhodamine-containing liposomes, with the lower molecular weight chondroitin sulfate causing a greater change in emission intensity (Appendix A). Reasons for this observation are

unclear, and further investigation is needed to fully deduce the mechanism responsible for this change.

Linear discriminant analysis (LDA) is used to identify the predictive power of the liposomes (see Appendix A for details).[19-21] Emission intensity data from the liposomes (the predictor variables) and the five GAGs shown in Table 1.1 (the dependent variables) were replicated a total of six times, yielding a sample of 30 observations with four variables (one for each liposome and one identifying the GAG). All statistical analyses were conducted using the PASW (formerly SPSS) Statistical Package, Version 18.

Table 1.2 shows means, F-statistics and Wilks' Lambda values for each liposome, disaggregated by GAGs. We note that smaller values for the Wilks' Lambda indicate a greater potential for the liposomes to discriminate across GAGs.[22] All F-statistics have associated p-values less than 0.05, indicating significant differences exist across group means for each GAG. For the chondroitin sulfate, dextran sulfate, heparin sulfate and hyaluronic acid, the dansyl liposomes have the highest mean fluorescence values. The pyranine liposomes have the second highest mean values, followed by rhodamine liposomes.

Table 1.2. **Tests of equality of group means**

GAG	**Pyranine[a,b]**	**Rhodamine[a,b]**	**Dansyl[a,b]**
Chondroitin Sulfate	1.562	1.297	1.563
Dermatan Sulfate	1.942	1.447	1.412
Dextran Sulfate	1.334	1.247	1.541
Heparin Sulfate	1.729	1.517	1.862
Hyaluronic Acid	1.487	1.124	2.243
Wilks' Lambda	0.068	0.214	0.560
F-Statistic	85.829	22.898	4.904
P-Value	<0.001	<0.001	1.541

[a] first panel provides group-specific means [b] second panel provides statistics and p-values.

The remaining GAG (dermatan sulfate) has the highest mean emission ratios when combined with pyranine, followed by dansyl and rhodamine containing liposomes. Wilks' Lambda values are lowest for pyranine, followed by rhodamine and dansyl liposomes. Chi-square tests indicate that three canonical functions are sufficient to explain our 5 GAGs (see Appendix A). Of these, the first canonical function is most important, as it explains 96.3% of the variation across GAGs. The remaining functions explain 3.0% and 0.7%, respectively. As such, we focus primarily on the first discriminant function. Figure 1.5 shows a canonical function plot of the first two canonical functions (explaining 99.3% of the variation in the GAGs). Note that each of the GAGs is clearly distinguished as a group in the plot. Moreover, traditional and cross-validated discriminant functions corrected predict 100% and 93.3% of the GAGs, respectively, indicating a high likelihood of interval validity.

To assess the overall contribution of each liposome to the discriminatory power of the LDA, we constructed cumulative potency indices (Appendix A). The potency indices suggest that pyranine (potency value = 0.215) provides the largest overall contribution to the model's ability to distinguish emission intensities across GAGs (rhodamine potency index = 0.057; dansyl potency index = 0.012).

The LDA results have a clear and intuitive interpretation; namely, that the pyranine liposomes are the "best" determinant of GAGs. Dansyl liposomes are identified as the least "potent" discriminator, even though its emission intensities are relatively high (Table 1.2). The Wilks' Lambda and structure matrices (see Appendix A for the latter) suggest that this is at least partly attributable to excess variation in dansyl emission intensities, which offsets the high mean values.

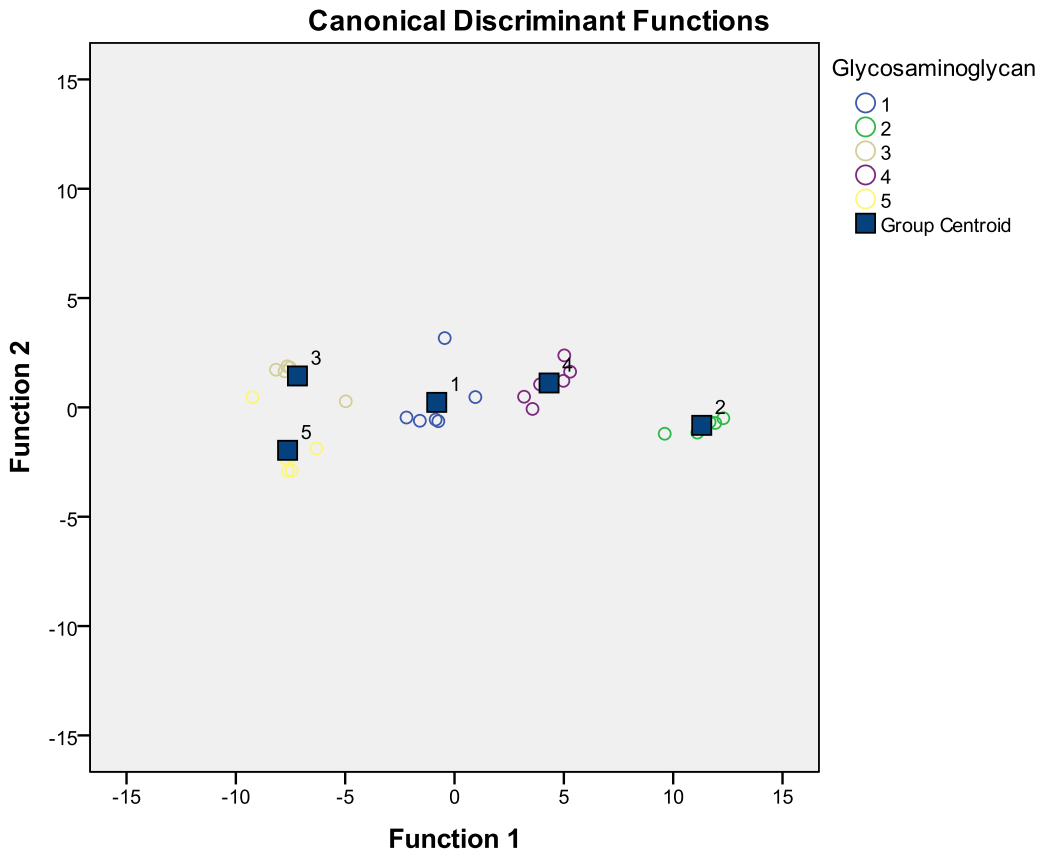

Figure 1.5. **Canonical correlation plot**. Canonical correlation plot between two largest canonical correlations and each of the five GAGs: chondroitin sulfate (group 1), dermatan sulfate (group 2), dextran sulfate (group 3), heparin sulfate (group 4) and hyaluronic acid (group 5).

One possible limitation of the analysis is that we have chosen a specific (50 nM) concentration to conduct our experiments. To check the robustness of our results, we replicated the LDA for the 100 nM concentrations (Appendix A). The results are qualitatively (but not quantitatively) similar to those at 50 nM.

Subsequently, we proceeded to determine if the pyranine-containing liposomes are capable of distinguishing an increase in GAG concentration in a complex mixture of proteins and other biomolecules, e.g., dilute human serum. According to the National Institute on Aging, currently there is no biochemical test to detect Alzheimer's disease. Indirect methods are used

by physicians for diagnosis.[§] However, it has been reported that the serum concentrations of glycosaminoglycans (uronic acids) increase in Alzheimer's disease patients (about 8.4 $\pm$ 0.8 mg/dL) relative to that of healthy individuals (about 4.6 $\pm$ 0.5 mg/dL).[6] Chondroitin sulfate concentration in the serum increases from about 0.58 mg/dL (healthy individuals) to about 2.36 mg/dL for Alzheimer's disease patients.[6] The LDA analysis indicated that the pyranine-containing liposomes are capable of distinguishing different GAGs at 100 nM and 50 nM concentrations. It follows that the pyranine liposomes have the capability to distinguish the GAGs in a very dilute human serum from an Alzheimer's disease patient (diluted 10^4 times).

In order to simulate serum from Alzheimer's disease patients, we spiked commercially available human serum (Sigma Chemical Company) with added chondroitin sulfate (MW: 35 kDa) such that the uronic acid concentration is about 8 mg/dL. We noted, *a priori*, that it is an increase in not one, but rather several GAGs which contributes to the overall increase in GAG concentration in Alzheimer's disease patients.[6] The use of chondroitin sulfate only as the GAG of choice is to provide a relevant model system to determine if the pyranine liposomes are capable of distinguishing changes in GAG concentration in a complex mixture of other physiological molecules. We noted also that the increase in chondroitin sulfate in Alzheimer's disease patients from that of healthy patients is among the highest percentage increases of all the GAGs, while also making up one of the highest fractions of the total GAGs present.[6] We diluted the simulated disease serum appropriately so that the concentration of the chondroitin sulfate is about 48 nM.

[§] Reported by the National Institutes of Health, National Institute on Aging; http://www.nia.nih.gov; updated January 10, 2011; accessed on April 18, 2011.

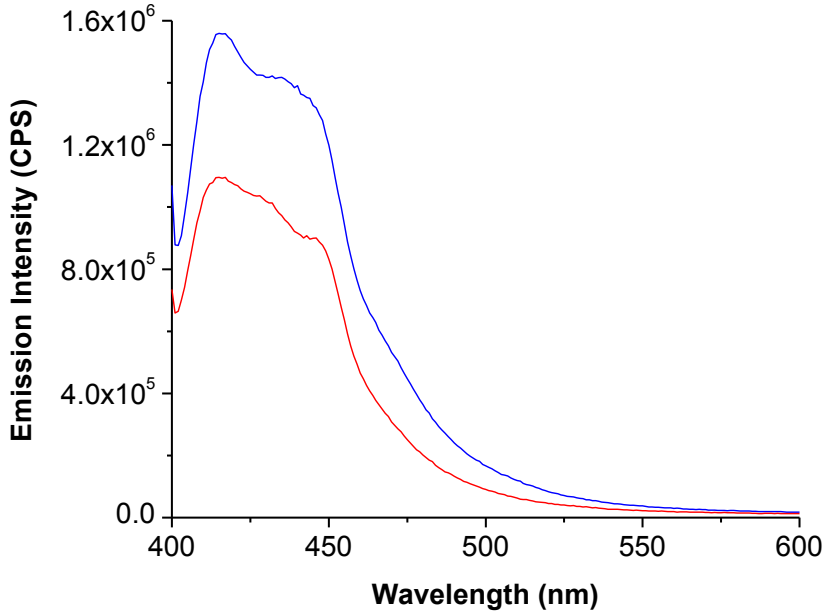

Figure 1.6. **Pyranine fluorescence in normal serum vs. Alzheimer's serum**. The fluorescence emission spectra for the pyranine liposomes (λ_{ex} = 390 nm) in the presence of diluted healthy serum (blue) and simulated Alzheimer's disease serum (red) are shown.

Results from the human serum experiment are shown in Figure 1.6. We observed a considerable decrease in the emission intensity from the pyranine liposomes in the presence of simulated Alzheimer's disease serum (Figure 1.6, red trace). It should be noted that the commercially available kit can detect the total concentrations of the GAGs (after enzymatic hydrolysis) with micromolar detection limits.[13] In contrast, the emission intensity from the pyranine liposomes changes considerably in the presence of 48 nM chondroitin sulfate (without prior enzymatic hydrolysis of the polymer). These results suggest that the pyranine fluorophore-containing liposomes may be very valuable in the successful diagnosis of Alzheimer's disease by monitoring the levels of the GAGs in the serum. The utility of such a test could be magnified further if the patient could be tested early in life, and then subsequently over time, monitoring any changes.

Conclusions

We have successfully synthesized a lipid with the pyranine dye as the hydrophilic head group. We have demonstrated (by fluorescence spectroscopy) that liposomes (with POPC as the major lipid component) incorporating suitable dyes will differentially interact with the different glycosaminoglycans. Linear discriminant analysis indicated that the liposomes incorporating the synthesized pyranine lipid have the highest discriminating ability amongst the GAGs. These liposomes are capable of distinguishing different levels of GAGs (e.g., chondroitin sulfate) even in a complex mixture of physiological molecules (human serum).

Acknowledgement

This research was supported by NIH grant 1R01 CA 132034 and NSF grant DMR 1005011 to Sanku Mallik. Steven Y. Qian acknowledges the support from the NIH grants R15CA140833 and P20RR015566.

References

(1) Zhang, F.; Zhang, Z.; Linhardt R. J. *The Handbook of Glycomics*; Cummings, R. D. and Pierce, M. J., Eds.; Elsevier: London, 2009.

(2) Gandhi, N. S.; Mancera, R. L. *Chem Biol Drug Des.* **2008**, *72*, 455-482.

(3) Varma, R.; Michos, G. A.; Gordon, B. J.; Varma, R. S.; Shirey, R. E. *Biochemical Medicine* **1983**, *30*, 206-214.

(4) Varma, R.; Hoshino, A. Y. *Carbohydrate Research* **1980**, *82*, 343-351.

(5) Varma, R. S.; Varma, R.; Allen, W. S.; Wardi, A. H. *Biochemical Medicine* **1974**, *11*, 358-369.

(6) Kurup, R. K.; Kurup, P. A. *Intern. J. Neuroscience* **2003**, *113*, 361-381.

(7) Masahiro, M.; Akiko, Y.; Yokohama, K. Y.; Kokuryo, T.; Tsunoda, N.; Oda, K.; Nagino, M.; Ishimaru, T.; Shimoyama, Y.; Utsunomiya, H.; Iwata, H.; Itoh, Y.; Itoh, J.; Kannagi, R.; Kyogashima, M. *Glycoconjugate J*. **2010**, *27*, 661-672.

(8) Corte, M. D.; Gonzalez, L. O.; Junquera, S.; Bongera, M.; Allende, M. T.; Vizoso, F. J. *J. Cancer Res. Clin. Oncol*. **2010**, *136*, 745-750.

(9) Platt, V. M.; Szoka Jr., F. C. *Mol. Pharmaceutics* **2008**, *5*, 474-486.

(10) Cengiz, N.; Baskin, E.; Anarat, R.; Agras, P. I.; Yildirim, S. V.; Tiker, F.; Anarat, A.; Saatci, U. *Pediatric Nephrology* **2005**, *20*, 937-939.

(11) Korir, A. K.; Larive, C. K. *Anal. Bioanal. Chem*. **2009**, *393*, 155-169.

(12) Pan, J.; Qian, Y.; Zhou, X.; Pazandak, A.; Frazier, S. B.; Weiser, P.; Lu, H.; Zhang, L. *Glycobiol. Insights* **2010**, *2*, 1-12.

(13) Bairstow, S.; McKee, J.; Nordhaus, M.; Johnson, R. *Anal. Biochem*. **2009**, *388*, 317-321.

(14) de Lima, C. R.; Baccarin, R. Y. A.; Michelacci, Y. M. *Clin. Chim. Acta* **2007**, *378*, 206-215.

(15) Krumbiegel, M.; Arnold, K. *Chem. Phys. Lipids* **1990**, *54*, 1-7.

(16) Satoh, A.; Toida, T.; Yoshida, K.; Kojima, K.; Matsumoto, I. *FEBS Letters* **2000**, *477*, 249-252.

(17) Lasch, J.; Weissig, V.; Brandl, M. *Liposomes: Second Edition;* Torchilin V. P. and Weissig V., Eds; Oxford University Press: New York, 2003.

(18) Banerjee, J.; Haldar, M. K.; Manokaran, S.; Mallik, S.; Srivastava, D. K. New Fluorescent Probes for Carbonic Anhydrases. *Chem. Commun*. **2007**, 3377-3379.

(19) Miranda, O. R.; Creran, B.; Rotello, V. M. *Curr. Opin. Chem. Biol*. **2010**, *14*, 728-736.

(20) Bunz, U. H. F.; Rotello, V. M. *Angew. Chem. Int. Ed*. **2010**, *49*, 3268-3279.

(21) Bajaj, A.; Miranda, O. R.; Phillips, R.; Kim, I. B.; Berry, J. D.; Bunz, U. H. F.; Rotello, V. M. *J. Am. Chem. Soc*. **2010**, *132*, 1018-1022.

(22) Johnson, R., Wichern, D. *Applied Multivariate Data Analysis*, 5th Ed. Prentice Hall: NJ, 2002.

This paper has been published:

Nyren-Erickson, E. K.; Haldar, M. K.; Gu, Y.; Qian, S. Y.; Friesner, D. L.; Mallik, S. Fluorescent Liposomes for Differential Interactions with Glycosaminoglycans. *Analytical Chemistry* **2011**, *83(15)*, 5989-5995.

PAPER 2. GLYCOSAMINOGLYCAN-MEDIATED SELECTIVE CHANGES IN THE AGGREGATION STATES, ZETA POTENTIALS, AND INTRINSIC STABILITY OF LIPOSOMES

Abstract

Though the aggregation of glycosaminoglycans (GAGs) in the presence of liposomes and divalent cations has been previously reported, the effect of different GAG species, as well as minor changes in GAG composition on the aggregates formed is yet unknown. If minor changes in GAG composition produce observable changes in liposome aggregate diameter or zeta potential, such a phenomenon may be used to detect potentially dangerous over-sulfated contaminants in heparin. We studied the mechanism of the interactions between heparin and its over-sulfated glycosaminoglycan contaminants with liposomes. Herein, we demonstrate that Mg^{2+} acts to shield the incoming glycosaminoglycans from the negatively-charged phosphate groups of the phospholipids, and that changes in the aggregate diameter and zeta potential are a function of glycosaminoglycan species and concentration, as well as liposome bilayer composition. These observations are supported by TEM studies. We have shown that organizational states of the liposome bilayers are influenced by the presence of GAG and excess Mg^{2+}, resulting in a stabilizing effect which increases the T_m value of DSPC liposomes; the magnitude of this effect is also dependent on GAG species and concentration present. There is an inverse relationship between the percent change of aggregate diameter and percent change of aggregate zeta potential, as a function of GAG concentration in solution. Finally, we demonstrate that the diameter and zeta potential changes of POPC liposome aggregates in the presence of different over-sulfated heparin contaminants at low concentrations allow accurate detection of over-sulfated chondroitin sulfate at concentrations as low as 1 mol%.

Introduction

Glycosaminoglycans (GAGs) are linear polysaccharides composed of disaccharide units of an amino sugar and uronic acid[1]. When incubated with phosphatidylcholine liposomes and divalent cations, GAGs cause the aggregation of liposomes[2,3]. The interaction between liposome charge and GAG concentration to cause this effect has been well documented[2-5]. However, studies conducted to date have focused primarily on mechanism of GAG binding, and have limited investigation of how average aggregate diameter and zeta potential are influenced by the species of GAG present in solution. In addition, there is no mention of how average aggregate diameter and zeta potential may co-vary as a function of GAG species and/or concentration, nor is information on how small changes in GAG composition affect these factors presently available. In the current study, we address a number of questions: do liposome aggregates demonstrate differences in their average aggregate diameter and zeta potential as a function of the GAG present in solution? If such changes are observed, how do the original diameter of the liposomes and the concentration of the GAG present influence these changes in aggregate diameter and zeta potential? Finally, if the composition of GAG present in solution varies slightly, can these changes in zeta potential and diameter be used to detect such variations in GAG composition? If so, such a phenomenon may prove useful in various industries, particularly the drug industry to detect potentially dangerous over-sulfated contaminants in heparin.

Heparin is a naturally occurring GAG which, when fully sulfated, has three sulfate groups per repeating disaccharide unit, making it the most negatively charged naturally occurring polyelectrolyte in mammalian tissues[6]. Its primary physiological function is highly varied;

however its pharmaceutical form (which is typically purified either from porcine intestine or bovine lung) is widely utilized as a drug for the prevention of blood clots in surgery patients[7].

In 2007 – 2008, several batches of heparin were found to be contaminated with over-sulfated chondroitin sulfate (OSCS), a product prepared by the synthetic oversulfation of chondroitin sulfate[8], at levels 0.5% by weight to 28% by weight[9]. Over-sulfated chondroitin sulfate has similar but considerably reduced physiological effects as compared to heparin; the anticoagulant effect of oversulfated chondroitin sulfate is approximately 20-25% of that is given by heparin[3]. In addition, its intravenous administration was associated with numerous allergic reactions, including 149 deaths[10]. The adverse effects of oversulfated chondroitin sulfate result from a potent anaphylactic response caused by the activation of the kinin-kallikrein pathway, leading to the release of bradykinin[11]. Other over-sulfated GAGs have also been shown to modulate this response[12].

To circumvent the onset of above noted side effects, many techniques have been explored/ developed for the detection of over-sulfated GAG contaminants in commercial preparations of heparin. These include ^{1}H NMR spectroscopy[13], potentiometric strip tests[14], enzyme immunoassay (ELISA)[15], polyanionic sensors[16], colorimetric assays[17], and activated partial thromboplastin times (aPTT) and prothrombin times (PT) performed with sheep and human plasma[18]. While each of these techniques presents advantages, all require specialized equipment, highly-trained personnel, and/or considerable time to obtain results. Approximately one billion doses of heparin are produced each year[19], and therefore a fast, simple, and readily available screen for the presence of over-sulfated contaminants would prove beneficial, both from the safety and economic standpoint. In pursuit of developing easily adaptable and sensitive protocol for detection of oversulfated GAG contaminates in heparin preparations, we

investigated the aforementioned tendency of liposomes to aggregate in the presence of GAG and Mg^{2+}, varying both liposome diameter and composition, as well as GAG species and concentration. Sensitivity of the changes in aggregate diameter and zeta potential with respect to these parameters were our interest.

Materials and methods

Materials and synthesis of over-sulfated GAGs: Chondroitin-6-sulfate, dermatan sulfate, and heparin were sourced from Spectrum Chemical Corp., CalBiochem, and Alfa Aesar, respectively. Each was over-sulfated using the procedures published by Maruyama, et al[3] and Nagasawa, et al[20].

Preparation of liposomes for aggregation: Stock solutions of 1-palmitoyl-2-oleoyl-*sn*-glycero-3-phosphocholine (POPC, commercially available from Avanti Polar Lipids, Alabaster, AL) and 1,2-distearoyl-*sn*-glycero-3-phosphocholine (DSPC, commercially available from Avanti Polar Lipids, Alabaster, AL) were prepared in chloroform at a concentration of 2 mg/mL. Stock solution of 1,2-dipalmitoyl-*sn*-glycero-3-phosphoethanolamine-N-(lissamine rhodamine B sulfonyl) (ammonium salt) (rhodamine lipid, commercially available from Avanti Polar Lipids, Alabaster, AL) was prepared in chloroform at a concentration of 0.01 mg/mL. Stock solution of pyranine lipid was prepared in chloroform at a concentration of 0.01 mg/mL. Lipid mixtures containing POPC were obtained by combining 2.4 mL POPC stock solution, and either 8.0 mL rhodamine lipid stock solution or 8.4 mL pyranine lipid stock solution. Mixtures containing DSPC were prepared by combining 2 mL DSPC stock solution and 6.5 mL rhodamine lipid stock solution.

The resulting mixtures had molar ratios of 99:1 POPC (or DSPC):rhodamine lipid/pyranine lipid, respectively. The mixture was subjected to rotary evaporation at 50ºC for

15 minutes, forming a thin film adhering to the sides of the flask. This thin film was then dried overnight under high vacuum to ensure complete removal of solvent. Lipid films containing POPC as the main lipid were then hydrated with 4.0 mL of 25 mM HEPES buffer at pH 8 by rapid rotation in a 50ºC water bath for 1hr. Lipid films containing DSPC as the main lipid were hydrated with 4.0 mL of 25 mM HEPES buffer at pH 8 by rapid rotation in a 70ºC water bath for 1hr. The procedure now varies for production of 50 nm, 200 nm, and 500 nm liposomes:

- For 50 nm diameter liposomes (POPC liposomes only): the hydrated solution was probe sonicated at 70ºC for 45 minutes, followed by extrusion at 70 ºC (15 times) through polycarbonate membrane filters (100 nm pore size). The average diameter of the prepared liposomes (by DLS) was approximately 55 nm $\pm$ 25 nm.
- For 200 nm diameter liposomes (POPC and DSPC liposomes): the hydrated solution was immediately extruded at 70 ºC (15 times) through polycarbonate membrane filters (100 nm pore size). Average measured diameters (by DLS) were approximately 185 $\pm$ 8 nm and 250 $\pm$ 90 nm for POPC and DSPC liposomes, respectively.
- For 550 nm diameter liposomes (POPC liposomes only): Following hydration, the resulting large vesicles were found to have an average diameter of 550 $\pm$ 70 nm (by DLS). These liposomes were used as such.

The final volume of each respective liposome solution was then measured using the extrusion syringes, and the total lipid per unit volume calculated from this volume. All liposome solutions were diluted to 1.4 mM total lipid before use.

Mechanistic studies--influence of GAG species and Mg^{2+} on diameter and zeta potential of aggregates: DSPC or POPC liposomes (200 nm diameter only) were incubated for 15 minutes at room temperature in the presence and absence of Mg^{2+} (33.4 mM final

concentration), as well as the presence and absence of heparin. Mixtures were produced according to Table 2.1 below.

***Table 2.1*. Preparation of liposomes for diameter and zeta potential mechanism tests (volume in μL)**

	HEPES buffer (25 mM, pH8)	**Liposomes (1.4 mM total lipid)**	**$MgSO_4$ (2 M in HEPES)**	**GAG (1 μM in HEPES)**
Liposomes only	306	50	---	---
Liposomes + GAG	246	50	---	60
Liposomes + Mg^{2+}	300	50	6	---
Liposomes + Mg^{2+} + GAG	240	50	6	60

Each mixture was allowed to incubate at room temperature for 15 minutes before reading. One hundred μL of this aggregated solution was mixed with 900 μL HEPES buffer at pH 8 in a disposable polystyrene cuvette, and read on a Malvern Zetasizer Nano ZS90 with the following settings: 5 measurements, each an average of 10 reads, each read 10 sec; 90° read angle; 60 second pre-equilibration; Auto Attenuation off, manual attenuation set to 7. For the corresponding zeta potential measurements, liposomes were aggregated in the same way as above. Zeta potential was read on a Malvern Zetasizer Nano ZS90 with the following settings: 5 measurements, each an average of 10 reads, each read 10 seconds; 60 second pre-equilibration; automatic attenuation on; automatic voltage selection on.

Mechanistic studies--influence of GAG species and concentration on the saturation of aggregate diameter and zeta potential: For tests with individual GAGs, POPC and DSPC liposomes were aggregated in the presence of eight different concentrations of each GAG (heparin, over-sulfated chondroitin sulfate, over-sulfated dermatan sulfate, or over-sulfated heparin) in preparation for DLS, according to Table 2.2 below.

Table 2.2. **Preparation of liposome aggregates for saturation tests (all volumes in μL)**

	HEPES buffer (25 mM, pH 8)	**Liposomes (1.4 mM total lipid)**	**$MgSO_4$ at 2 M**	**GAG (concentration in parentheses)**
Liposomes only + Mg^{2+}	300	50	6	---
100 nM GAG	264	50	6	35.6 (1 μM)
500 nM GAG	122	50	6	178 (1 μM)
1 μM GAG	296	50	6	3.6 (100 μM)
10 μM GAG	264	50	6	35.6 (100 μM)
50 μM GAG	122	50	6	178 (100 μM)
100 μM GAG	264	50	6	35.6 (1 mM)
250 μM GAG	211	50	6	89 (1 mM)
500 μM GAG	122	50	6	178 (1 mM)

Measurement of aggregate diameter and zeta potential proceeded in the same way as stated above. Three measurements were collected for each GAG concentration for both average diameter and zeta potential, each an average of 10 reads, each read 10 seconds. Equipment settings remained the same.

TEM imaging: To aggregate liposomes, 50 μL of liposomes (200 nm diameter) at 1.4 mM, were incubated with 60 μL of GAG at 1 μM (approximately 20% v/v, 170 nM final concentration) and 6 μL of $MgSO_4$ at 2 M in 240 μL HEPES buffer at pH 8 for 15 minutes at room temperature. For liposome only control, 60 μL GAG was substituted with 60 μL additional HEPES buffer. Copper TEM grids (300-mesh, formvar-carbon coated, Electron Microscopy Sciences, Hatfield, Pennsylvania, USA) were prepared by applying a drop of 0.01% poly-L-lysine, allowing it to stand for 30 seconds, wicking off the liquid with torn filter paper, and allowing the grids to air dry. A drop of the aggregated liposome suspension was placed on a prepared grid for 30 seconds and wicked off; grids were allowed to air dry again.

Phosphotungstic acid 1%, pH adjusted to 7-8, was dropped onto the grid containing the liposome sample, allowed to stand for 1.5 min, and wicked off. After the grids were dry, images were obtained using a JEOL JEM-2100 LaB_6 transmission electron microscope (JEOL USA, Peabody, Massachusetts) running at 200 keV.

Differential scanning calorimetry: DSPC liposomes were incubated with 1 μM and 250 μM GAG for 15 minutes at room temperature, before being degassed for 15 minutes and loaded into a Nano DSC (TA instruments New Castle, DE) without further dilution. A sample of DSPC liposomes incubated with only Mg^{2+} was used as the control. The DSC reference cell was filled with HEPES buffer at 25 mM, pH 8, containing 33.4 mM $MgSO_4$, the same as that of the samples. Machine was pressurized to three atmospheres, and scans were conducted from 25 °C to 75 °C, and rate of temperature change was 2 °C/minute. Heat required during transition was calculated using NanoAnalyze software provided by the instrument vendor, using the sigmoidal baseline function to produce the pre- and post-transition baseline.

Mechanistic studies—combined influence of liposome diameter and GAG concentration on diameter and zeta potential changes: POPC liposomes of diameters 50, 200, and 550 nm diameter liposomes were each incubated with heparin, OSH, OSCS, and OSD (individually) at concentrations of 50, 170, and 500 nM. Measurement of aggregate diameter and zeta potential were measured in the same way as stated above. Five measurements were collected for each GAG concentration for both diameter and zeta potential, each an average of 10 reads, each read 10 seconds. Equipment settings remained the same. Following collection of data, each over-sulfated contaminant was compared to the corresponding measurement of heparin by calculating the percent change from heparin, using the following formula:

$$\left(\frac{size\ of\ contaminant\ aggregate - size\ of\ heparin\ aggregate}{size\ of\ heparin\ aggregate}\right) x\ 100$$

The same formula was applied to calculate zeta potential percent change.

Heparin contamination studies: For contaminated heparin studies, final concentrations of 170 nM and 500 nM total GAG were used with 200 nm and 500 nm diameter liposomes, respectively. Solutions of heparin with an over-sulfated contaminant were prepared according to Tables 2.3 and 2.4 below.

Table 2.3. **Preparation of liposome aggregates for 170 nM contamination study (all volumes in μL)**

	HEPES buffer (25 mM, pH 8)	**Liposomes (1.4 mM total lipid)**	**$MgSO_4$ at 2 M**	**Heparin (1 μM concentration)**	**Over-sulfated contaminant**
Heparin only	240	50	6	60	--
0.5 mol% contamination	237.3	50	6	59.7	3 (100 nM)
1.0 mol% contamination	234.3	50	6	59.4	6 (100 nM)
2.5 mol% contamination	240	50	6	58.5	1.5 (1 μM)
5.0 mol% contamination	240	50	6	57	3 (1 μM)
10.0 mol% contamination	240	50	6	54	6 (1 μM)
15.0 mol% contamination	240	50	6	51	9 (1 μM)
20.0 mol% contamination	240	50	6	48	12 (1 μM)
30.0 mol% contamination	240	50	6	42	15 (1 μM)

Measurement of aggregate diameter and zeta potential proceeded in the same way as stated above. Five measurements were collected for each GAG concentration for both diameter and zeta potential, each an average of 10 reads, each read 10 seconds. Equipment settings remained the same.

Statistical analysis: Analysis of variance and Dunnett's post-tests were run using Minitab software, version 16.1.1.

Table 2.4. **Preparation of liposome aggregates for 500 nM contamination study (all volumes in μL)**

	HEPES buffer (25 mM, pH 8)	**Liposomes (1.4 mM total lipid)**	**$MgSO_4$ at 2 M**	**Heparin (1 μM concentration)**	**Over-sulfated contaminant**
Heparin only	122	50	6	178	--
0.5 mol% contamination	114	50	6	177.11	8.9 (100 nM)
1.0 mol% contamination	122	50	6	176.2	1.78 (1 μM)
2.5 mol% contamination	122	50	6	173.6	4.45 (1 μM)
5.0 mol% contamination	122	50	6	169.1	8.9 (1 μM)
10.0 mol% contamination	122	50	6	160.2	17.8 (1 μM)
15.0 mol% contamination	122	50	6	151.3	26.7 (1 μM)
20.0 mol% contamination	122	50	6	142.4	35.6 (1 μM)
30.0 mol% contamination	122	50	6	124.6	53.4 (1 μM)

Results and discussion

In our previous work, we have demonstrated that phosphocholine liposomes having either the pyranine lipid or the lissamine-rhodamine lipid present in the bilayer at 1 mol% were able to distinguish between different GAG species in solution[21]. In these studies, we have found the optimal liposomes for GAG discrimination contain the pyranine or the rhodamine lipid (Figure 2.1 shows structures of these lipids); however preliminary studies demonstrated that liposomes containing the pyranine head group tend to aggregate in the presence of excess of divalent cations (i.e., in the absence of GAG; data not shown). Based on these prior results, we prepared 1-palmitoyl-2-oleoyl-*sn*-glycero-3-phosphocholine (POPC) liposomes incorporating 1 mol% of 1,2-dipalmitoyl-*sn*-glycero-3-phosphoethanolamine-N-(lissamine rhodamine B sulfonyl; rhodamine lipid), as well as 1,2-distearoyl-*sn*-glycero-3-phosphocholine (DSPC) liposomes

incorporating 1 mol% rhodamine lipid for use in these studies. We employed transmission electron microscopy (TEM) and dynamic light scattering (DLS) to evaluate the relative diameter differences between aggregates produced by different GAGs. Changes in diameter and zeta potential in the presence of different GAGs were also evaluated. We used DLS and zeta potential changes to determine if there are any variations upon contamination of heparin with over-sulfated GAGs. Inclusion of the fluorophore in the liposomal bilayer was originally intended for study of fluctuations in fluorescence emission intensity as a function of the aggregation phenomenon. However, due to non-uniformity of the liposomal solution upon aggregation, fluorescence studies produced very variable results, and were thus removed from this study.

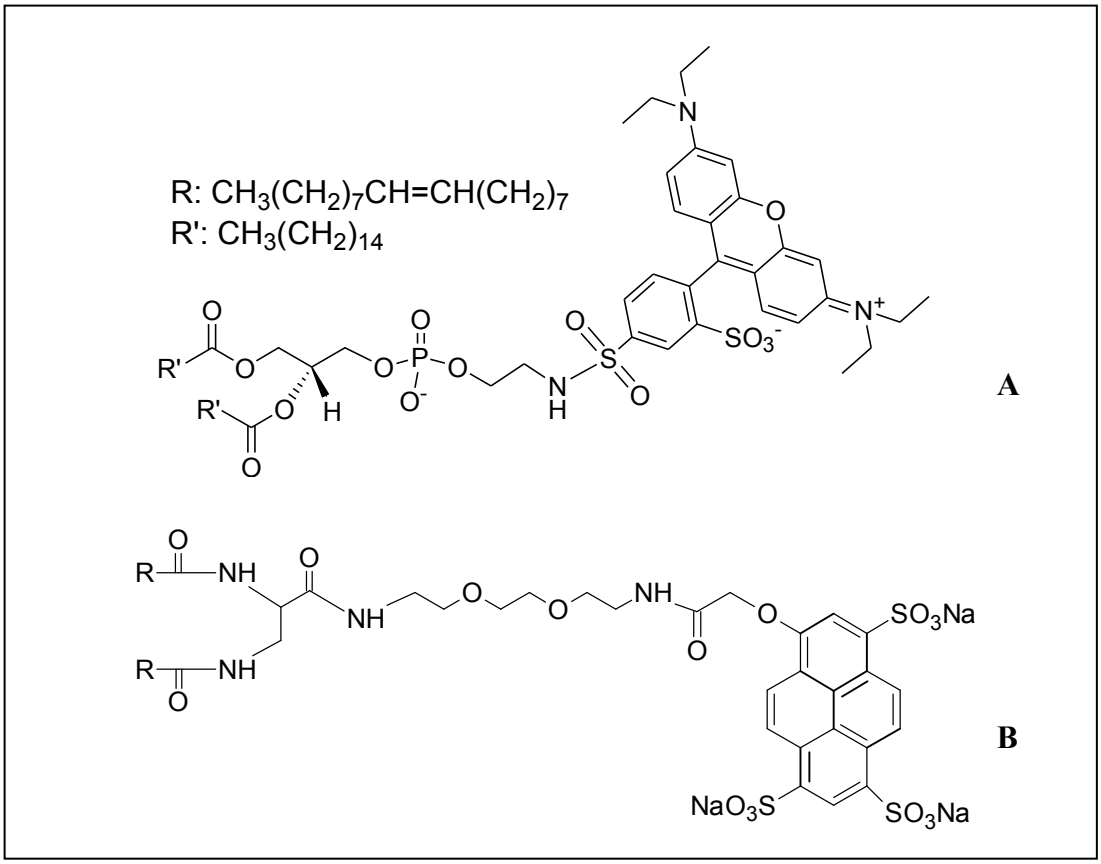

Figure 2.1. **Structures of rhodamine (A) and pyranine (B) lipids.**

Preparation of liposomes: We have previously shown that 100 nm diameter liposomes composed of 99 mol% POPC and 1 mol% fluorophore-conjugated lipid (either pyranine, rhodamine, or dansyl) are able to discriminate between various GAGs[21]. Although these liposomes undergo modulations in fluorescence intensity in the presence of GAGs only, we wish to utilize the tendency of these liposomes to undergo rapid changes in the aggregate diameter and zeta potential in the presence of GAG and divalent cations to develop a rapid screen for these contaminants. To achieve this, we have chosen Mg^{2+} as a flocculating agent[22], and have produced POPC liposomes of three diameters (50, 200, and 550 nm) and aggregated each of these in the presence of three concentrations (50, 170, and 500 nM) of each GAG of interest: heparin, over-sulfated heparin (OSH), over-sulfated chondroitin sulfate (OSCS), and over-sulfated dermatan sulfate (OSD). We demonstrate that high concentrations of Mg^{2+} aggregate liposomes in the presence of GAG, but not in the absence of GAG (as shown in Tables 2.5 and 2.6).

Mechanistic studies--liposomes selectively aggregate upon binding of different GAG species when Mg^{2+} is present, and liposome-GAG interactions influence the zeta potentials and diameters of overall assembly: Kim and Nishida had proposed that the divalent cation (Mg^{2+} in our case) form bridges between the negative phosphate groups of the phospholipid head groups[5]. This interaction shields the incoming GAGs from the negative charges on liposome surface, allowing them to bind to the positively charged choline[5], leading to the formation of aggregates (see Figure 2.2).

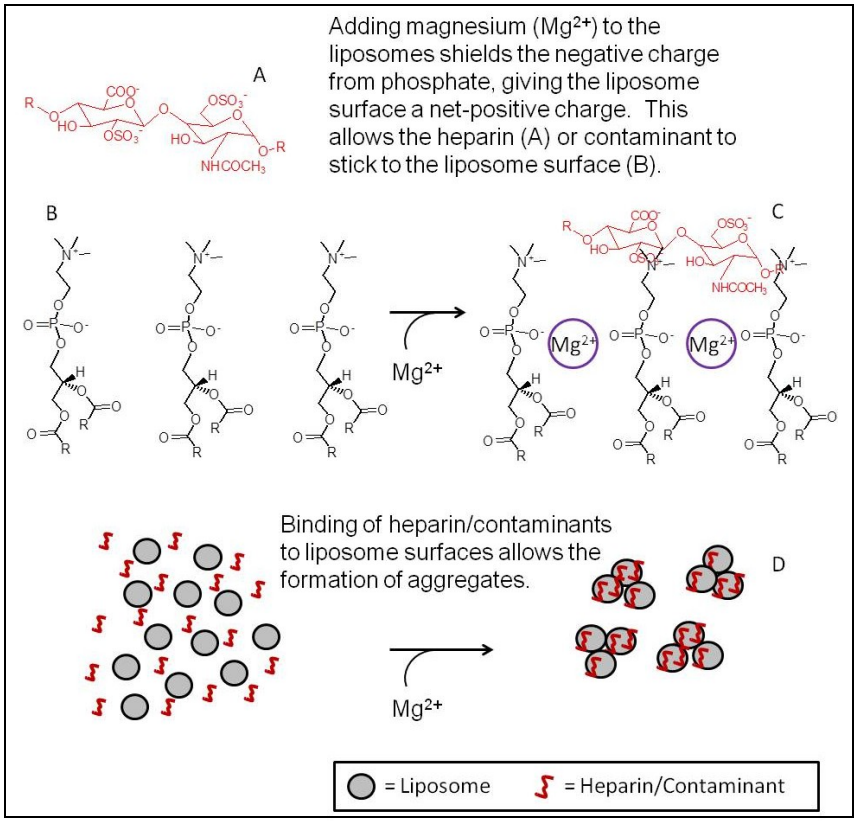

Figure 2.2. **The addition of Mg^{2+} allows liposomes to form strong interactions with heparin/contaminants (C), resulting in liposome aggregates (D).**

To study this effect, we used both DSPC-rhodamine liposomes and POPC-rhodamine liposomes (200 nm diameter) in the presence of Mg^{2+} only, in the presence of each GAG only (no Mg^{2+}), and finally in the presence of both GAG and Mg^{2+} (GAG concentration was held constant at 170 nM). Both diameters and zeta potentials of the resulting aggregates were measured. Results of these studies are as shown in Tables 2.5 and 2.6.

Table 2.5. **Diameters and zeta potentials of POPC-containing liposomes in the presence of GAG, with and without Mg^{2+}**

Formulation	Zeta potential (mV)	Diameter (nm)
Liposomes only	-13.3 ± 0.78	183.1 ± 8.01
Liposomes + Heparin	-11.6 ± 1.16	177.0 ± 3.94
Liposomes + OSH	-12.1 ± 0.80	174.4 ± 6.35
Liposomes + OSCS	-12.3 ± 0.37	186.8 ± 3.2
Liposomes + OSD	-12.2 ± 0.41	173.5 ± 4.45
Liposomes + Mg^{2+}	4.4 ± 0.61	179.5 ± 1.58
Liposomes + Mg^{2+} + Heparin	4.6 ± 0.58	540.8 ± 50.49
Liposomes + Mg^{2+} + OSH	4.7 ± 0.75	773.9 ± 78.54
Liposomes + Mg^{2+} + OSCS	3.2 ± 0.97	2098.6 ± 192.87
Liposomes + Mg^{2+} + OSD	3.7 ± 0.80	3325.8 ± 543.79

Table 2.6. **Diameters and zeta potentials of DSPC-containing liposomes in the presence of GAG, with and without Mg^{2+}.**

Formulation	Zeta potential (mV)	Diameter (nm)
Liposomes only	-11.8 ± 0.28	254.9 ± 90.97
Liposomes + Heparin	-11.4 ± 0.81	374.2 ± 61.16
Liposomes + OSH	-11.9 ± 0.44	445.9 ± 68.92
Liposomes + OSCS	-11.7 ± 0.43	429.4 ± 36.72
Liposomes + OSD	-12.7 ± 0.34	426.6 ± 58.89
Liposomes + Mg^{2+}	10.3 ± 0.91	397.7 ± 96.19
Liposomes + Mg^{2+} + Heparin	6.7 ± 1.11	2603 ± 189.51
Liposomes + Mg^{2+} + OSH	6.7 ± 1.08	1873 ± 162.66
Liposomes + Mg^{2+} + OSCS	-16.0 ± 0.62	2483 ± 200.76
Liposomes + Mg^{2+} + OSD	-2.7 ± 0.67	3489 ± 762.22

As the zeta potentials of both POPC and DSPC-containing liposomes do not appear to change significantly without the presence of Mg^{2+}, we conclude that the GAGs alone do not bind to the surface of liposomes, as has been previously reported[4]. However in contrast to previous studies[4], we find that excess Mg^{2+} does result in liposomal charge inversion[23], changing the zeta potential of the liposomes. It is likely that previous studies did not use divalent cations in sufficiently large excess to observe this effect. Consistent with previous findings, we note a significant change in the zeta potential upon the addition of both Mg^{2+} and GAG in the presence of DSPC liposomes; however this effect is negligible for POPC liposomes. Interesting to note is the drop in zeta potential of the DSPC aggregates to -16 mV in the presence of OSCS, 4 mV below that of the original liposomes. This effect likely results from overcharging of the liposome surface, due to excess charge from the OSCS[23]. Both liposomes experience significant changes in aggregate diameter in the presence of GAG and Mg^{2+}, and these diameter changes appear to be dependent on the species of GAG present, particularly for POPC liposomes. It must also be noted that previous studies by M. Krumbiegel and K. Arnold describe the measurement of zeta potential in the presence of liposomes aggregated by glycosaminoglycans, and they have found that this aggregation in no way interferes with the measurement of zeta potential[2].

Mechanistic studies—diameter and zeta potential of liposome aggregates reach saturation upon addition of sufficient concentrations of GAG: To determine how the aggregate hydrodynamic diameters and zeta potentials of both DSPC and POPC containing liposomes changed with increasing concentrations of each GAG, and to determine if there were any differences between GAGs at these concentrations, DSPC and POPC liposomes were incubated with heparin, over-sulfated chondroitin sulfate, over-sulfated dermatan sulfate, and over-sulfated heparin at eight concentrations (100 nM, 500 nM, 1 μM, 10 μM, 50 μM, 100 μM,

250 μM, and 500 μM). Results are summarized in Figure 2.3 below; each data point is the average of three collected aggregate diameters or zeta potential measurements. We note that some of the diameter measurements are outside the range which the Zetasizer Nano may accurately measure (5 x 10^3 nm diameter), however the purpose of these experiments was to investigate whether each species of GAG caused the eventual saturation of both aggregate diameters and zeta potentials, and if so above what concentration does this saturation take place. *Measurements are of interest in terms of general trend only*. Notable are the progression of aggregate diameters from small to quite large and then to small again for both DSPC and POPC containing liposomes, as concentration increases. This is consistent with theoretical analysis of McClements[24] and Guzey[25], according to which below a specific critical concentration of charged polymers (e.g., GAGs), the surface of the colloid particles (liposomes) will be incompletely covered by the polymer, resulting in an imbalance between attractive and repulsive forces acting on the colloidal particles. Below this critical concentration, these imbalances will allow sections of liposome surface coated with GAG to attract sections of neighboring liposomes which have not been so coated, resulting in aggregate formation. Above this critical concentration however, the surfaces of the colloidal particles will become saturated as the charged polymer forms a continuous coat on the surface, and allows the repulsive forces between the colloid particles in solution to become re-balanced, preventing significant aggregation. McClements[24] also notes that at concentrations much higher than the critical concentration may cause "depletion flocculation" due to excesses of polymer electrolyte in solution, which may be sufficient to overcome the repulsive forces between colloid particles. This depletion flocculation may be one explanation for the sudden increase in diameter of the POPC liposomes in presence of 500 μM over-sulfated heparin.

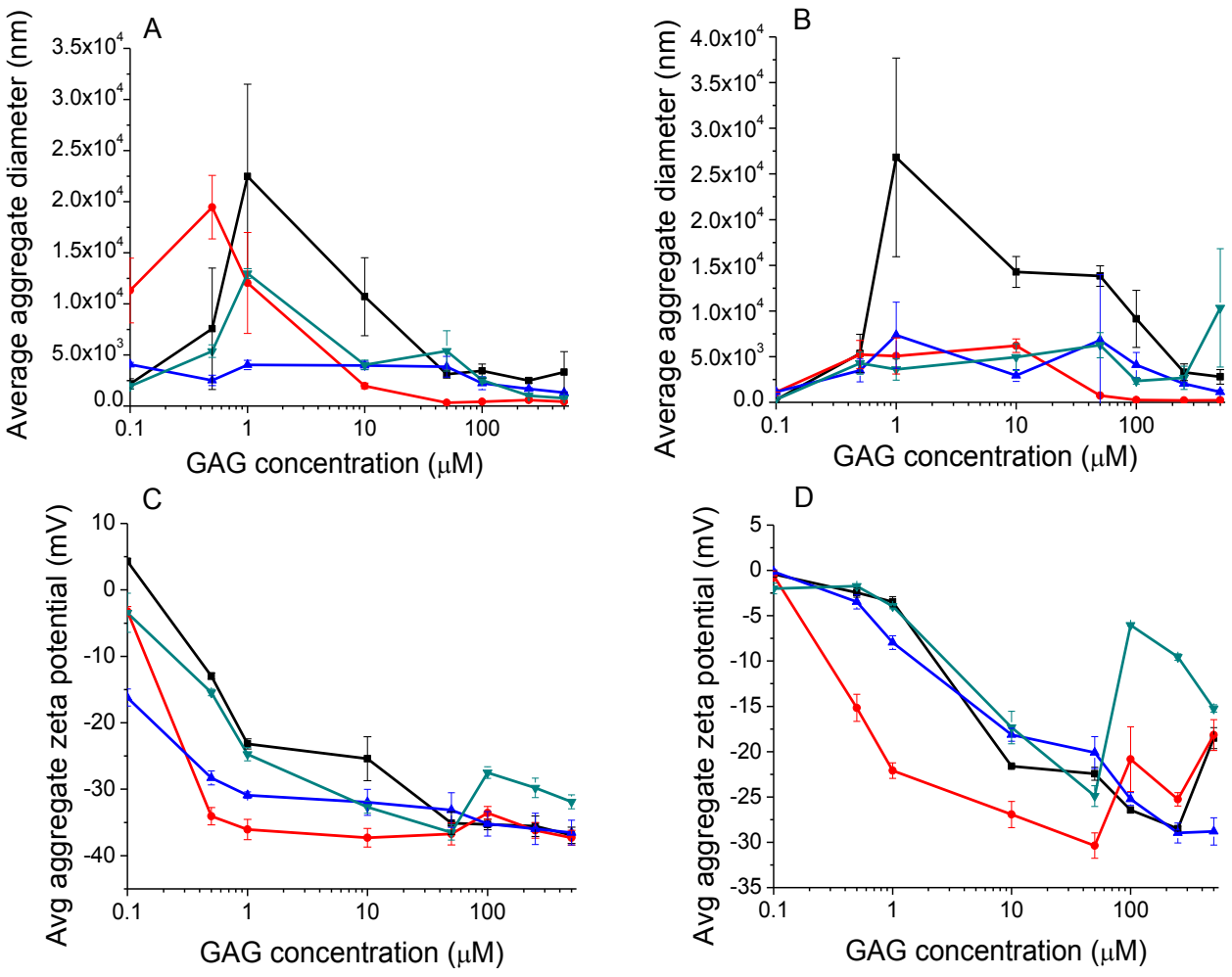

Figure 2.3. **DSPC and POPC aggregate diameters and zeta potentials with increasing GAG concentration.** Average aggregate diameters of DSPC liposome aggregates (**A**) and POPC liposomes (**B**); and average zeta potentials of DSPC liposome aggregates (**C**) and POPC liposomes (**D**) in the presence of increasing concentrations of heparin (black squares), over-sulfated chondroitin sulfate (blue triangles), over-sulfated dermatan sulfate (red circles), and over-sulfated heparin (green upside-down triangles).

For the DSPC containing liposomes, as the aggregate diameter becomes saturated, the zeta potential becomes likewise saturated (at high GAG concentration), and does not change appreciably at higher concentrations. For the POPC containing liposomes however, there is a tendency for the zeta potential to reach a minimum, and then return to smaller absolute values at

higher concentrations. This difference is clearly due to the difference in composition of the fatty acid tails of the liposomal lipids. In the case of DSPC, both tails are constituted of saturated (stearic acid) and thus they will pack more efficiently (*vis a vis* the palmitoyl and oleyl tails of POPC) within the lipid phase. These differences will impart greater rigidity to the head groups of the DSPC liposomes, and thus will allow homogeneous distribution of GAG induced aggregates of the liposomes. The above feature is unlikely to prevail in the case of POPC liposomes. It is worth noting that other studies involving changes in the liposome's zeta potential upon addition of GAGs and divalent cations were focused on lipid bilayers, harboring saturated lipids (DMPC, DLPC, and egg lecithin)[2,4], and these studies produced zeta potential results similar to our DSPC liposomes. However, irrespective of the underlying physical forces responsible for our observed experimental data of Figure 2.2, it is evident that POPC and DSPC formulated liposomes elicit marked differences in their aggregational states and zeta potentials as a function of different types of GAGs. Whether or not such features are intimately involved in discriminatory changes in the liposome's resident fluorescence probes[21] as a function of different types of GAGs are currently being investigated in our laboratory, and we will report these findings subsequently.

TEM images demonstrate differential aggregation of liposomes in the presence of different GAG species: The diameters of the POPC liposomes and DSPC liposomes in the presence of Mg^{2+} only were compared with those in the presence of heparin, over-sulfated chondroitin sulfate, over-sulfated dermatan sulfate, and over-sulfated heparin. Figure 2.4 presents the TEM images of the POPC liposomes in the presence of Mg^{2+} alone (panel **A**) and in the presence of Mg^{2+} and different GAG species. Figure 2.5 presents the corresponding TEM images involving DSPC liposomes. In each figure, panels **A**-**E** are images of liposomes magnified 5,000 times, and panel **F** is an image of one OSCS aggregate magnified 25,000 to

show detail of the stacked liposomes. The TEM images of Figures 3 and 4 clearly reveal that the liposomes are aggregated in the presence of Mg^{2+} and different GAG species, and such aggregates are asymmetrical and polydisperse. However, notable in these TEM images is the presence of considerably larger aggregates in the presence of over-sulfated GAGs as compared to those observed in the presence of heparin. Also notable is the apparent size in these images; it is evident that the liposomes and aggregates have collapsed during the preparation of the samples. It is therefore necessary to consider these sizes as relative; *aggregate images should only be compared with images of the liposomes in the presence of* Mg^{2+} *only.*

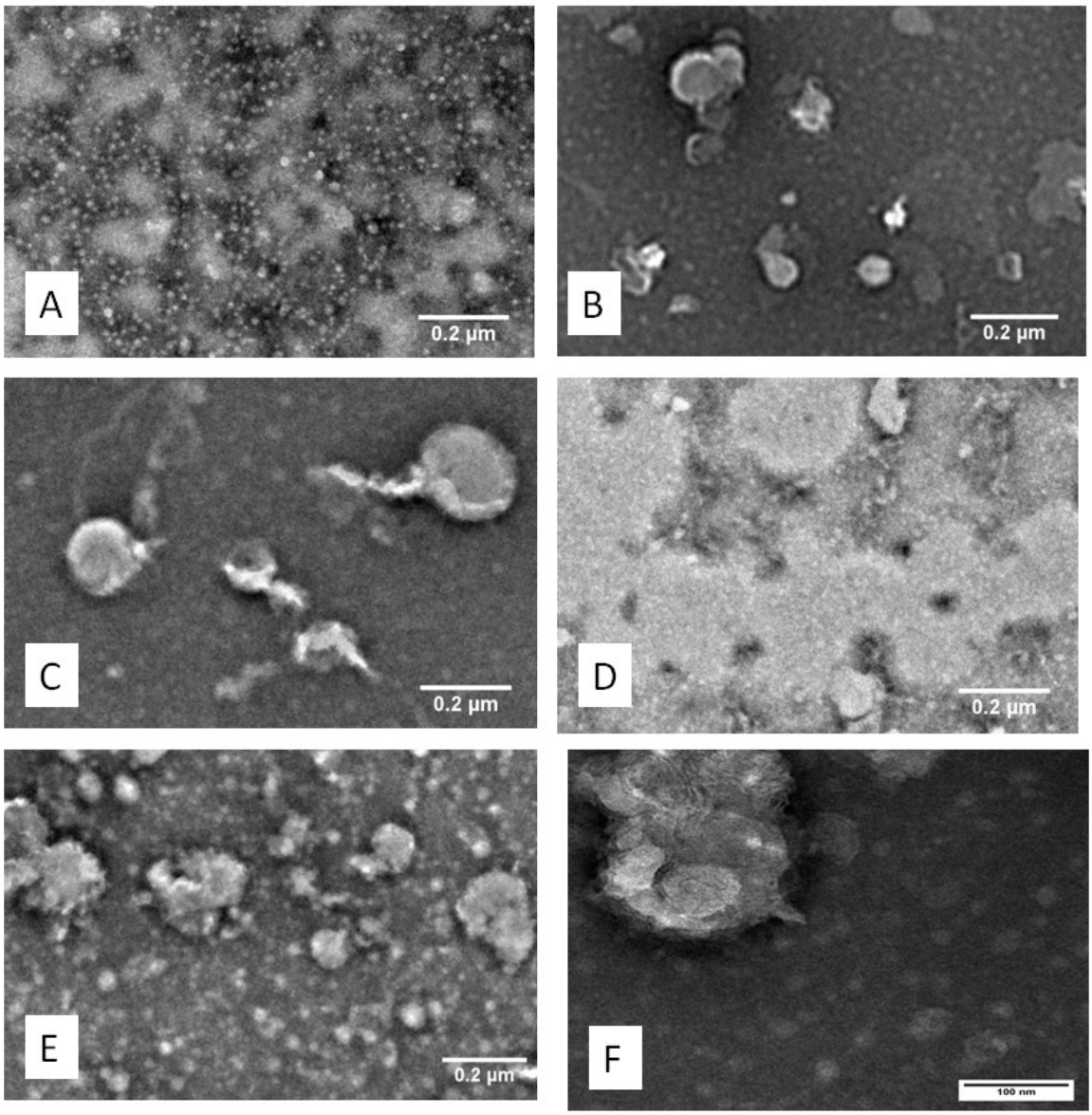

Figure 2.4. **TEM images of POPC liposomes in presence of different GAGs**. TEM images of POPC liposomes with Mg^{2+} only (**A**): red arrows denote individual liposomes), and aggregated in the presence of heparin (**B**), over-sulfated chondroitin sulfate (**C**), over-sulfated dermatan sulfate (**D**), and over-sulfated heparin (**E**) magnified 5,000x. Notable is the increase in average size of the aggregates of over-sulfated GAGs over heparin, as well as the polydispersity of these aggregates. Shown also is an image of liposomes aggregated with over-sulfated chondroitin sulfate magnified 25,000x (**F**). Clearly shown are the clustered bilayers in one section of the aggregate, denoted by the red arrows.

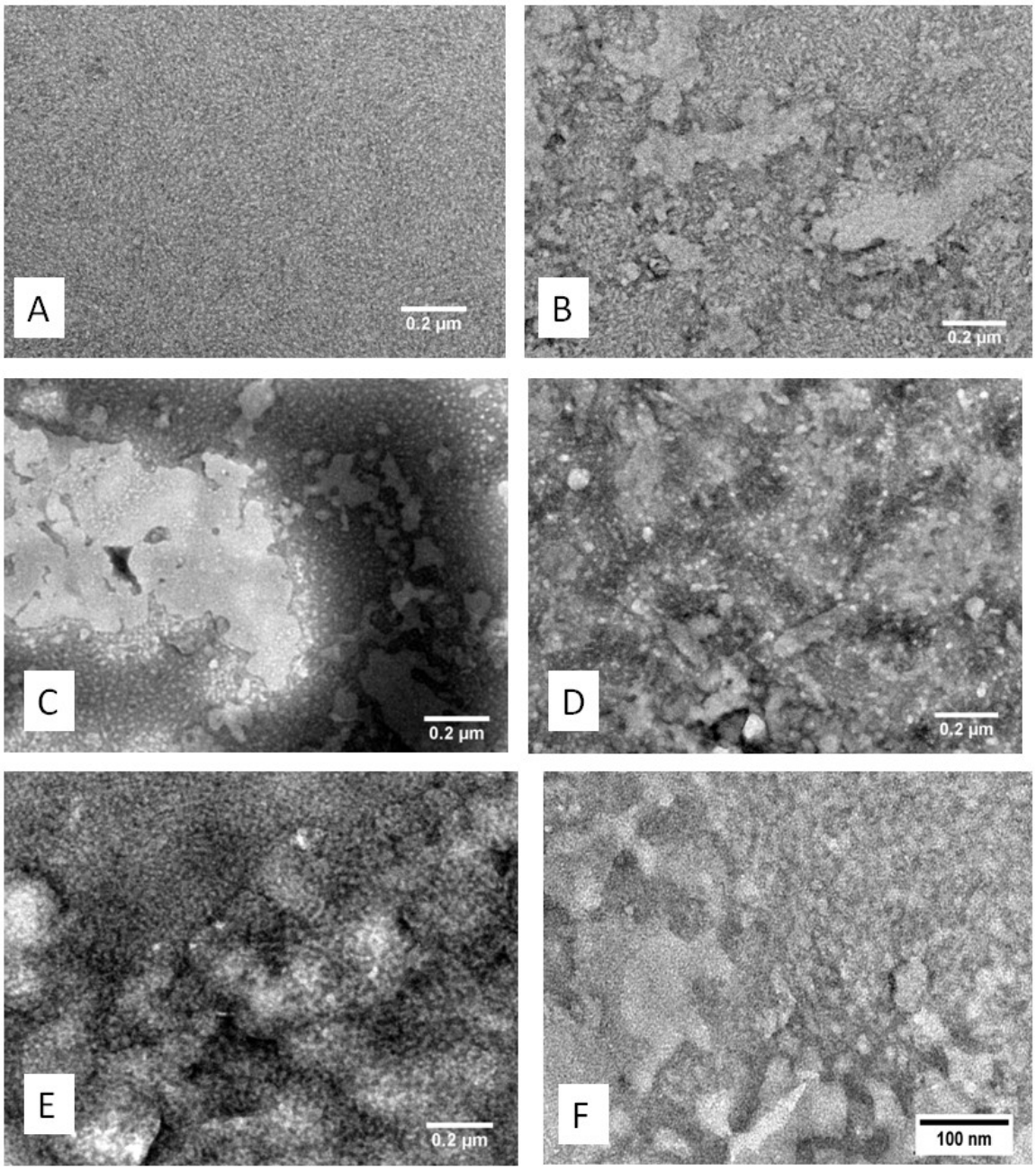

Figure 2.5. **TEM images of DSPC liposomes in presence of different GAGs.** TEM images of DSPC liposomes with Mg^{2+} only (**A**), and aggregated in the presence of heparin (**B**), over-sulfated chondroitin sulfate (**C**), over-sulfated dermatan sulfate (**D**), and over-sulfated heparin (**E**) magnified 5,000x. Notable is the the polydispersity of these aggregates. Shown also is an image of liposomes aggregated with over-sulfated chondroitin sulfate magnified 25,000x (**F**). Visible are the closely associated liposomes within a single aggregate.

Differential scanning calorimetry demonstrates intrinsic and differential stability of liposomes upon binding of GAGs to liposomes: Having established that the liposomes are aggregated in the presence of both Mg^{2+} and different GAG species, it was of interest to investigate whether the above "effectors" modulated the intrinsic stability of liposomes. To probe this, we performed DSC studies for melting of DSPC liposomes in the presence of Mg^{2+} and two concentrations (i.e., 1 μM and at 250 μM) of each different GAG species. The DSC endotherms reveal that the presence of Mg^{2+} and GAGs influence both the melting temperature (T_m value) of the liposomes as well as the area under the peaks (measure of the enthalpic changes between native and denatured/melted forms of the liposomes; see Figure 2.6). The observed shifting of the 250 μM trace to a lower relative heat rate reflects the increase of dissolved solutes over the control[26], and the widening and flattening of the DSC trace with increasing GAG concentration, accompanied by a rightward shift in T_m, indicates that structural changes are taking place within the bilayers of the liposomes (increased T_m), and that these changes are dispersed somewhat unevenly within the "population" of the liposomes (widening and flattening of the T_m peak)[26]. To our further interest, we observed that the second DSC scan (performed after cooling the heated sample after the first scan) yielded essentially identical T_m values in the presence of different GAG species, albeit the enthalpic changes were slightly decreased (data not shown). This suggests that there is a marked reversibility in the organizational states of the liposomes, and such feature is intrinsic to the nature of the GAG species. Table 2.7 summarizes the T_m values and enthalpic changes under our selected experimental conditions. A perusal of the data of Table 2.6 reveals that among different GAGs used herein, heparin and oversulfated heparin exhibit the least and most stabilizing influence on the liposomes as evident by their corresponding enthalpic changes.

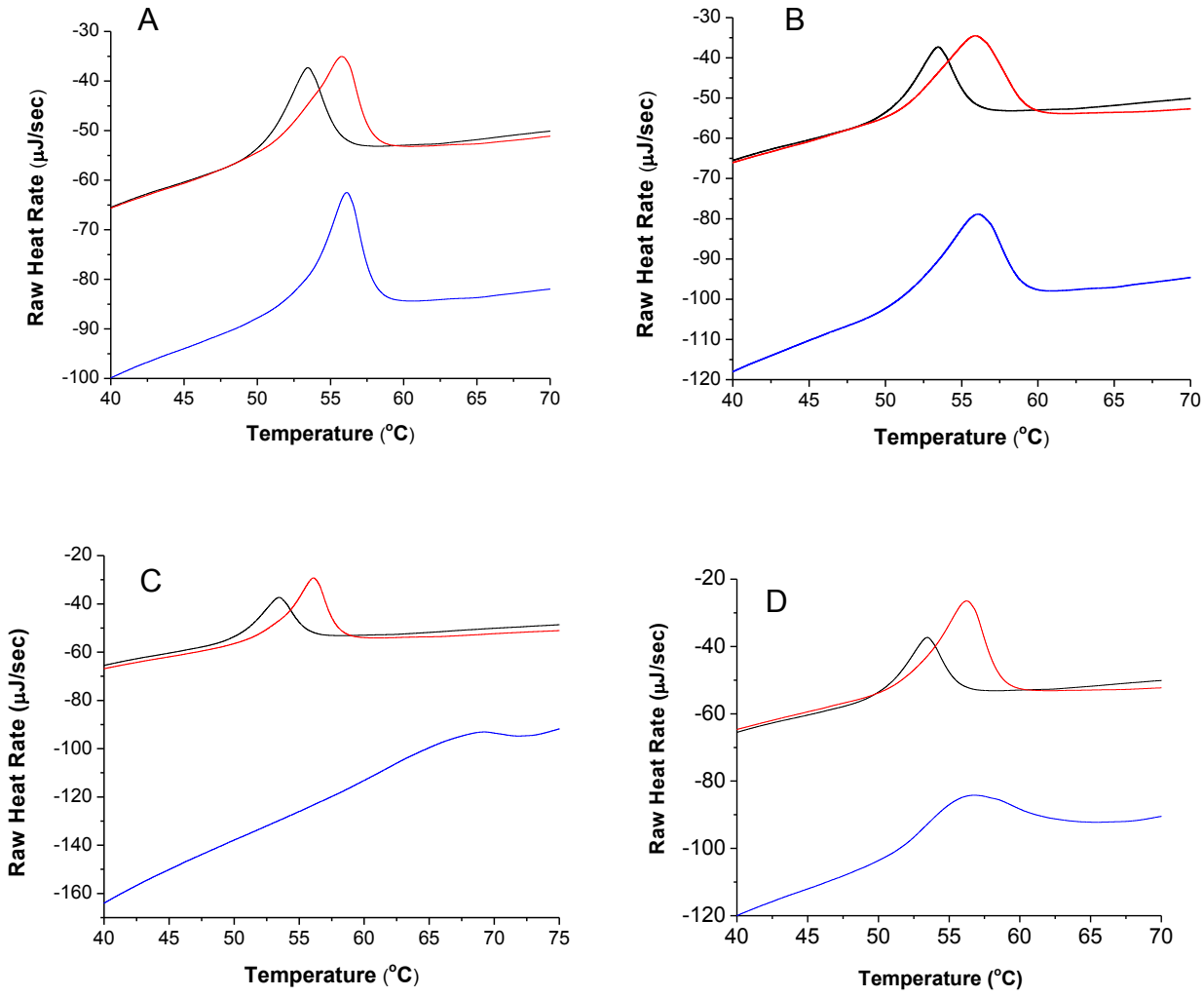

Figure 2.6. **Differential scanning calorimetry of DSPC liposomes with GAGs.** DSC traces of DSPC liposomes with heparin (**A**), over-sulfated chondroitin sulfate (**B**), over-sulfated dermatan sulfate (**C**), and over-sulfated heparin (**D**): liposomes only (black trace), GAG at 1 μM (red trace), GAG at 250 μM (blue trace).

We conclude from these studies that binding of GAGs and Mg^{2+} to the liposomal bilayer causes the liposomal assembly to become more stable, and thus requires more heat energy (enthalpic changes) to bring it to the fully disorganized (melted) states with concomitant increase in the transition temperature. We believe the above feature is due to the intercalation of the GAGs between the individual phosphocholine molecules, thus forcing the exclusion of

intervening water molecules and thus allowing the liposomal lipids to pack more efficiently in their native states.

Table 2.7. **Heat required for liposome melting (μJ)**

GAG	Liposomes only	1 μM	250 μM
Heparin	1709.1	2814.9	2887.1
OSCS	1709.1	3338.2	3367.5
OSD	1709.1	3693.2	2793.5
OSH	1709.1	3653.9	3853.4

Mechanistic studies--there is an inverse relationship between the percent change of aggregate diameter and the percent change of aggregate zeta potential as the concentration of GAG increases, independent of liposome diameter: For studies comparing the relative contribution of liposome diameter and GAG concentration to the overall average diameter and zeta potential changes of the resulting aggregates, only POPC liposomes were used. This is due to the high variability of the DSPC liposomes' diameters, which is clear from results shown in Table 2.6 (the standard deviation for the diameter of these liposomes alone as measure by DLS is 36% of their diameter). Additionally, DLS shows the presence of both very large (>1000 nm) and very small (<50 nm) particles in the DSPC liposome solution. Due to this difficulty in controlling the liposome diameter, DSPC liposomes have been excluded from this, as well as the contamination studies.

As one considers the percent change of each over-sulfated contaminant relative to heparin at each concentration, while holding the diameter of the liposomes constant, an interesting pattern emerges: there appears to be an inverse relationship between the percent change in aggregate diameters, and the percent change in aggregate zeta potential (i.e.—as the percent

change in diameter goes down with increasing GAG concentration, the percent change in zeta potential becomes greater with increasing GAG concentration). These results are summarized in Figure 2.7. Notable from this figure is that at 50 nM concentration (represented by a black trace with black squares), OSCS always produces the greatest change in aggregate diameter, regardless of the liposomes' starting diameter. At 170 nM GAG, OSD causes the greatest changes in aggregate diameter, and at 500 nM GAG results depend on the starting liposome diameter. Reasons for this are unclear, and will require further investigation. However it is obvious from these results that as GAG concentration increases, overall percent change decreases. Results for percent change in aggregate zeta potential are also very consistent for liposomes of all diameters tested: as GAG concentration increases, the magnitude of percent change in aggregate zeta potential also increases. We hypothesize the mechanism for this may be due to differences in the percent overall coverage of the liposome surface by the GAG. When the concentration of GAG in solution is relatively low relative to the total lipid concentration in solution (~200 nM), the liposomal surface is covered with GAG to a lesser extent, resulting in greater imbalance between the attractive and repulsive colloidal forces. As such, the number of liposomes which form aggregates will be dependent on the charge density of the GAG present on the liposome surface, as well as the surface area between oppositely charged sections of each bilayer (a function both of liposome diameters and the percent of surface area covered). However, as the concentration of GAG in solution increases, the surface of each liposome bilayer will be covered to a greater extent, which will not only begin to re-balance the repulsive forces between them in solution, but it will also reduce the amount of available surface area for aggregation between liposomes. This will reduce the percent change in the aggregate diameter (as fewer liposomes will be able to aggregate together), as well as increasing the change

observed in the zeta potentials (as a function of the amount and charge density of the GAG bound). Studies to confirm this mechanism are currently being undertaken.

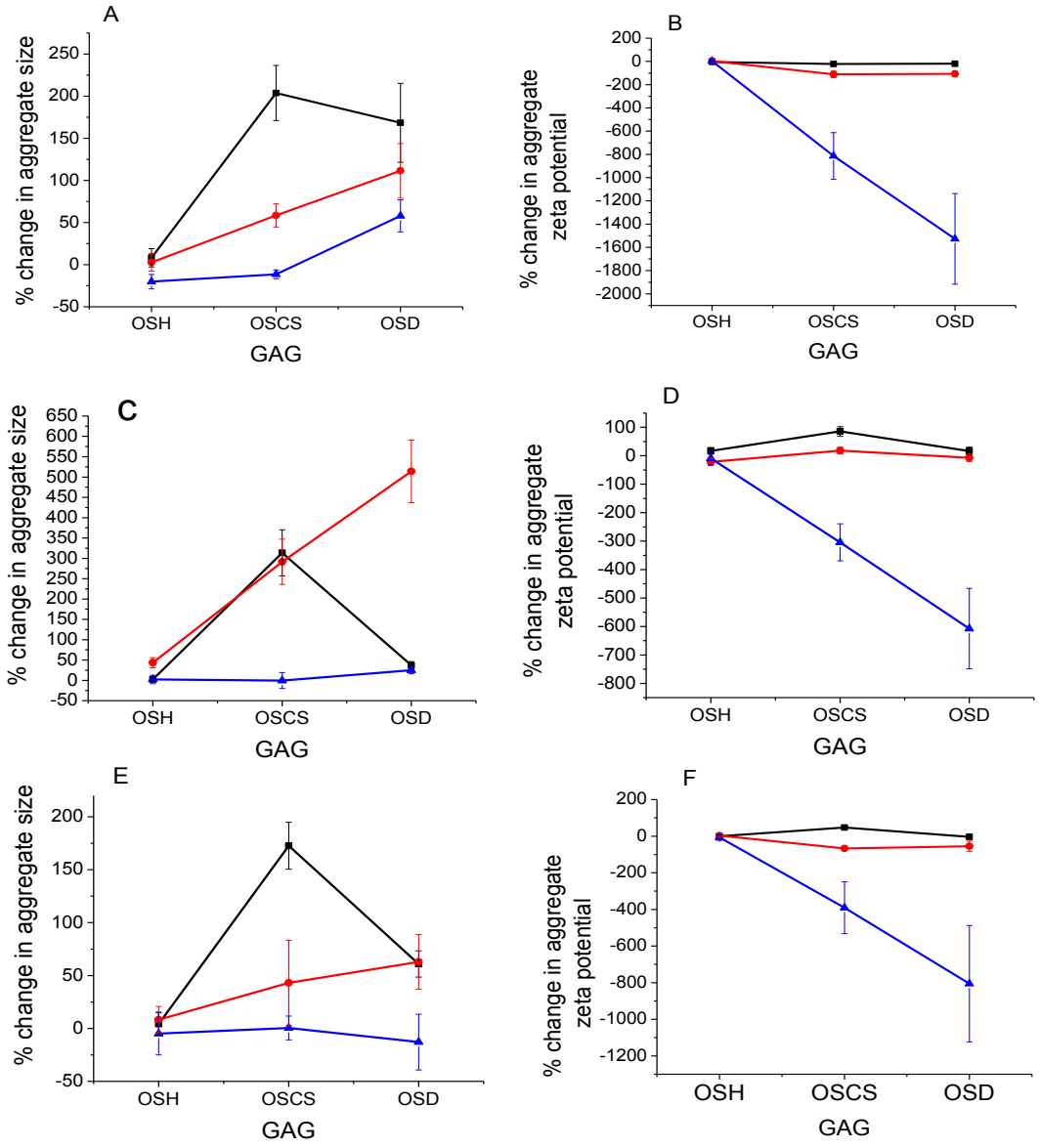

Figure 2.7. **Percent changes for 50 nm diameter liposomes (A, B), 200 nm liposomes (C, D), and 500 nm liposomes (E, F).** Shown are percent changes in aggregate diameter (A, C, E) and percent changes in aggregate zeta potential (B, D, F). Concentrations used for this study are 50 nM (black squares), 170 nM (red circles), and 500 nM (blue triangles).

Contamination studies demonstrate that changes in diameter and zeta potential of POPC liposomes can distinguish small changes in GAG composition: The insights gained from the previous studies were employed to probe whether the presence of low concentrations of over-sulfated contaminants in a heparin sample could be detected using DLS and zeta potential measurements of liposomal aggregates. We chose to incubate 200 nm diameter liposomes with 170 nM contaminated heparin (produced the greatest percent changes in diameter), and 500 nm diameter liposomes with 500 nM contaminated heparin (produced the greatest percent changes in zeta potential). Heparin samples in 2008 were found by Beyer, et al, to be contaminated in the range of 0.5% to 28% by weight[9]. As such, for both of these liposome/GAG concentration combinations, eight contamination levels were prepared: 0.5, 1.0, 2.5, 5, 10, 15, 20, and 30 mol% contaminations with each over-sulfated contaminant. Each combination was measured for changes in aggregate diameter and zeta potential by DLS.

Analysis of variance ($\alpha = 0.05$) was conducted for each of these sets of data (see statistical results in Appendix B). Included in this analysis is a comparison of means for each contamination level against heparin alone using Dunnett's method for pairwise comparisons[27]. This method allows us to compare each contamination level to the control (heparin only) while controlling the family-wise error of all comparisons together to 0.05. Results for both 200 nm and 500 nm diameter liposomes indicate that OSH could not be consistently detected, and thus will be eliminated from further discussion.

Results for OSCS and OSD are far more promising. Analysis of variance indicates that for the 200 nm liposomes, changes in average aggregate diameter could detect contamination by OSCS at concentrations from 5 mol% to 30 mol%, and OSD contamination from concentrations of 10 mol% to 30 mol%. Changes in aggregate zeta potential could not consistently detect

contamination. Results for the 500 nm diameter liposomes indicate detection of OSCS contamination at concentrations from 1 mol% through 30 mol% by changes in zeta potential, and from 2.5 mol% to 30 mol% by changes in aggregate diameter. OSD could be detected by this method from 10 mol% to 30 mol% by changes in zeta potential, and from 0.5 mol% to 30 mol% by changes in aggregate diameter. (For detailed statistical results please see Appendix B). If we consider percent heparin contamination by weight, the lowest contamination level we can detect using these methods is approximately 1.6% by weight of OSD, and 2.2% by weight of OSCS, making it an attractive screening tool for heparin intended for clinical use. These calculations are based on the estimated molecular weights of heparin, over-sulfated chondroitin sulfate, and over-sulfated dermatan sulfate, summarized in Table 2.8 below.

Table 2.8. **Molecular weight of GAGs (g/mol)**

GAG	Liposomes only
Heparin	13,500
OSCS	29,560
OSD	42,529

It must be stated that despite the relative consistency and significance of the DLS diameter measurements, the presence of fluorescence, high polydispersity, and large precipitating particles in the sample lead us to favor the use of zeta potential for measurements of over-sulfated heparin contaminants, as these measurements are unaffected by any of the aforementioned concerns.

A comparison of current methods used to detect heparin quality reported in 2011 by Alban, et al., has been very revealing. The authors reported that while NMR and other spectroscopic methods are useable, other heparin mimetic may cause deviating results, and thus

accurate detection of OSCS in heparin will be in large part dependent on the skill of the individual running the tests, and only currently known heparin contaminants may be recognized[18]. Additionally, the PT and aPTT, while they are able to detect overall heparin quality, cannot actually detect contamination, and have an LOD of 3%[18]. Further, it must be recognized that no reported adverse effects were observed from enexoparin contaminated with up to 7% OSCS[15]. Based on this, the analysis by Alban and Beyer of original contaminated samples[9,18], and the above statistical analysis of our data, we believe that zeta potential measurements combined with DLS diameter measurements of POPC based liposomes incubated with heparin samples at 170/500 nM and excess Mg^{2+} may be a rapid and economical initial screen for contamination in these samples.

Conclusions

We have demonstrated that liposomes containing 1 mol% lissamine-rhodamine lipid form aggregates of varying diameters and zeta potentials depending on the species and concentration of GAG present. This has been verified by TEM studies. We have shown that organizational states of the liposome bilayers are influenced by the presence of GAG and excess Mg^{2+}, resulting in a stabilizing effect, and the magnitude of this effect is also dependent on GAG species and concentration present. Additionally, there is an inverse relationship between the percent change of aggregate diameter and percent change of aggregate zeta potential, as a function of GAG concentration in solution. Finally, the presence of small concentrations of over-sulfated contaminants in heparin samples cause statistically significant variations in the average aggregate diameter and zeta potential POPC liposomes. Significant variations of POPC liposome aggregate zeta potentials enables detection of over-sulfated chondroitin sulfate and over-sulfated dermatan sulfate at 1 mol% and 0.5 mol % (2.2% w/w and 1.6% w/w,

respectively). Based on the work of Bayer, the use of this method would have been able to detect the contaminants in the majority of the original heparin samples which caused allergic reactions and deaths of patients in 2007 and 2008[9]. These results offer insight into the potential of these interactions for a rapid and economical screen for the presence of over-sulfated contaminants in heparin or other drugs.

Acknowledgement

This research was supported by NIH grants 1R01 CA CA113746, 1R01 CA 132034 to SM and DKS and NSF grant DMR 1005011 to SM. The ITC and the DSC instruments were purchased through the NSF ARRA award CBET-0959422.

References

(1) Zhang, F.; Zhang, Z.; Linhardt, R. J. *The Handbook of Glycomics*; Elsevier: London, UK, 2009.

(2) Krumbiegel, M.; Arnold, K. *Chemistry and Physics of Lipids* **1990**, *54*, 1-7.

(3) Satoh, A.; Toida, T.; Yoshida, K.; Kojima, K.; Matsumoto, I. *FEBS Letters* **2000**, *477*, 249-252.

(4) Zschornig, O.; Richter, W.; Paasche, G.; Arnold, K. *Colloid Polymer Science* **2000**, *278*, 637-646.

(5) Kim, Y. C.; Nishida, T. *J Biol Chem* **1977**, *252*, 1243-1249.

(6) Voet, D.; Voet, J. *Biochemistry*; 3rd ed.; John Wiley & Sons, Inc.: Hoboken, NJ, 2004.

(7) Linhardt, R. J. *Journal of Medicinal Chemistry* **2003**, *46*, 2551-2564.

(8) Maruyama, T.; Toida, T.; Imanari, T.; Yu, G.; Linhardt, R. *Carbohydrate Research* **1998**, *306*, 35-43.

(9) Beyer, T.; Matz, M.; Brinz, D.; Radler, O.; Wolf, B.; Norwig, J.; Baumann, K.; Alban, S.; Holzgrabe, U. *Eur J Pharm Sci* **2010**, *40*, 297-304.

(10) Pan, J.; Qian, Y.; Zhou, X.; Pazandak, A.; Frazier, S. B.; Weiser, P.; Lu, H.; Zhang, L. *Nature Biotechnology* **2010**, *28*, 203-207.

(11) Li, B.; Suwan, J.; Martin, J. G.; Zhang, F.; Zhang, Z.; Hoppensteadt, D.; Clark, M.; Fareed, J.; Linhardt, R. J. *Biochemical Pharmacology* **2009**, *78*, 292-300.

(12) Pan, J.; Qian, Y.; Zhou, X.; Lu, H.; Ramacciotti, E.; Zhang, L. *Journal of Biological Chemistry* **2010**, *285*, 22966-22974.

(13) Zhang, Z.; Li, B.; Suwan, J.; Zhang, F.; Z., W.; Liu, H.; Mulloy, B.; Linhardt, R. *Journal of Pharmaceutical Sciences* **2009**, *98*, 4017-4026.

(14) Kang, Y.; Gwon, K.; Shin, J. H.; Nam, H.; Meyerhoff, M.; Cha, G. *Analytical Chemistry* **2011**, *83*, 3957-3962.

(15) Bairstow, S.; McKee, J.; Nordhaus, M.; Johnson, R. *Analytical Chemistry* **2009**, *288*, 317-321.

(16) Wang, L.; Buchanan, S.; Meyerhoff, M. *Analytical Chemistry* **2008**, *80*, 9845-9847.

(17) Sommers, C.; Mans, D.; Mecker, L.; Keire, D. *Analytical Chemistry* **2011**, *8*, 3422-3420.

(18) Alban, S.; Luhn, S.; Schiemann, S.; Beyer, T.; Norwig, J.; Schilling, C.; Radler, O.; Wolf, B.; Matz, M.; Baumann, K.; Holzgrabe, U. *Anal Bioanal Chem* **2011**, *399*, 605-620.

(19) Bertozzi, C. R.; Freeze, H. H.; Varki, A.; Esko, J. D. *Glycans in biotechnology and the pharmaceutical industry*; Cold Spring Harbor Laboratory Press: Cold Spring Harbor, NY, 2009.

(20) Nagasawa, K.; Uchiyama, H.; Wajima, N. *Carbohydrate Research* **1986**, *158*, 183-190.

(21) Nyren-Erickson, E. K.; Haldar, M. K.; Gu, Y.; Qian, S. Y.; Friesner, D. L.; Mallik, S. *Analytical Chemistry* **2011**, *83*, 5989-5995.

(22) Semerjian, L. A., G. M. *Advances in Environmental Research* **2003**, *7*, 389-403.

(23) Hsiao, P. Y. *J Phys Chem B* **2008**, *112*, 7347-7350.

(24) McClements, D. J. *Langmuir* **2005**, *21*, 9777-9785.

(25) Guzey, D.; McClements, D. J. *Adv Colloid Interface Sci* **2006**, *128-130*, 227-248.

(26) Gabbott, P. *Principles and applications of thermal analysis*; Blackwell Pub.: Oxford ; Ames, Iowa, 2008.

(27) Mendenhall, W.; Sincich, T. *A second course in statistics : regression analysis*; 7th ed.; Pearson Education: Boston, 2012.

This paper has been published:

Nyren-Erickson, E. K.; Haldar, M. K.; Totzauer, J. R.; Ceglowski, R.; Patel, D. S.; Friesner, D. L.; Srivastava, D. K.; Mallik, S. Glycosaminoglycan-Mediated Selective Changes in the Aggregation States, Zeta Potentials, and Intrinsic Stability of Liposomes. *Langmuir* **2012**, *28*, 16115-16125

PAPER 3. URINARY CONCENTRATIONS OF ADAM 12 FROM BREAST CANCER PATIENTS PRE- AND POST-SURGERY VS. CANCER-FREE CONTROLS: A CLINICAL STUDY FOR BIOMARKER VALIDATION

Abstract

The ADAMs (A Disintegrin and Metalloproteinases) are a family of 35 multi-domain, zinc-dependent metalloproteinase enzymes. ADAM isozyme 12 (ADAM 12) has been previously associated with the onset and progression of breast cancer, and elevated levels of the secreted form (ADAM 12-S) have been previously found in the urine of breast cancer patients. Aims of the current study are: **1**) establish the viability of urinary ADAM 12 as a screening marker for breast cancer, and **2**) explore the effects of surgical tumor removal on the levels of urinary ADAM 12. A total of 68 patients have been recruited for this study, including 37 patients diagnosed with cancer, and 31 age-matched controls. Commercially available ELISA kits for ADAM 12 were used to quantify the presence and concentration of this enzyme in the urine from cancer patients with ductal carcinoma *in situ* (DCIS) and invasive breast cancer (IBC) both prior to any treatment and approximately two weeks following surgery, as well as from controls. We find no statistically significant differences between the concentrations of ADAM 12 in the urine of breast cancer patients prior to treatment and that of their age-matched controls; however the concentration of ADAM 12, both alone and as a function of urine total protein, are significantly elevated following surgery ($p < 0.0001$). Patients who underwent a mastectomy have significantly higher urinary ADAM 12 concentrations than those who underwent a lumpectomy (significant at $p = 0.0271$). Based on these results, a screen for urinary ADAM 12 is unlikely to prove useful for breast cancer diagnosis.

Introduction

Breast cancer is currently the second leading cause of cancer deaths among women in the United States (second only to lung cancer), and it is now estimated that in the U.S. one in eight women will be diagnosed with breast cancer during her lifetime[1]. However, if breast cancer is detected during its earlier stages, the 5-year survival rate may be as high as 93%[**] (at stage 0); when detected at stage IIIB and later, 5-year survival rate drops below 50%[2], making early detection of breast cancer essential for favorable prognosis. Blood-based antigens currently measured to screen for breast cancer include (but are not limited to) cancer antigen 15-3 and 27.29 (CA15-3, CA27.29), carcinoembryonic antigen (CEA), and HER2/neu[3,4]; however these show little potential for early detection[5]. Recent studies have begun exploring the potential of urinary biomarkers for breast cancer detection[6,7], and among those studied are the ADAM proteases, particularly ADAM 12.

The ADAMs (A Disintegrin and Metalloproteinases) are a family of 35 multi-domain, zinc-dependent metalloproteinase enzymes. ADAMs are usually membrane bound (although some isozymes have secreted forms, including ADAM-9[8], -10[9], -12[10] and -28[11]), and their physiological roles include extracellular matrix restructuring[12-14], to cell adhesion[15-17], to cell-surface protein processing[18-20]. ADAM 12, which is transcribed as both a membrane bound and a secreted form, has roles in cell adhesion and matrix restructuring during cell differentiation[15-17,21], and also has regulatory functions[22] in healthy tissues. ADAM 12 has also been associated with development and progression of a number of disease states, including arthritis[23], cardiac hypertrophy[24], liver fibrogenesis[25], and various cancers, including bladder [26], lung [27], brain [28] and breast[29].

[**] These numbers reflect death from all causes.

One study in 2004 indicated a strong correlation between excretion of urinary ADAM 12-S (the short, secreted form of the enzyme), and breast cancer status and stage[29]. This report concluded that patients with ductal carcinoma *in situ* (DCIS), invasive breast cancer (IBC), and metastatic breast cancer had significantly higher levels of ADAM 12-S present in their urine than controls (i.e. patients with "no discernible disease")[29]. The report further concluded that only 15% of the control subjects had detectable levels of ADAM 12 present in their urine, while 82%, 86%, and 85% of patients with DCIS, IBC and metastatic disease, respectively, were positive for the presence of ADAM 12-S[29]. These results strongly suggest that a urine screen for the presence of ADAM 12 would prove especially useful for the diagnosis of breast cancers, stage DCIS and later.

The aims of the current study are twofold: **1**) establish the viability of urinary ADAM 12 as a screening marker for breast cancer, and **2**) explore the effects of surgical tumor removal on the levels of urinary ADAM 12. Our primary objective is to establish a simple, practical screening test for the early detection of breast cancer. As such, we have chosen to utilize commercially available ELISA kits for urinary ADAM 12 screening: we reason that they are a well accepted technology, which will provide reliable, reproducible results in a clinic setting.

Materials and methods

Ethics review and approval: This study was conducted in compliance with the Helsinki Declaration. The protocol, informed consent form, and laboratory manuals for this study were reviewed and approved by the Sanford Health Institutional Review Board in compliance with its Federalwide Assurance (#00016819). All patients' participation was voluntary, and all enrolled participants were given the right to refuse or exit the study at any time. Participants' were given a unique study number; and therefore their specimens and related medical information were de-

identified. Participant's study related medical record information was protected in accordance with HIPAA regulation.

Materials: Coomasie Blue (Bradford) Assay Kit was obtained from Thermo Scientific (Rockford, IL), and 96-well polystyrene plates for this assay were obtained from Greiner Bio-One (Monroe, NC). ADAM 12 enzyme linked immunosorbent assay (ELISA) kits obtained from R&D Systems (Minneapolis, MN). All supplies used without any further modification.

Patient recruitment: Study participants were screened during their visit either to the Sanford Breast Clinic and/or breast surgeon consultation visit by their treatment provider. If they wished to participate in the study, the clinical research coordinator met with them to discuss and/or complete the Informed Consent Form (ICF) document and process. After consent was obtained, the coordinator collected the pre-surgery or control urine sample, and informed those participants with breast cancer of the need to leave a second sample at a follow-up visit after their surgery. Control patients were matched for age and co-morbidities. They were selected from Sanford Medical Center Breast Clinic or other clinics. If they had benign and non interventional breast findings they were approached at their clinic visit about participation in the study and appropriately consented. Controls were consented using the same ICF document and process as breast cancer subjects.

Inclusion criteria:

- Females age 21 years of age or older
- Recent diagnosis of breast cancer
- No previous diagnosis of cancer, excepting non-melanoma skin cancer.
- Treatment naïve (i.e.no chemotherapy or radiation therapy prior to surgery for this breast cancer diagnosis)

Exclusion criteria:

- Pregnancy
- Advanced stage breast cancer disease (i.e.—stage 4 cancer with multiple metastasis)

Age-matched controls were females with no positive history of breast cancer or other previous diagnosed cancers, excluding non-melanoma skin cancer. All patients were recruited for study from the Sanford Medical Breast Clinics, and were consented in accordance with institutional regulatory board guidelines. All breast cancer patients had surgery as their initial treatment. The surgeries involved either a lumpectomy or a mastectomy for local control of their cancer; and in most cases included either an axillary sentinel lymph node dissection. When indicated a level I and II axillary lymph node dissection was done as part of the same procedure based on frozen section evaluation on the sentinel lymph nodes. The decision of surgery options was made after multidisciplinary treatment planning, consultation with the patients, and followed National Cancer Cooperative Network (NCCN) guidelines.

Urine collection and processing: Following consent, patients and controls were brought to a private area and asked to leave a urine sample. Immediately following collection, the urine was well mixed, and ten milliliters (10 mL) was aliquoted into a sterile, 10 mL screw cap test tube, and labeled with the patients de-identified information only; available information includes only patient age, stage of cancer, tumor size and co-morbidities. These samples were immediately placed upright in a -80ºC freezer for storage. Recruited breast cancer patients provided two samples of urine, one just following diagnosis, and a second approximately two weeks following surgery to remove the tumor mass (all patients recruited for this study were

scheduled for surgery). Controls have provided one sample only. Upon collection of 20 samples, tubes were transported to North Dakota State University on dry ice for testing.

Prior to testing, samples were thawed on ice and centrifuged at 200 rcf for 15 minutes to remove any particulates. The resulting supernatant was diluted 1:5 in one of two buffers: for the Bradford assay, 50 mM Tris at pH 8 was used, and for ELISA the calibrator diluent provided with the kit was used, as per the manufacturer's suggestion. Preliminary data demonstrated the necessity of dilution such that the ADAM 12 concentration in the patient samples would fit within the standard curve of the ADAM 12 ELISA.

Bradford assay: Manufacturer's instructions for the "micro microplate procedure" obtained with the kit were followed regarding volumes of samples, standards, and assay reagent. Bovine serum albumin was provided with the kit, and was used to produce the standard curve. The 2 mg/mL albumin standard was diluted in 50 mM Tris buffer (pH 8) to produce a standard curve ranging from zero µg/mL to 100 µg/mL. Twenty patient and/or control urine samples diluted 1:5 (see section on urine collection and processing) were loaded into four wells each of a 96-well standard clear bottom polystyrene plate, 150 µL per well. Standard samples were also loaded, two wells each sample, 150 µL per well. Bradford assay reagent provided was loaded into each well, 150 µL per well, and the plate was mixed on a shaker for 10 seconds, followed by incubation at room temperature for 10 minutes. Reading of plate absorbance, production of the standard curve and analysis of the samples was performed according to manufacturer's instructions.

ELISA: Twenty patient and/or control urine samples diluted 1:5 (see section on urine collection and processing) were loaded into four wells each of the provided 96-well plate of a commercially available ELISA kit. Standard samples were also loaded, two wells each.

Manufacturer's instructions were followed for production of standard curve and analysis of samples.

Statistical analysis: Groups were compared using nonparametric Mann-Whitney test ($\alpha = 0.05$). Analysis was performed using Minitab (v. 16.1.1).

Results

A total of 37 patients with the diagnosis of breast cancer and 31 age matched control patents were recruited into the study. Based on the data collected, no significant differences exist between the urinary ADAM 12 concentrations of the control patients and the cancer patients prior to their surgery. The urinary concentration of ADAM 12 increased significantly following patient surgery ($p < 0.0001$), both in ng/mL and as a function of total urine protein. Results are summarized in Table 3.1 and Figure 3.1 below.

Table 3.1. **Cancer patient group vs. control group**

	Cancer Group: Pre-surgery (n = 37)	**Cancer Group: Post-surgery (n = 35)**	**Control group (n = 31)**
Age	Mean: 61 ± 13 Median: 60	Mean: 61 ± 12.4 Median: 60	Mean: 58 ± 10.7 Median: 58
[ADAM 12] (ng/mL)	Mean: 3.22 ± 2.35 Median: 2.52	Mean: 18.3 ± 17.0 Median: 12.78	Mean: 3.74 ± 3.1 Median: 2.85
% Increase in ADAM 12 Concentration Post-Surgery	Mean: 3.2 ± 2.4 Median: 2.5	Mean: 18.3 ± 17.0 Median: 12.8	Mean: 3.74 ± 3.1 Median: 2.9
Total protein (μg/mL)	Mean: 59.8 ± 54.5 Median: 39.0	Mean: 62.3 ± 26.5 Median: 62.8	Mean: 79.6 ± 75.3 Median: 50.6
ADAM 12 as % of total protein	Mean: 0.009 ± 0.012 Median: 0.005	Mean: 0.031 ± 0.32 Median: 0.017	Mean: 0.007 ± 0.007 Median: 0.005
Cancer group consists of DCIS (n = 10) and IBC (n = 27) diagnoses.			

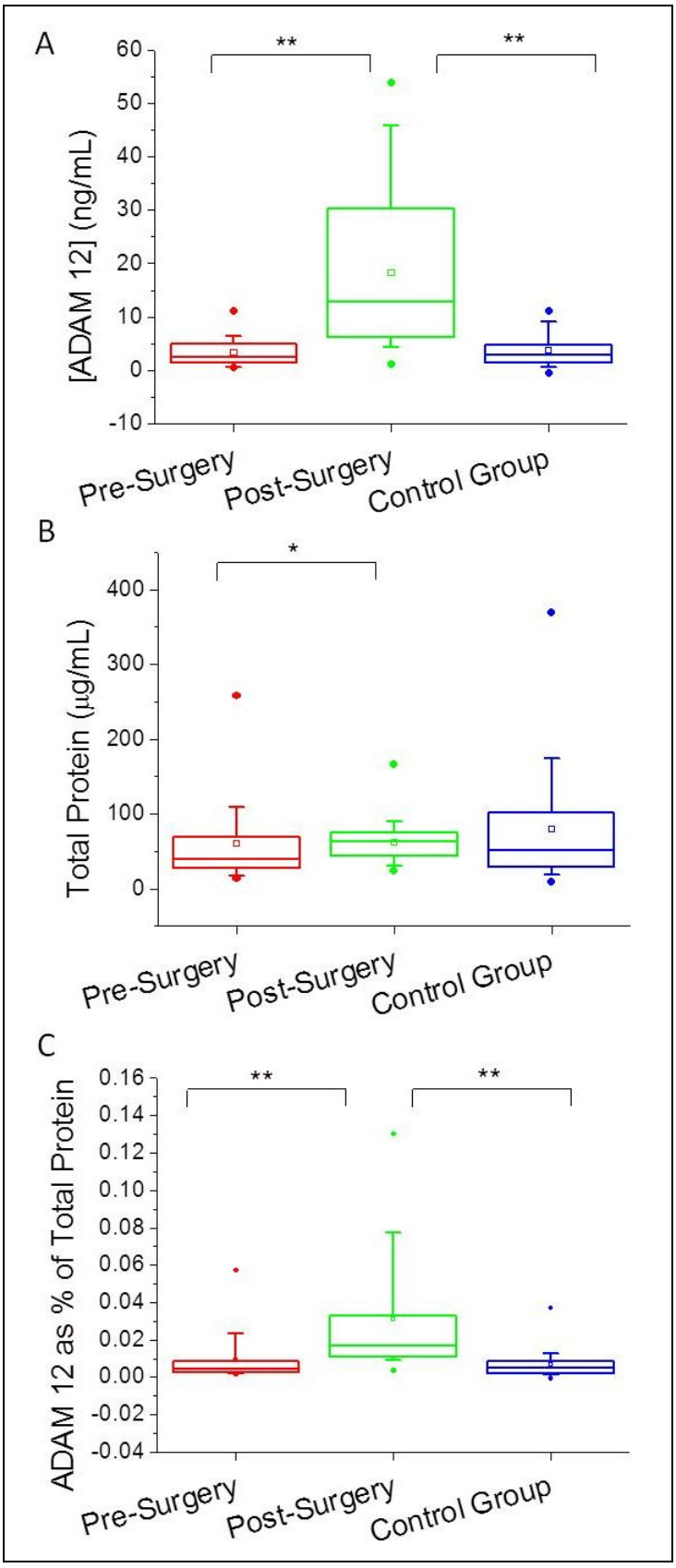

Figure 3.1. **Boxplots showing urinary ADAM 12-S levels in patient groups (pre- and post-surgery) vs. control group.** Concentration of ADAM 12-S denoted in ng/mL (A), total protein concentration (B), and ADAM 12 as a % of total protein (C) are shown for each respective group. Circles above and below the box denote 99% and 1%, respectively; vertical bars denote 10-90%; the box denotes 25-75%; the square in the middle of the box denotes the mean; and the horizontal bar denotes the median. * $p = 0.049$, ** $p < 0.0001$

The cancer patients recruited for this study consist of 10 women with a diagnosis of DCIS, and 27 women with a diagnosis of IBC (27% and 73% of the total group, respectively). If we consider these as separate groups and compare these groups individually to the control group the results do not change, nor do the DCIS and IBC patients differ significantly from each other pre-surgery (see Figure 3.2). The ADAM 12 concentration ranges, median changes in concentration, and median percent change from pre- to post-surgery are also consistent between the DCIS and IBC groups (see Table 3.2). Significant elevation of urinary ADAM 12 does take place after patients have undergone surgery (overall p-value < 0.0001).

Table 3.2. **Ranges and median change of ADAM 12 concentration for controls and cancer patients (by stage)**

Stage	Pre-surgery	Post-surgery	Median change	Median % change
Control	0--11.01 ng/mL	NA	NA	NA
DCIS	0.6--6.4 ng/mL	2.9--53.8 ng/mL	9.5	500.2%
IBC	0.4--11.1 ng/mL	1.1--53.8 ng/mL	7.5	423.7%

Results further suggest a link between the extent of patient surgery and urinary ADAM 12 elevation. Of the cancer patients recruited for this study, 29 of these underwent lumpectomies, and 9 underwent mastectomies (83% and 17% of the total group, respectively; two of the recruited patients failed to leave post-operative samples). The concentration of ADAM 12 in the urine of mastectomy patients was significantly higher than that of lumpectomy patients ($p = 0.0271$); the median increase in ADAM 12 concentration for mastectomy patients was 14.7 ng/mL , versus 7.0 ng/mL for lumpectomy patients. When considered as a percentage of total protein, the percent urinary ADAM 12 following a mastectomy versus that following a lumpectomy was significant at $p = 0.0731$. There were no statistically significant differences between the total urine protein concentrations of these groups. These results are summarized in

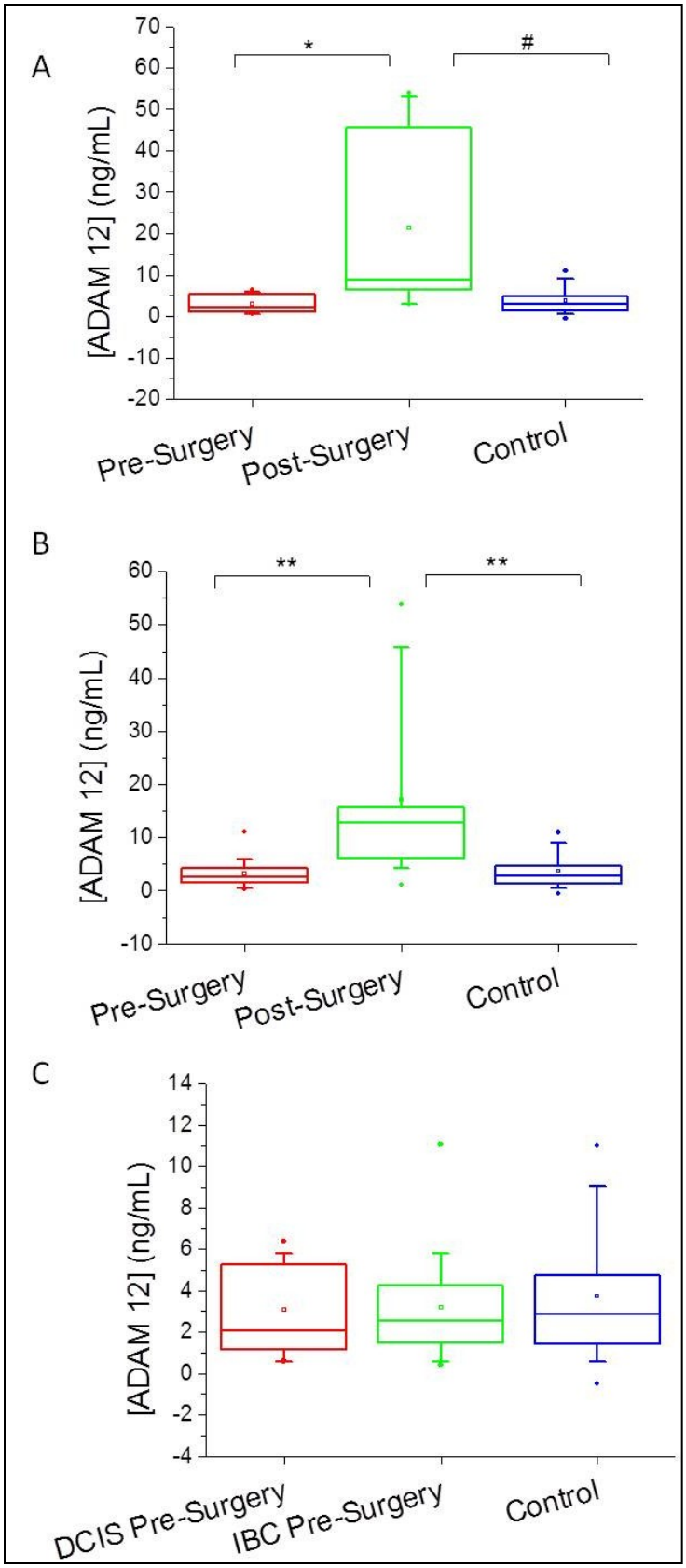

Figure 3.2. **Boxplots showing urinary ADAM 12-S concentration in ng/mL pre- and post- surgery for DCIS patients only (A), IBC patients only (B), and both DCIS and IBC patients pre-surgery (C) with comparison to the control group**. Circles above and below the box denote 99% and 1%, respectively; vertical bars denote 10-90%; the box denotes 25-75%; the square in the middle of the box denotes the mean; and the horizontal bar denotes the median.
* $p = 0.0017$, # $p = 0.0005$,
** $p < 0.0001$

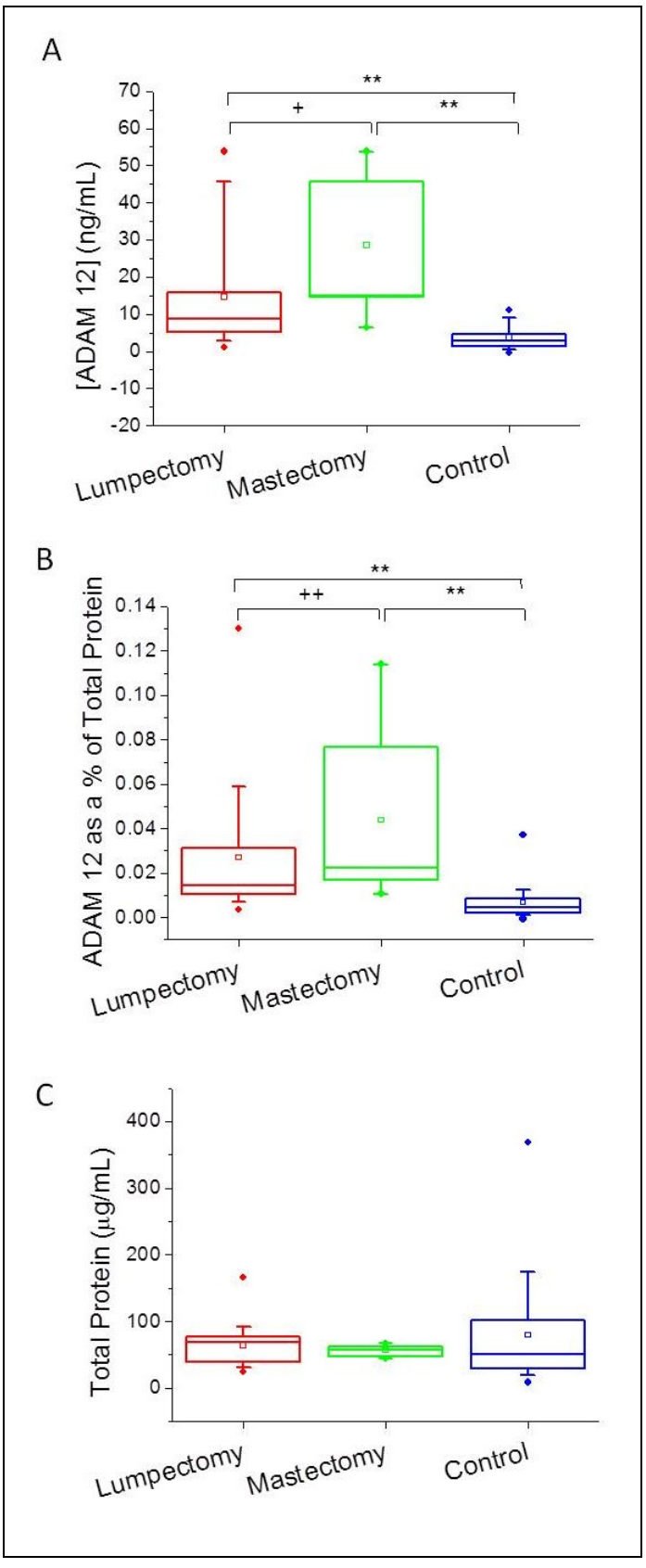

Figure 3.3. **Boxplots showing urinary ADAM 12-S levels in patients who underwent lumpectomies or mastectomies vs. control group**. Concentration of ADAM 12-S denoted in ng/mL (A), total protein concentration (B), and ADAM 12 as a % of total protein (C) are shown for each respective group. Circles above and below the box denote 99% and 1%, respectively; vertical bars denote 10-90%; the box denotes 25-75%; the square in the middle of the box denotes the mean; and the horizontal bar denotes the median.
+ $p = 0.0271$, ++ $p = 0.0731$, ** $p < 0.0001$

Table 3.3 and Figure 3.3. There were no significant differences between the urinary ADAM 12 concentrations of lumpectomy and mastectomy patients prior to their surgeries (data not shown).

***Table 3.3*. Ranges and median change of ADAM 12 concentration for lumpectomy patients vs. mastectomy patients (compared with controls)**

Surgery	Pre-surgery	Post-surgery	Median change	Median % change
Control	0--11.0 ng/mL	NA	NA	NA
Lumpectomy	0.5--11.1 ng/mL	1.08--53.8 ng/mL	7.0	322.2%
Mastectomy	0.4--7.0 ng/mL	6.44--53.8 ng/mL	14.7	764.5%

Discussion

Interestingly, these results appear to contradict those published in 2004 [29]; while these authors have concluded that patients with DCIS and IBC had significantly higher levels of ADAM 12 in their urine, our data shows no significant difference between the cancer and control groups.

These results raise a number of interesting questions. The observed elevation in ADAM 12 following surgery is not surprising: many matrix metalloproteinase enzymes are upregulated during wound healing [30], and evidence suggests that ADAM 12 is involved in tissue remodeling [31], making it likely to undergo upregulation following surgical or other trauma to the tissues. We also note *a priori* that many patients recruited for this study have co-morbidities which may affect levels of ADAM 12 (e.g. osteoarthritis [23], allergic rhinitis [32], and asthma [32]), however these co-morbidities are well balanced between the cancer group and the control group, and based on our analysis they have had no significant effect on the concentrations of urinary ADAM 12. The data also shows that some cancer and control patients having levels of ADAM 12 above the median did not have obvious comorbidities. It remains to be determined under what circumstances members of a certain group could have significantly elevated levels of urinary ADAM 12 compared to members of another group, assuming these groups are age-matched.

Based on our observations, these circumstances could easily occur if the group having elevated urinary ADAM 12 had undergone surgery within four weeks of having been tested. Further, as those patients with more advanced stages of cancer would be likely to have had more extensive surgery; it would follow that those patients with higher stage breast cancers would appear to have higher urinary ADAM 12 concentrations. Other tissue trauma could also play a role, such as biopsies. Further, had existing comorbidities not been balanced between the control and test groups, it is likely these may play a role in the elevation of urinary ADAM 12 levels in one group over another.

Conclusions

In conclusion, we find no significant difference between urinary ADAM 12 concentrations in patients diagnosed with DCIS or IBC and their age-matched controls prior to any surgery or other therapeutic treatment. Further, we find no significant differences in urinary ADAM 12 concentrations between DCIS patients and IBC patients either prior to or following surgical treatment. Following surgical treatment, the concentrations of urinary ADAM 12 are elevated significantly over age-matched controls, and the degree of this increase depends upon the severity of the surgery. These results are in contrast to those published by another group in 2004 [29]. However, as a final consideration we note that in 2011, the same group (which concluded in 2004 that DCIS patients have significantly elevated urinary ADAM 12 vs. controls) has conducted another study (utilizing fluorescent metalloproteinase substrates) to simultaneously detect a number of matrix metalloproteinases (MMPs) and ADAMs (MMP-1, -2, -3, -8, -9, and -13; ADAM-8, -9, -10, -12, and -17) in the urine of cancer patients and age-matched controls. This study concluded that no statistical difference exists between DCIS patients and age-matched controls when this fluorescence-based method is used [33]. Based on

these findings, it is unlikely that a screen for the presence of urinary ADAM 12 will become a viable method for the diagnosis of breast cancer.

Acknowledgments

We would like to thank Abby Zimmerman for her contributions as a study coordinator, and for her assistance consenting and coordinating the patients. We thank BreAnn Neiger for compiling information regarding patient surgeries. Support provided by the Sanford Seed Grant Research Fund, Grant# 2012-211.

References

(1) *National Breast Cancer Statistics,* Northeast Ohio Affiliate of Susan G. Komen, January 2012,www.komenneohio.org

(2) *Breast cancer survival rates by stage,* The American Cancer Society, 2/26/2013,www.cancer.org

(3) Sturgeon, C. M.; Duffy, M. J.; Stenman, U. H.; Lilja, H.; Brunner, N.; Chan, D. W.; Babaian, R.; Bast, R. C., Jr.; Dowell, B.; Esteva, F. J.; Haglund, C.; Harbeck, N.; Hayes, D. F.; Holten-Andersen, M.; Klee, G. G.; Lamerz, R.; Looijenga, L. H.; Molina, R.; Nielsen, H. J.; Rittenhouse, H.; Semjonow, A.; Shih Ie, M.; Sibley, P.; Soletormos, G.; Stephan, C.; Sokoll, L.; Hoffman, B. R.; Diamandis, E. P. *Clin Chem* **2008**, *54*, e11-79.

(4) Ludwig, J. A.; Weinstein, J. N. *Nat Rev Cancer* **2005**, *5*, 845-856.

(5) Opstal-van Winden, A. W.; Rodenburg, W.; Pennings, J. L.; van Oostrom, C. T.; Beijnen, J. H.; Peeters, P. H.; van Gils, C. H.; de Vries, A. *Int J Mol Sci* **2012**, *13*, 13587-13604.

(6) Nolen, B. M.; Lokshin, A. E. *Int J Biol Markers* **2011**, *26*, 141-152.

(7) Silva, C. L.; Passos, M.; Camara, J. S. *Talanta* **2012**, *89*, 360-368.

(8) Hotoda, N.; Koike, H.; Sasagawa, N.; Ishiura, S. *Biochem Biophys Res Commun* **2002**, *293*, 800-805.

(9) Yavari, R.; Adida, C.; Bray-Ward, P.; Brines, M.; Xu, T. *Hum Mol Genet* **1998**, *7*, 1161-1167.

(10) Gilpin, B. J.; Loechel, F.; Mattei, M. G.; Engvall, E.; Albrechtsen, R.; Wewer, U. M. *J Biol Chem* **1998**, *273*, 157-166.

(11) Roberts, C. M.; Tani, P. H.; Bridges, L. C.; Laszik, Z.; Bowditch, R. D. *J Biol Chem* **1999**, *274*, 29251-29259.

(12) Millichip, M. I.; Dallas, D. J.; Wu, E.; Dale, S.; McKie, N. *Biochem Biophys Res Commun* **1998**, *245*, 594-598.

(13) Alfandari, D.; Cousin, H.; Gaultier, A.; Smith, K.; White, J. M.; Darribere, T.; DeSimone, D. W. *Curr Biol* **2001**, *11*, 918-930.

(14) Martin, J.; Eynstone, L. V.; Davies, M.; Williams, J. D.; Steadman, R. *J Biol Chem* **2002**, *277*, 33683-33689.

(15) Zolkiewska, A. *Exp Cell Res* **1999**, *252*, 423-431.

(16) Iba, K.; Albrechtsen, R.; Gilpin, B. J.; Loechel, F.; Wewer, U. M. *Am J Pathol* **1999**, *154*, 1489-1501.

(17) Iba, K.; Albrechtsen, R.; Gilpin, B.; Frohlich, C.; Loechel, F.; Zolkiewska, A.; Ishiguro, K.; Kojima, T.; Liu, W.; Langford, J. K.; Sanderson, R. D.; Brakebusch, C.; Fassler, R.; Wewer, U. M. *J Cell Biol* **2000**, *149*, 1143-1156.

(18) Selvais, C.; D'Auria, L.; Tyteca, D.; Perrot, G.; Lemoine, P.; Troeberg, L.; Dedieu, S.; Noel, A.; Nagase, H.; Henriet, P.; Courtoy, P. J.; Marbaix, E.; Emonard, H. *FASEB J* **2011**, *25*, 2770-2781.

(19) Saftig, P.; Hartmann, D. *ADAM10: A major membrane protein ectodomain sheddase involved in regulated intramembrane proteolysis.*; Springer, 2005.

(20) Brou, C.; Logeat, F.; Gupta, N.; Bessia, C.; LeBail, O.; Doedens, J. R.; Cumano, A.; Roux, P.; Black, R. A.; Israel, A. *Mol Cell* **2000**, *5*, 207-216.

(21) Kawaguchi, N.; Sundberg, C.; Kveiborg, M.; Moghadaszadeh, B.; Asmar, M.; Dietrich, N.; Thodeti, C. K.; Nielsen, F. C.; Moller, P.; Mercurio, A. M.; Albrechtsen, R.; Wewer, U. M. *J Cell Sci* **2003**, *116*, 3893-3904.

(22) Stautz, D.; Sanjay, A.; Hansen, M. T.; Albrechtsen, R.; Wewer, U. M.; Kveiborg, M. *Exp Cell Res* **2010**, *316*, 55-67.

(23) Okada, A.; Mochizuki, S.; Yatabe, T.; Kimura, T.; Shiomi, T.; Fujita, Y.; Matsumoto, H.; Sehara-Fujisawa, A.; Iwamoto, Y.; Okada, Y. *Arthritis Rheum* **2008**, *58*, 778-789.

(24) Wang, X.; Chow, F. L.; Oka, T.; Hao, L.; Lopez-Campistrous, A.; Kelly, S.; Cooper, S.; Odenbach, J.; Finegan, B. A.; Schulz, R.; Kassiri, Z.; Lopaschuk, G. D.; Fernandez-Patron, C. *Circulation* **2009**, *119*, 2480-2489.

(25) Bourd-Boittin, K.; Le Pabic, H.; Bonnier, D.; L'Helgoualc'h, A.; Theret, N. *J Biol Chem* **2008**, *283*, 26000-26009.

(26) Frohlich, C.; Albrechtsen, R.; Dyrskjot, L.; Rudkjaer, L.; Orntoft, T. F.; Wewer, U. M. *Clin Cancer Res* **2006**, *12*, 7359-7368.

(27) Mino, N.; Miyahara, R.; Nakayama, E.; Takahashi, T.; Takahashi, A.; Iwakiri, S.; Sonobe, M.; Okubo, K.; Hirata, T.; Sehara, A.; Date, H. *J Surg Oncol* **2009**, *100*, 267-272.

(28) Kanakis, D.; Lendeckel, U.; Theodosiou, P.; Dobrowolny, H.; Mawrin, C.; Keilhoff, G.; Bukowska, A.; Dietzmann, K.; Bogerts, B.; Bernstein, H. G. *Disease Markers* **2013**, *34*, 81-91.

(29) Roy, R.; Wewer, U. M.; Zurakowski, D.; Pories, S. E.; Moses, M. A. *J Biol Chem* **2004**, *279*, 51323-51330.

(30) Veeravalli, K. K.; Dasari, V. R.; Tsung, A. J.; Dinh, D. H.; Gujrati, M.; Fassett, D.; Rao, J. S. *Neurobiol Dis* **2009**, *36*, 200-212.

(31) Kim, J.; Kim, H.; Lee, S. J.; Choi, Y. M.; Lee, J. Y. *Reprod Fertil Dev* **2005**, *17*, 543-555.

(32) Estrella, C.; Rocks, N.; Paulissen, G.; Quesada-Calvo, F.; Noel, A.; Vilain, E.; Lassalle, P.; Tillie-Leblond, I.; Cataldo, D.; Gosset, P. *Am J Respir Cell Mol Biol* **2009**, *41*, 449-458.

(33) Roy, R.; Zurakowski, D.; Pories, S.; Moss, M.; Moses, M. *Clinical Biochemistry* **2011**, *44*, 1434-1439.

FUTURE STUDIES

Clinical investigation of sera from Alzheimer's disease patients

In our previous studies it became evident that increases in the serum concentration of glycosaminoglycan from 26 nM to 48 nM (corresponding to those of a healthy individual and an Alzheimer's disease patient, respectively, after dilution) may be distinguished by decreases in the fluorescence emission intensity from liposomes composed of 99 mol% POPC (1-palmitoyl-2-oleoyl-*sn*-glycero-3-phosphocholine), and 1 mol% of a pyranine-containing lipid[1]. These experiments were carried out using commercially available serum from healthy patients, and addition of chondroitin sulfate was made following dilution to simulate the serum of a patient afflicted with Alzheimer's disease. To further confirm this effect, and to verify the efficacy of this method for the accurate diagnosis of Alzheimer's disease, it will be necessary to conduct a clinical study. Briefly, such a study would recruit patients diagnosed with Alzheimer's disease and age-matched controls (individuals with no cognitive impairment) from a local hospital, and patient consent would be obtained in accordance with the Institutional Review Board of Sanford Health. Blood would be taken from each patient and control, and the serum separated from the cells and clotting factors. This serum would then be diluted and combined with pyranine-containing liposomes as in our previous study, and the extent of fluorescence emission intensity changes recorded. Non-parametric Mann-Whitney tests would be used to make statistical comparisons between the control group and Alzheimer's group. As a means of gaining access to study participants, collaboration with Sanford Medical Center would be sought.

Enzymatic digestion of heparin to increase OSCS/OSD detection sensitivity

Our previous studies indicate that contamination of heparin with over-sulfated chondroitin sulfate or over-sulfated dermatan sulfate may be detected by aggregation of POPC

liposomes containing 1 mol% of a lissamine-rhodamine-containing lipid[2]. The lowest limit of detection of this method was found to be 1 mol% over-sulfated chondroitin sulfate and 0.5 mol% over-sulfated dermatan sulfate, when using liposomes with a diameter of 500 nm. It may be possible to increase the sensitivity of this method by selectively digesting the heparin in solution using the enzyme Heparin Lyase I. Heparin Lyase I selectively cleaves substrates having 2-O-sulfated α-L-idopyranosyluronic acid at the cleaved linkages[3], and as such should selectively degrade heparin allowing the over-sulfated contaminants to remain in solution at approximately their original molecular weight. The presence of these proportionately larger over-sulfated glycosaminoglycans in solution should result in the presence of large liposomal aggregates, whereas a solution of uncontaminated heparin should be fully digested, and thus should result in very little liposomal aggregation. Heparin Lyase I is commercially available, as is heparin sulfate; over-sulfated glycosaminoglycan contaminants could be produced as in our previous studies. Optimization studies would be conducted to determine appropriate amounts of enzyme to add to solutions of heparin and contaminant, as well as appropriate duration of the digest. Confirmation of the anticipated effect would be determined using dynamic light scattering, as in our previous studies.

Continued monitoring of breast cancer patients following completion of chemotherapy

In our previous studies, we have concluded that there are no significant differences between the urinary ADAM 12 concentrations of breast cancer patients prior to surgical treatment and those of their age-matched controls (no cancer present). We further conclude that urinary concentrations of ADAM 12 are elevated following patient surgery, and that this elevation is significantly greater for patients following a mastectomy than a lumpectomy (the greater the severity of the surgery, the greater the elevation of urinary ADAM 12). To further

understand the role of wound healing and other inflammation processes on the elevation of urinary ADAM 12, we will collect an additional sample of urine from the cancer patient group following the completion of their chemotherapy treatments (if any). These samples will be analyzed in the same way as previously obtained samples. In addition, patient records will be monitored for the reappearance of cancer for five years following the completion of treatment; possible correlations between elevation of ADAM 12 following surgery and reappearance of cancer will be explored. Any required approval by the Sanford Health Institutional Review Board will be sought prior to the commencement of any study.

References

(1) Nyren-Erickson, E. K.; Haldar, M. K.; Gu, Y.; Qian, S. Y.; Friesner, D. L.; Mallik, S. *Analytical Chemistry* **2011**, *83*, 5989-5995.

(2) Nyren-Erickson, E. K.; Haldar, M. K.; Totzauer, J. R.; Ceglowski, R.; Patel, D. S.; Friesner, D. L.; Srivastava, D. K.; Mallik, S. *Langmuir* **2012**, *28*, 16115-16125.

(3) Desai, U. R.; Wang, H. M.; Linhardt, R. J. *Arch Biochem Biophys* **1993**, *306*, 461-468.

Synthesis of pyranine containing lipid

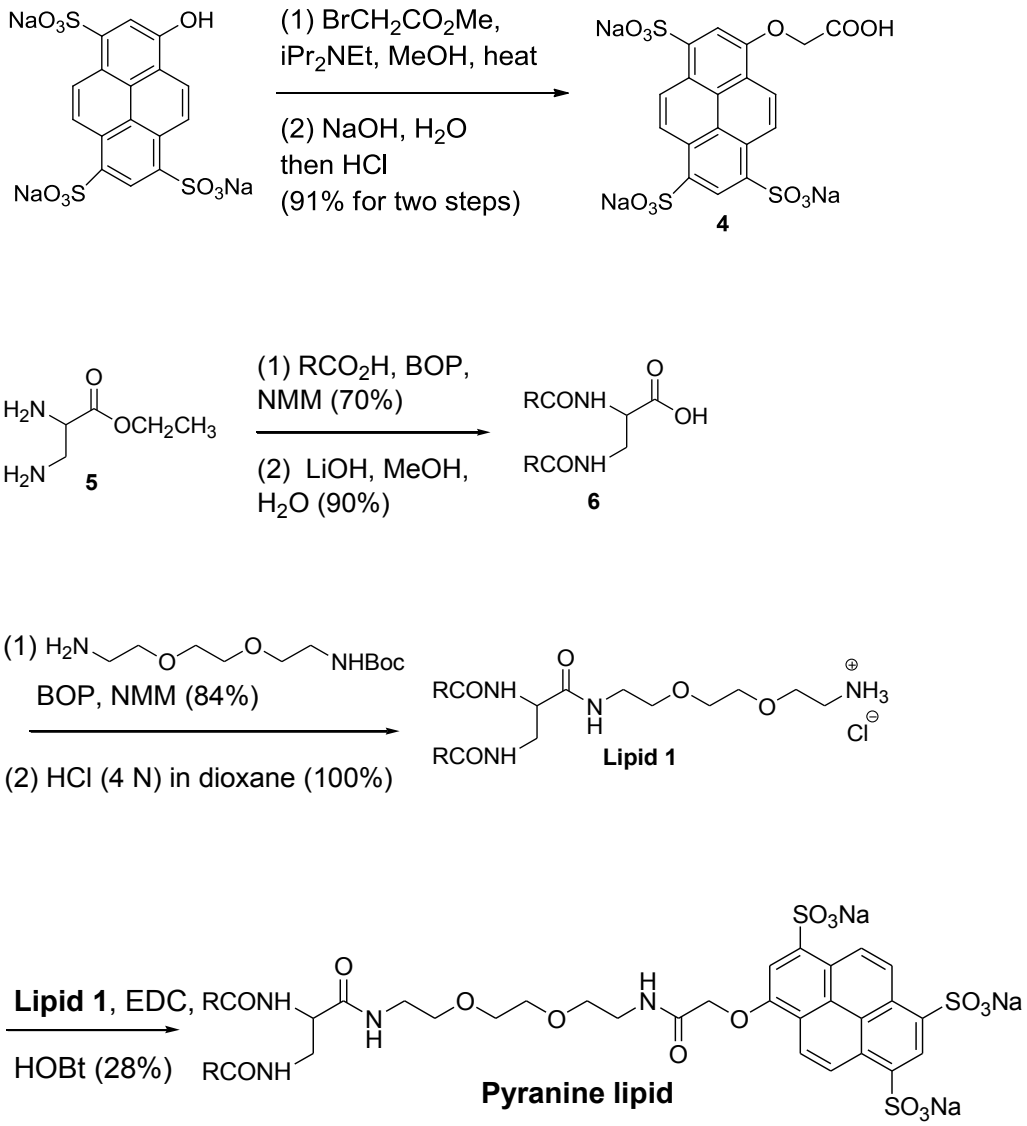

Figure A1. **Pyranine lipid synthesis.**

MW = 1329.61 g/mol

λ_{ex} = 390 nm; λ_{em} = 400-600 nm

Cascade Blue (**4**)**:** Methyl ester derivative of cascade blue (1.28 g, 2.14 mmol) was dissolved in water (20 mL) and stirred with NaOH (0.086 g, 2.15 mmol) for 30 min at 60^0 C. After cooling the reaction mixture, 100 μL of HCl was added. To this clear solution isopropanol (60 mL) was added to effect precipitation. The mixture was stirred for 20 minutes, filtered and dried to afford free flowing yellow powder (1.131 g, 91%). ^{1}H NMR (400 MHz, CD_3OD): δ 5.07 (s, 2H), 8.33(s, 1H), 8.76 (d, 1H, J = 10 Hz,), 9.11(d, 1H, J = 10 Hz), 9.19-9.24 (overlapping doublet, 2H, J = 10.8 Hz and 10 Hz), 9.378 (s, 1H). ^{13}C NMR (100 MHz, D_2O):δ 66.64, 109.92, 120.87, 121.67, 123.26, 124.39, 124.69, 124.73, 125.63, 125.71, 127.41, 129.64, 130.28, 134.84, 138.88, 152.43, 174.10.

Compound 6: To a stirred mixture of diamino propanoic acid, 2PTSA ethyl ester (5.12 g, 10 mmol) and oleic acid (5.64 g, 20 mmol) in $CHCl_3$ (150 mL) and DMF (50 mL), BOP (8.85 g, 20 mmol) was added. The reaction mixture was stirred for 5 minutes and NMM (6.5 mL, 60 mmol) was added dropwise. Overnight stirring at room temperature resulted in a clear reaction mixture. The reaction mixture was then diluted with 250 mL additional $CHCl_3$, quenched with brine, and the organic phase was washed successively with brine, 5% citric acid and 5% $NaHCO_3$ solution. Organic layer was dried on sodium sulfate and solvent evaporated under reduced pressure. Oily residue was purified by SiO_2 column chromatography employing 3:1 to 3:2 hexane ethyl acetate. (R_f = 0.3 in 1:1 ethyl acetate/hexane) to obtain the pure product as a colorless oil(4.6 g, 70%) ^{1}H NMR (400 MHz, $CDCl_3$): δ 0.83-0.87 (t, 6H, J = 6.8 Hz), 1.18-1.32 (m, 43H), 1.56-1.61 (m, 4H), 1.94-2.01 (m, 8H), 2.11-2.3 (m, 4H), 3.58-3.62 (m, 2H), 4.15-4.21 (m, 2H), 4.53-4.58 (m, 1H), 5.26-5.33 (m, 4H), 6.15-6.18 (m, 1H), 6.71 (d, 1H, J = 7.2 Hz). Bis oloeyl diaminopropanoic acid ethyl ester (3.6 g, 5.44 mmol) in CH_2Cl_2/MeOH (2:1, 45 mL) was treated with $LiOH.H_2O$ (0.458 g, 10.89 mmol) overnight at room temperature. After

complete consumption of starting material the reaction was stopped and acidified to pH 2 with dilute HCl and solvent was evaporated under reduced pressure. The residue was taken into CH_2Cl_2 and was washed with water to remove LiCl. Drying of organic phase over sodium sulfate and solvent evaporation afforded clear liquid which slowly became waxy solid. This was used in the next step without further purification. Compound **6** was obtained in 90% yield (3.1 g). ^{1}H NMR (400 MHz, $CDCl_3$): δ 0.78-0.82 (distorted triplet, 6H, J = 7.2 and 6.8 Hz), 1.17-1.25 (m, 40H), 1.47-1.54 (m, 4H), 1.89-1.94 (m, 8H), 2.06-2.25 (m, 4H), 3.28-3.34 (m, 1H), 3.51-3.55 (dd, 1H, J = 4 Hz and J = 9.6 Hz), 4.12-4.14 (q, 1H), 5.23-5.27 (m, 4H).

Lipid 1: Following a similar protocol as above, compound **6** (3.6 g, 5.696 mmol) was conjugated with the mono BOC protected linker (1.447 g, 5.98 mmol) by employing BOP (2.646 g, 5.98 mmol) and NMM (1.876 mL, 17.08 mmol) in chloroform (100 mL). After work-up and solvent evaporation it was purified by chromatography with CH_2Cl_2/MeOH (R_f = 0.3 in 5% methanol in CH_2Cl_2, iodine active). Pure product obtained 4.1 g (yield: 84%). ^{1}H NMR (400 MHz, $CDCl_3$): δ 0.83-0.87 (distorted triplet, 6H, J = 7.2 and 6.8 Hz), 1.2-1.38 (m, 40H), 1.41 (s, 9H), 1.54-1.62 (m, 4H), 1.95-1.99 (m, 8H), 2.14-2.22 (m, 4H), 3.32-3.36 (m, 2H), 3.42-3.58 (m, 12H), 4.44 (br s, 1H), 5.29-5.33 (m, 4H), 6.46 (br s, 1H).

The obtained Boc-protected compound (2.5 g, 2.90 mmol) was dissolved in minimum quantity of CH_2Cl_2 (5 mL) and stirred with 4 N HCl in dioxane (10 mL) for 3 hours. Evaporation of solvent afforded the compound **7** as HCl in quantitative yield. ^{1}H NMR (500 MHz, $CDCl_3$/2 drops CD_3OD): δ 0.88-0.90 (dd, 6H, J = 5.2 and 5.6 Hz), 1.28-1.32 (m, 40H), 1.58-1.61 (m, 4H), 2.00-2.02 (m, 8H), 2.21-2.28 (m, 4H), 3.15-3.3 (br s, 2H), 3.37-3.47 (m, 1H), 3.63-3.72 (m, 9H), 3.85-3.86 (m, 2H), 4.6-4.7 (m, 1H), 5.32-5.37 (m, 4H), 7.24 (br s, 1H), 7.73 (d, 1H, J = 5.2Hz), 8.20 (br s, 1H), 8.36 (br s, 3H).

Pyranine lipid: To a DMF (10 mL) solution of compound **7** (0.2 g, 0.25 mmol), cascade blue (0.161 g, 0.27 mmol) was added and stirred for 10 minutes to make a homogeneous solution. HOBt (0.036 g, 0.27 mmol) followed by EDC (0.052 g, 0.27 mmol) were added to the reaction mixture and stirred at room temperature for 36 hours. Solvent was evaporated under reduced pressure and little water was added to the residue followed by large excess of isopropyl alcohol. The resulting precipitate was filtered, dried and was subjected to chromatographic purification using 2:1 dichloromethane methanol mixture ($R_f = 0.3$) to afforded the pure product as a yellow waxy solid (92 mg, 28%). ^{1}H NMR (400 MHz, DMSO-d_6): δ 0.80-0.84 (distorted triplet, 6H, J = 7.2 and 6.4 Hz), 1.13-1.31 (m, 40H), 1.40-1.44 (m, 4H), 1.93-2.01 (m, 10H), 2.05-2.09 (t, 2H, J = 7.6 Hz), 3.14-3.51 (m, 14H), 4.26-4.29 (m, 1H), 4.85 (s, 2H), 5.26-5.31 (m, 4H), 7.68-7.73 (m,2H), 7.84-7.86 (m, 1H), 8.11 (s, 1H), 8.25-8.28 (m,1H), 8.51 (d, 1H, J = 9.6 Hz), 8.96 (d, 1H, J = 10 Hz), 9.02-9.04 (m, 2H), 9.15 (d, 1H, J = 9.6 Hz). ^{13}C NMR (100 MHz, DMSO-d_6): δ 14.95, 22.74, 25.41, 25.76, 25.89, 27.23, 27.30, 29.25, 29.33, 29.49, 29.63, 29.75, 29.83, 31.94, 36.02, 39.03, 69.50, 69.58, 70.23, 85.59, 109.78, 120.43, 121.37, 121.67, 124.51, 125.17, 125.69, 126.09, 126.68, 127.01, 128.29, 128.69, 130.26, 130.53, 134.25, 140.29, 140.41, 143.79, 151.28, 168.18, 170.71, 172.92, 173.43. MH^+ calcd. for $C_{63}H_{89}N_4Na_3O_{16}S$: 1324.51; found: 1324.57.

Lissamine Rhodamine B lipid: This lipid is commercially available from Avanti Polar Lipids, Alabaster, AL. MW = 1267.68 g/mol; λ_{ex} = 557 nm; λ_{em} = 567-700 nm

Dansyl lipid: This lipid is commercially available from Avanti Polar Lipids, Alabaster, AL. MW = 994.35 g/mol; λ_{ex} = 336 nm; λ_{em} = 400-650 nm

Fluorescence emission ratio graphs

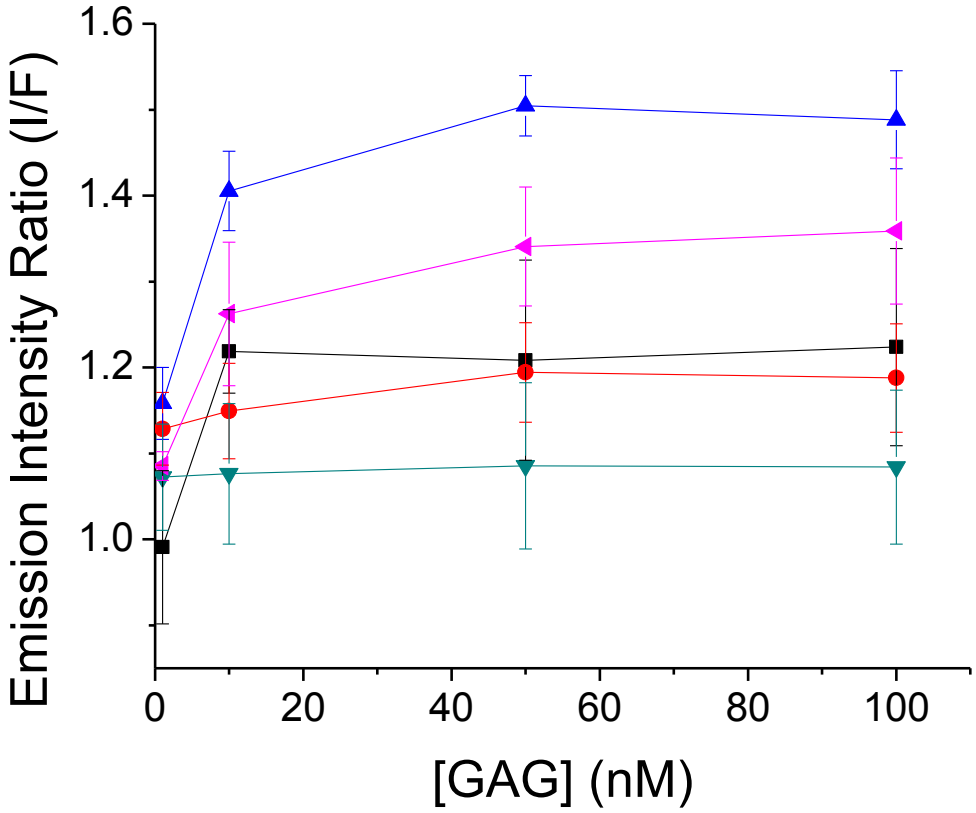

Figure A2. **Fluorescence emission intensity changes of liposomes containing rhodamine fluorophore in presence of glycosaminoglycans**. The emission intensity ratios for the rhodamine liposomes (λ_{ex} = 557 nm) in the absence and presence of added GAGs are shown. The GAGs include chondroitin sulfate (black squares), dextran sulfate (red circles), heparin sulfate (blue triangles), hyaluronic acid (dark cyan inverted triangles), and dermatan sulfate (magenta diamonds). The data points are connected by straight lines.

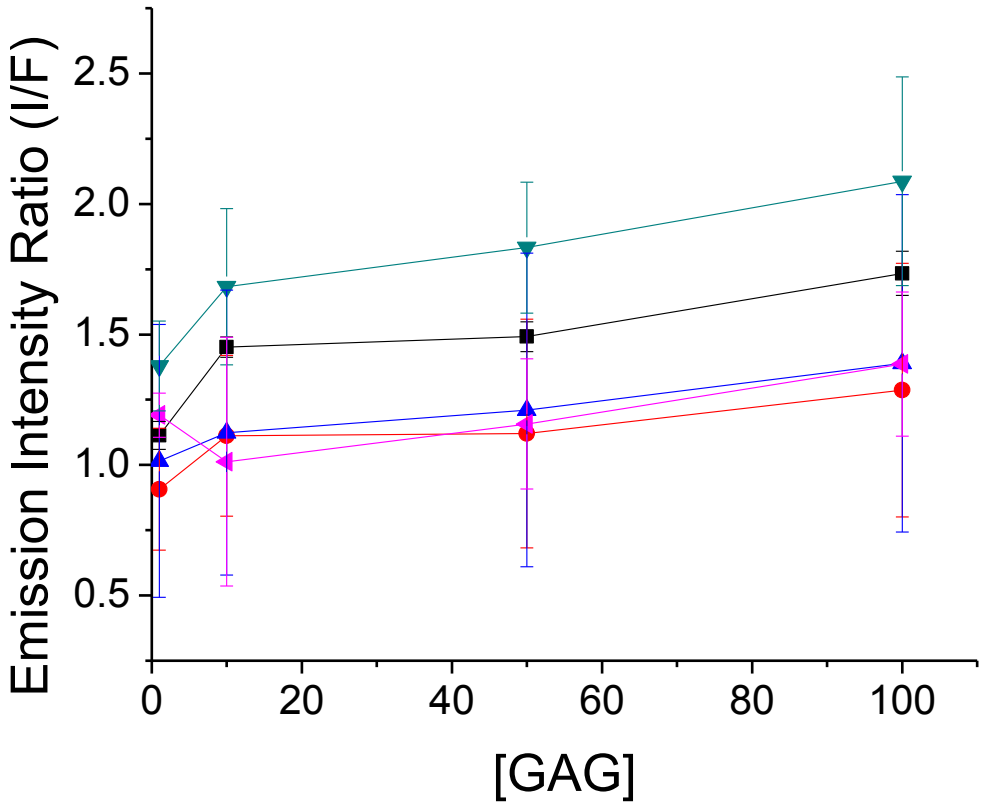

Figure A3. **Fluorescence emission intensity changes of liposomes containing dansyl fluorophore in presence of glycosaminoglycans**. The emission intensity ratios for the dansyl liposomes (λ_{ex} = 336 nm) in the absence and presence of added GAGs are shown. The GAGs include chondroitin sulfate (black squares), dextran sulfate (red circles), heparin sulfate (blue triangles), hyaluronic acid (dark cyan inverted triangles), and dermatan sulfate (magenta diamonds). The data points are connected by straight lines.

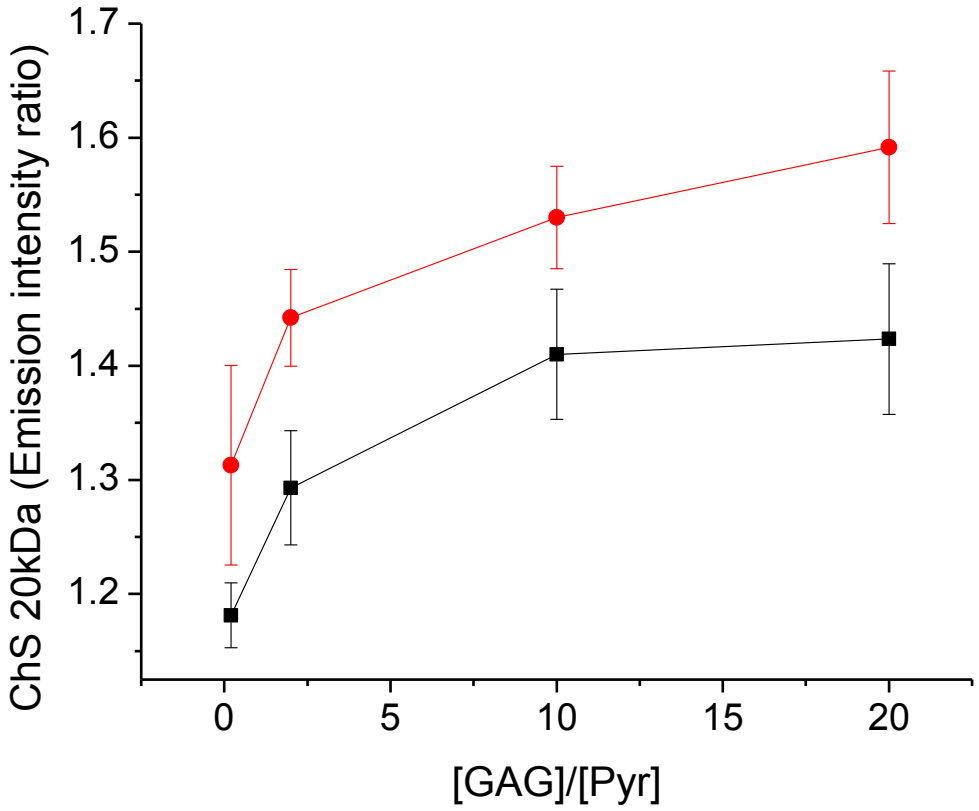

Figure A4. **Comparison of liposome fluorescence emission intensity changes of pyranine-containing liposomes in the presence of chondroitin sulfate of two molecular weights**. The emission intensity ratios for the pyranine liposomes (λ_{ex} = 415 nm) in the presence of 20kDa MW chondroitin sulfate (black squares), and 35kDa MW chondroitin sulfate (red circles). The data points are connected by straight lines.

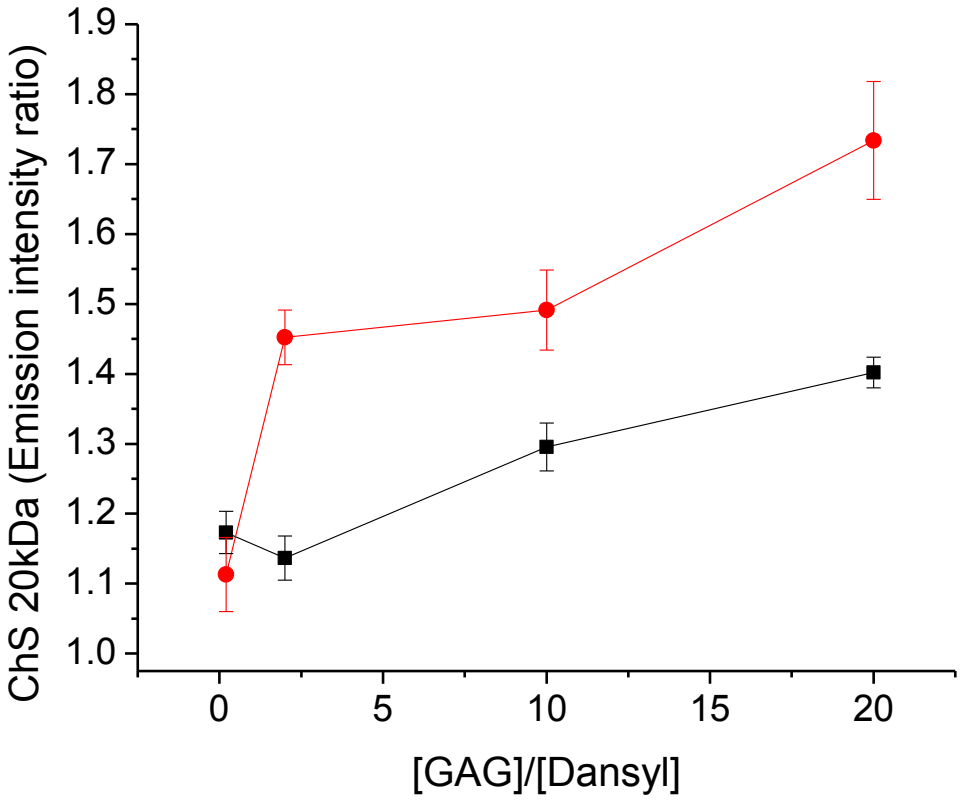

Figure A5. **Comparison of liposome fluorescence emission intensity changes of dansyl-containing liposomes in the presence of chondroitin sulfate of two molecular weights.** The emission intensity ratios for the dansyl liposomes (λ_{ex} = 587 nm) in the presence of 20kDa MW chondroitin sulfate (black squares), and 35kDa MW chondroitin sulfate (red circles). The data points are connected by straight lines.

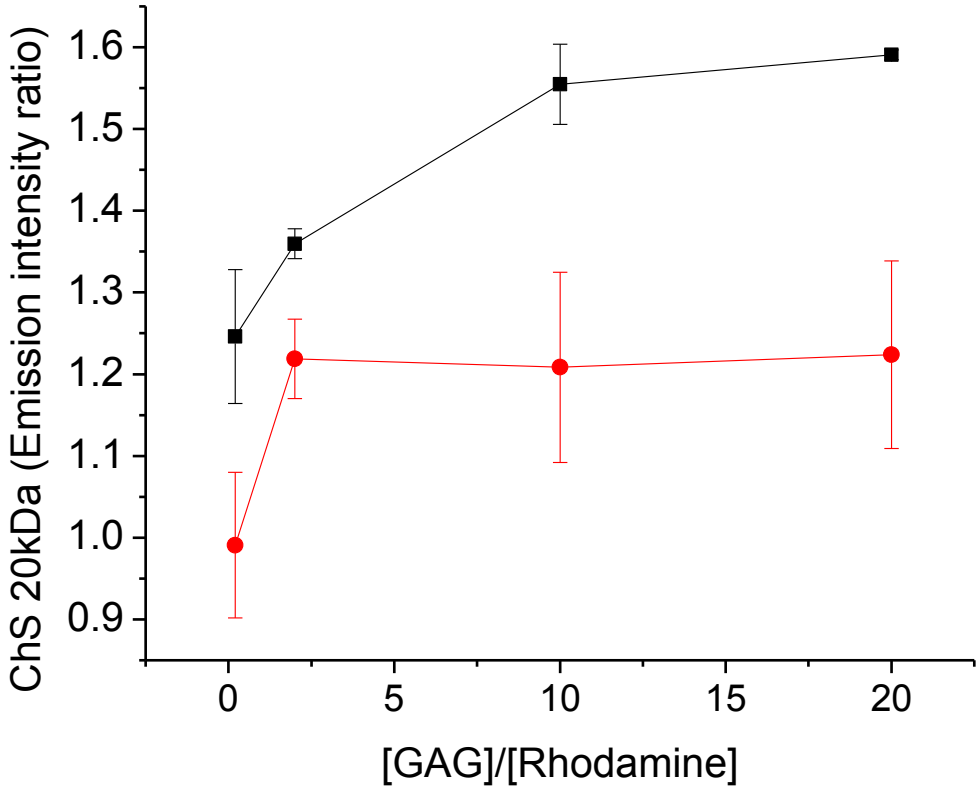

Figure A6. **Comparison of liposome fluorescence emission intensity changes of rhodamine-containing liposomes in the presence of chondroitin sulfate of two molecular weights.** The emission intensity ratios for the rhodamine liposomes (λ_{ex} = 587 nm) in the presence of 20kDa MW chondroitin sulfate (black squares), and 35kDa MW chondroitin sulfate (red circles). The data points are connected by straight lines.

Statistical data analysis

The following discussion presents the full set of LDA results for the analysis at 50 nM. For simplicity, these are labeled as Tables A1-A5 and Figure A1. Note that several of these tables (A1 and A5), Figure A1 and some of the language are identical to those presented in the body of the text.

Linear discriminant analysis (LDA) is used to identify the predictive power of the liposomes. Emissions intensity data from the three liposomes (the predictor variables) and the

five GAGs (the dependent variables) were replicated a total of six times, yielding a sample of 30 observations with four variables (one for each liposome and one identifying the GAG). Each liposome is included in the model using a stepwise procedure, where inclusion is based on minimizing the Mahalanobis D^2, or generalized squared inter-point distance, between each individual observation to the corresponding group centroid.

Once the appropriate number of liposomes is determined, LDA identifies canonical correlations (i.e., synthetic variables which are linear combinations of the predictor variables) which maximize the ratio of the between-group variation to the within-group variation across the GAGs. That is, LDA identifies the set of predictive factors that leads to maximum discrimination between our GAGs. Note that, for K = 5 possible GAGs, it is possible to identify as many as K-1 = 4 possible canonical correlations, and by extension as many as K-1 = 4 discriminant functions, each of which relates a single canonical correlation to a linear combination of liposome fluorescence intensities. It is common practice to identify and interpret only those correlations that are both orthogonal and explain a significant portion of the variation in the GAGs. The coefficients characterizing the linear combination of the predictor variables can also be used (with a bit of algebraic manipulation) to identify the relative contribution of each liposome to a discriminant function. Liposomes with larger coefficient values (in absolute value) play a larger role in the formation of a given discriminant function, and by extension in predicting the GAGs. To characterize the contribution of each liposome to the model's overall ability to discriminate across GAGs (rather than the ability of a single canonical function), we utilize the correlations between each liposome and each of the discriminant functions to generate a structure matrix. The elements of the structure matrix are subsequently combined with the eigenvalues of canonical functions to generate an overall "potency index" for each liposome.

Higher values for each index signal the overall importance of each liposome to the model as a whole.

Overall model fit is assessed by examining canonical function plots to identify whether each of the group centroids (one for each of the five GAGs) is sufficiently distinct. Overlap between the data points of two or more groups indicates that the model does not adequately discriminate across these GAGs. Internal validity is assessed by comparing the percentage of GAG observations that are correctly predicted by the model. All model predictions are computed using both traditional and (leave one out) cross-validation techniques. Internally valid results should correctly predict a high percentage of observations, and display consistency in predicted values across both techniques. All statistical analyses were conducted using the PASW (formerly SPSS) Statistical Package, Version 18.

Table A1 contains means, F-statistics and Wilks' Lambda values for each liposome, disaggregated by GAGs. We note in passing that smaller values for the Wilks' Lambda indicate a greater potential for the liposome to discriminate across GAGs. All F-statistics have associated p-values less than 0.05, indicating significant differences exist across group means for each GAG. For the chondroitin sulfate, dextran sulfate, heparin sulfate and hyaluronic acid GAGs, the dansyl liposome has the highest mean fluorescence values. The pyranine liposomes have the second highest mean values, followed by rhodamine. The remaining GAG (dermatan sulfate) has the highest mean emission ratios when combined with pyranine, followed by dansyl and rhodamine. Wilks' Lambda values are lowest for pyranine, followed by rhodamine and dansyl.

Table A1. **50 nM LDA tests of equality of group means**

GAG	Pyranine[a,b]	Rhodamine[a,b]	Dansyl[a,b]
Chondroitin Sufate	1.562	1.297	1.563
Dermatan Sulfate	1.942	1.447	1.412
Dextran Sulfate	1.334	1.247	1.541
Heparin Sulfate	1.729	1.517	1.862
Hyaluronic Acid	1.487	1.124	2.243
Wilks' Lambda	0.068	0.214	0.560
F-Statistic [4, 25]	85.829	22.898	4.904
P-Value	<0.001	<0.001	0.005

[a] first panel provides group-specific means [b] second panel provides statistics and p-values.

Table A2 contains a summary of the stepwise variable selection process. All three liposomes are found worthy of inclusion, and no variables are removed from the analysis. Table A3 identifies the number of significant canonical correlations, and by extension the number of significant canonical functions. Chi-square tests indicate that three canonical functions are sufficient to explain our 5 GAGs. Of these, the first canonical function is most important, as it explains 96.3% of the variation across GAGs. The remaining functions explain 3.0% and 0.7%, respectively. As such, we focus primarily on the first discriminant function.

Table A2. **50nM LDA variables in the analysis[a]**

Step Entered	Predictor	D^2	Between Groups	F-Statistic	P-Value
1	Pyranine	1.475	1 and 5	4.426	0.046
2	Dansyl	6.150	3 and 5	8.857	0.001
3	Rhodamine	12.499	3 and 5	11.499	<0.001

[a] Variables are entered in a manner that maximizes the Mahalanobis D^2 between the two closest groups. [b] Each of five GAGs groups are: chondroitin sulfate (group 1), dermatan sulfate (group 2), dextran sulfate (group 3), heparin sulfate (group 4) and hyaluronic acid (group 5).

Table A3. **50 nM LDA canonical function summary**[a]

Fct.	Eigen-Value	Pct. of Variance Explained	Canonical Correl.	Wilks' Lambda[a]	Chi-Square Statistic	P-Value
1	61.693	96.3	0.992	0.004[b]	139.166	<0.001
2	1.893	3.0	0.809	0.240[c]	35.710	<0.001
3	0.442	0.7	0.554	0.693[d]	9.151	0.010

[a] Lower values for Wilks' Lambda indicate greater discrimination. Wilks' Lambda and chi-square tests apply sequentially. [b] tests functions 1 – 3 cumulatively. [c] tests functions 2 – 3 cumulatively [d] tests function 3.

Figure A7 contains a canonical function plot of the first two canonical functions (explaining 99.3% of the variation in the GAGs). Note that each of the GAGs is clearly distinguished as a group in the plot. Moreover, traditional and cross-validated discriminant functions corrected predict 100% and 93.3% of the GAGs, respectively, indicating a high likelihood of interval validity.

Table A4 contains the standardized discriminant function coefficients, which measure the relative contributions of each liposome to a specific discriminant function. For function one, the dansyl liposome exhibits the largest coefficient in absolute value (signs merely denote the magnitude of the relationship) followed closely by the pyranine liposome. While still meaningful (coefficients with values above 0.3 are generally considered "significant" or meaningful), the rhodamine liposome is over twice as small as the other two coefficients. Concomitantly, rhodamine carries the largest weight in the second canonical function, and is twice as large in absolute magnitude compared to the other coefficients. Lastly, the Dansyl liposome has the largest canonical weight in the third canonical function.

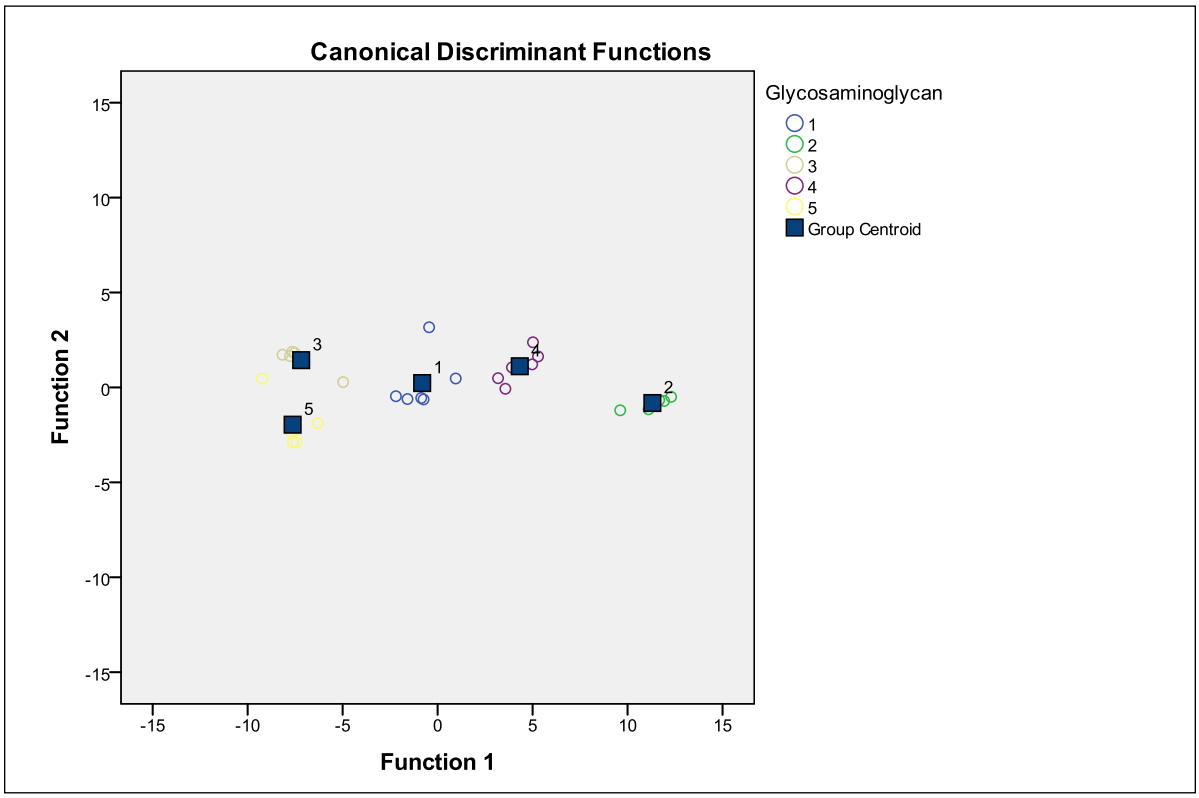

Figure A7. **50nM LDA canonical correlation plot between two largest canonical correlations and each of the five GAGs.** Chondroitin sulfate (group 1), dermatan sulfate (group 2), dextran sulphate (group 3), heparin sulphate (group 4) and hyaluronic sulphate (group 5).

Table A4. **50 nM LDA standardized canonical discriminant function coefficients**

Predictor	Canonical Function 1	Canonical Function 2	Canonical Function 3
Pyranine	1.615	-0.478	-0.059
Rhodamine	0.795	0.924	0.352
Dansyl	-1.708	-0.426	0.811

To assess the overall contribution of each liposome to the discriminatory power of the LDA, we present Table A5, which contains the structure matrix and the cumulative potency indices. The potency indices suggest that pyranine provides the largest overall contribution to the model's ability to distinguish emission intensities across GAGs.

Table A5. **50 nM LDA structure matrix and potency index**

Predictor	Canonical Function 1	Canonical Function 2	Canonical Function 3	Potency Index
Pyranine	0.456	-0.631	0.628	0.215
Rhodamine	0.209	0.613	0.762	0.057
Dansyl	-0.057	-0.312	0.948	0.012

On total, the LDA has a clear and intuitive interpretation. The results in Table A2 suggest that the first canonical function is, by far, the most important discriminant function. Tables A4 and A5 jointly suggest that pyranine is the largest contributor to this discriminant function, and to the model overall. This implies that the pyranine liposome is the "best" determinant of GAGs. Dansyl is identified as the least "potent" discriminator, even though its emission intensities are relatively high (Table A1). The Wilks' Lambda and structure matrix (Table A5) suggest (but do not prove) that this is at least partly attributable to excess variation in dansyl emission intensities, which offsets the high mean values.

The following tables present the full set of LDA results for the analysis at 100 nM. For simplicity, these are labeled as Tables A6 – A10 and Figure A8. Since the discussion of each of the following tables is analogous to what was described previously, we simply present the tables for the reader's consumption.

Table A6. **100 nM LDA tests of equality of group means**

GAG	Pyranine[a,b]	Rhodamine[a,b]	Dansyl[a,b]
Chondroitin Sulfate	1.687	1.315	1.816
Dermatan Sulfate	2.035	1.495	1.712
Dextran Sulfate	1.388	1.253	1.728
Heparin Sulfate	1.766	1.530	2.093
Hyaluronic Acid	1.551	1.130	2.506
Wilks' Lambda	0.153	0.209	0.623
F-Statistic [4,25]	34.489	0.626	3.775
P-Value	<0.001	<0.001	0.016

[a] first panel provides group-specific means [b] second panel provides statistics and p-values.

Table A7. **100 nM LDA variables in the analysis[a]**

Step Entered	Predictor	D^2	Between Groups	F-Statistic	P-Value
1	Pyranine	0.615	1 and 4	1.845	0.187
2	Dansyl	4.928	1 and 5	7.097	0.004
3	Rhodamine	9.514	1 and 4	8.753	<0.001

[a] Variables are entered in a manner that maximizes the Mahalanobis D^2 between the two closest groups. [b] Each of five GAGs groups are: chondroitin sulfate (group 1), dermatan sulfate (group 2), dextran sulfate (group 3), heparin sulfate (group 4) and hyaluronic acid (group 5)

Table A8. **100 nM LDA canonical function summary[a]**

Fct.	Eigen-Value	Pct. of Variance Explained	Canonical Correl.	Wilks' Lambda[a]	Chi-Square Statistic	P-Value
1	23.726	85.3	0.980	0.006[b]	126.396	<0.001
2	3.749	13.5	0.889	0.158[c]	46.199	<0.001
3	0.336	1.2	0.502	0.748[d]	7.250	0.027

[a] Lower values for Wilks' Lambda indicate greater discrimination. Wilks' Lambda and chi-square tests apply sequentially. [b] tests functions 1 – 3 cumulatively. [c] tests functions 2 – 3 cumulatively [d] tests function 3.

Table A9. **100 nM LDA standardized canonical discriminant function coefficients**

Predictor	Canonical Function 1	Canonical Function 2	Canonical Function 3
Pyranine	1.546	-1.117	-0.058
Rhodamine	0.438	1.412	0.281
Dansyl	-1.686	-0.245	0.830

Table A10. **100 nM LDA structure matrix and potency index**

Predictor	Canonical Function 1	Canonical Function 2	Canonical Function 3	Potency Index
Pyranine	0.456	-0.308	0.835	0.199
Rhodamine	0.346	0.435	0.831	0.136
Dansyl	-0.085	-0.169	0.982	0.022

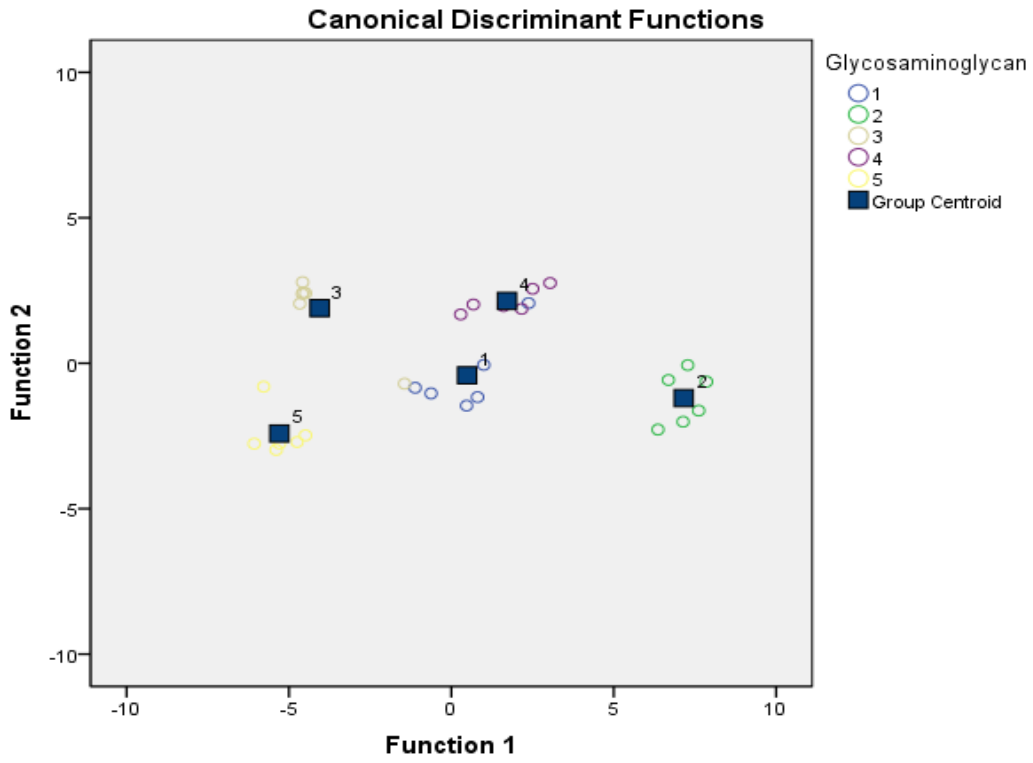

Figure A8. **100 nM LDA canonical correlation plot between two largest canonical correlations and each of the five GAGs.** Chondroitin sulfate (group 1), dermatan sulfate (group 2), dextran sulphate (group 3), heparin sulphate (group 4) and hyaluronic sulfate (group 5).

APPENDIX B. SUPPLIMENTARY INFORMATION FROM PAPER 2

Example of calculation of total lipid concentration

MW of DSPC = 790.145 g/mol, MW of Rhodamine lipid = 1,249.641 g/mol

Concentration of Total Lipid:

4.0×10^{-3} g DSPC x 1 mol/760.076 g = 5.26×10^{-6} mol

6.5×10^{-5} g rhodamine lipid x 1 mol/ 1,249.641 g = 5.2×10^{-8} mol

5.26×10^{-6} mol + 5.2×10^{-8} = 5.312×10^{-6} mol

5.312×10^{-6} mol/3.8 mL = 1.4×10^{-6} mol/mL

1.4×10^{-6} mol/mL x 1000mL/L = 1.4×10^{-3} mol/L

= 1.4 mM

Statistical analysis

All statistical analysis was carried out using Minitab (version 16.1.1, State College, PA). Raw data from the Zetasizer Nano (Malvern, Westborough, MA), including measurements of average diameter and zeta potential, were entered into the Minitab spreadsheets, and analysis was carried out using these numbers in their original form.

Minitab spreadsheets

One-way ANOVA: 200 nm liposomes OSCS size versus contamination:

```
Source         DF        SS       MS       F      P
contamination   8  11431736  1428967  103.26  0.000
Error          36    498172    13838
Total          44  11929908

S = 117.6   R-Sq = 95.82%   R-Sq(adj) = 94.90%


                        Individual 95% CIs For Mean Based on
                        Pooled StDev
Level  N    Mean  StDev  --+---------+---------+---------+-------
 0.0   5   540.8   50.5   (-*-)
 0.5   5   502.2   37.0  (-*-)
 1.0   5   661.2  103.8     (-*-)
 2.5   5   689.1  129.4      (-*-)
 5.0   5  1013.6   65.5            (-*-)
10.0   5  1458.0  116.3                    (-*-)
15.0   5  1374.4  139.8                   (-*--)
20.0   5  1696.8  196.0                          (-*-)
30.0   5  1929.4  131.7                              (--*-)
                        --+---------+---------+---------+-------
                        500       1000      1500      2000
Pooled StDev = 117.6
Grouping Information Using Dunnett Method

Level           N    Mean  Grouping
 0.0 (control)  5   540.8  A
30.0            5  1929.4
20.0            5  1696.8
10.0            5  1458.0
15.0            5  1374.4
 5.0            5  1013.6
 2.5            5   689.1  A
 1.0            5   661.2  A
 0.5            5   502.2  A

Means not labeled with letter A are significantly different from control
level mean.


Dunnett's comparisons with a control

Family error rate = 0.05
Individual error rate = 0.0084

Critical value = 2.79

Control = level (0) of contamination
```

```
Intervals for treatment mean minus control mean

Level   Lower  Center   Upper  -----+---------+---------+---------+----
 0.5   -246.0   -38.6   168.9  (---*---)
 1.0    -87.0   120.5   327.9     (---*----)
 2.5    -59.1   148.3   355.8      (---*---)
 5.0    265.4   472.9   680.3            (---*----)
10.0    709.8   917.2  1124.7                    (---*---)
15.0    626.2   833.6  1041.1                   (---*---)
20.0    948.6  1156.0  1363.5                         (---*---)
30.0   1181.2  1388.6  1596.1                              (---*---)
                                -----+---------+---------+---------+----
                                     0       500      1000      1500
```

One-way ANOVA: 200 nm liposome OSD size versus contamination:

```
Source         DF       SS      MS      F      P
contamination   8  4679965  584996  59.78  0.000
Error          36   352295    9786
Total          44  5032260

S = 98.92   R-Sq = 93.00%   R-Sq(adj) = 91.44%


                          Individual 95% CIs For Mean Based on
                          Pooled StDev
Level  N    Mean  StDev  -------+---------+---------+---------+--
 0.0   5   540.8   50.5    (--*--)
 0.5   5   483.2   63.8  (--*--)
 1.0   5   674.9  108.3        (-*--)
 2.5   5   656.9   73.6       (--*--)
 5.0   5   609.1   64.5     (--*--)
10.0   5   947.4   83.4                 (--*--)
15.0   5  1132.4  134.0                       (--*--)
20.0   5  1312.0   90.6                             (--*--)
30.0   5  1377.2  164.4                               (--*--)
                          -------+---------+---------+---------+--
                               600       900      1200      1500

Pooled StDev = 98.9

Grouping Information Using Dunnett Method

Level           N    Mean  Grouping
 0.0 (control)  5   540.8  A
30.0            5  1377.2
20.0            5  1312.0
15.0            5  1132.4
10.0            5   947.4
 1.0            5   674.9  A
 2.5            5   656.9  A
 5.0            5   609.1  A
 0.5            5   483.2  A
```

```
Means not labeled with letter A are significantly different from control
level mean.
Dunnett's comparisons with a control

Family error rate = 0.05
Individual error rate = 0.0084

Critical value = 2.79

Control = level (0) of contamination

Intervals for treatment mean minus control mean

Level   Lower  Center   Upper  -------+---------+---------+---------+--
 0.5   -232.1   -57.6   116.9  (----*----)
 1.0    -40.3   134.1   308.6        (----*----)
 2.5    -58.3   116.2   290.6       (----*----)
 5.0   -106.1    68.4   242.8      (----*----)
10.0    232.2   406.6   581.1                (----*----)
15.0    417.2   591.6   766.1                     (----*----)
20.0    596.8   771.2   945.7                          (----*----)
30.0    662.0   836.4  1010.9                            (----*----)
                                -------+---------+---------+---------+--
                                       0       350       700      1050
```

One-way ANOVA: 200 nm liposome OSCS zeta versus contamination:

```
Source         DF      SS     MS      F      P
contamination   8  34.117  4.265  20.28  0.000
Error          36   7.571  0.210
Total          44  41.688

S = 0.4586   R-Sq = 81.84%   R-Sq(adj) = 77.80%


                         Individual 95% CIs For Mean Based on
                         Pooled StDev
Level  N    Mean   StDev  --+---------+---------+---------+-------
 0.0   5  4.6280  0.5840               (---*---)
 0.5   5  3.9260  0.3182        (---*---)
 1.0   5  5.5340  0.8384                        (---*---)
 2.5   5  4.0040  0.1435         (---*---)
 5.0   5  3.2480  0.4206  (---*----)
10.0   5  3.9140  0.3577        (---*---)
15.0   5  5.2860  0.2964                      (---*---)
20.0   5  5.8180  0.4274                           (---*---)
30.0   5  5.5580  0.3892                        (----*---)
                         --+---------+---------+---------+-------
                         3.0       4.0       5.0       6.0

Pooled StDev = 0.4586
```

```
Grouping Information Using Dunnett Method

Level           N    Mean  Grouping
 0.0 (control)  5  4.6280  A
20.0            5  5.8180
30.0            5  5.5580
 1.0            5  5.5340
15.0            5  5.2860  A
 2.5            5  4.0040  A
 0.5            5  3.9260  A
10.0            5  3.9140  A
 5.0            5  3.2480

Means not labeled with letter A are significantly different from control
level mean.


Dunnett's comparisons with a control

Family error rate = 0.05
Individual error rate = 0.0084

Critical value = 2.79

Control = level (0) of contamination

Intervals for treatment mean minus control mean

Level    Lower   Center    Upper  --------+---------+---------+---------+-
 0.5   -1.5107  -0.7020   0.1067       (------*------)
 1.0    0.0973   0.9060   1.7147                    (------*-----)
 2.5   -1.4327  -0.6240   0.1847        (------*------)
 5.0   -2.1887  -1.3800  -0.5713  (-----*------)
10.0   -1.5227  -0.7140   0.0947       (------*------)
15.0   -0.1507   0.6580   1.4667                  (-----*------)
20.0    0.3813   1.1900   1.9987                      (------*------)
30.0    0.1213   0.9300   1.7387                    (------*-----)
                                 --------+---------+---------+---------+-
                                      -1.2       0.0       1.2       2.4
```

One-way ANOVA: 200 nm liposomes OSD zeta versus contamination:

```
Source         DF      SS    MS     F      P
contamination   8   41.03  5.13  3.12  0.009
Error          36   59.23  1.65
Total          44  100.26

S = 1.283   R-Sq = 40.92%   R-Sq(adj) = 27.79%
```

```
                          Individual 95% CIs For Mean Based on
                          Pooled StDev
Level  N   Mean  StDev  ------+---------+---------+---------+--
 0.0   5  4.628  0.584                    (-------*-------)
 0.5   5  4.604  0.528                    (-------*------)
 1.0   5  1.656  3.078  (-------*-------)
 2.5   5  4.716  0.742                     (------*-------)
 5.0   5  4.830  0.857                     (-------*-------)
10.0   5  4.872  0.984                      (------*-------)
15.0   5  4.590  0.738                    (-------*------)
20.0   5  4.672  1.133                    (-------*-------)
30.0   5  4.446  0.796                   (-------*------)
                          -------+---------+---------+---------+--
                               1.5       3.0       4.5       6.0

Pooled StDev = 1.283

Grouping Information Using Dunnett Method

Level           N   Mean  Grouping
 0.0 (control)  5  4.628  A
10.0            5  4.872  A
 5.0            5  4.830  A
 2.5            5  4.716  A
20.0            5  4.672  A
 0.5            5  4.604  A
15.0            5  4.590  A
30.0            5  4.446  A
 1.0            5  1.656

Means not labeled with letter A are significantly different from control
level mean.

Dunnett's comparisons with a control

Family error rate = 0.05
Individual error rate = 0.0084

Critical value = 2.79

Control = level (0) of contamination

Intervals for treatment mean minus control mean

Level   Lower  Center   Upper  ------+---------+---------+---------+---
 0.5   -2.286  -0.024   2.238                (----------*----------)
 1.0   -5.234  -2.972  -0.710  (----------*----------)
 2.5   -2.174   0.088   2.350                (----------*-----------)
 5.0   -2.060   0.202   2.464                 (----------*----------)
10.0   -2.018   0.244   2.506                 (----------*-----------)
15.0   -2.300  -0.038   2.224               (-----------*----------)
20.0   -2.218   0.044   2.306                (----------*-----------)
30.0   -2.444  -0.182   2.080               (----------*----------)
                                  ------+---------+---------+---------+---
                                     -4.0      -2.0       0.0       2.0
```

One-way ANOVA: OSCS size versus contamination:

```
Source         DF       SS      MS     F      P
contamination   8  4087429  510929  4.57  0.001
Error          36  4026851  111857
Total          44  8114280

S = 334.5   R-Sq = 50.37%   R-Sq(adj) = 39.35%


                          Individual 95% CIs For Mean Based on Pooled StDev
Level  N    Mean  StDev    -+---------+---------+---------+--------
 0.0   5  3223.6  645.7                           (-------*------)
 0.5   5  2754.2  479.3                 (-------*------)
 1.0   5  2903.2  207.2                     (-------*------)
 2.5   5  2416.8  273.9          (------*-------)
 5.0   5  2361.0  297.0        (-------*-------)
10.0   5  2370.4  136.9         (------*-------)
15.0   5  2452.6  260.4           (------*-------)
20.0   5  2268.2  204.7      (-------*------)
30.0   5  2387.0  159.5         (-------*------)
                          -+---------+---------+---------+--------
                         2000      2400      2800      3200

Pooled StDev = 334.5


Grouping Information Using Dunnett Method

Level           N    Mean  Grouping
 0.0 (control)  5  3223.6  A
 1.0            5  2903.2  A
 0.5            5  2754.2  A
15.0            5  2452.6
 2.5            5  2416.8
30.0            5  2387.0
10.0            5  2370.4
 5.0            5  2361.0
20.0            5  2268.2

Means not labeled with letter A are significantly different from control
level mean.
Dunnett's comparisons with a control

Family error rate = 0.05
Individual error rate = 0.0084

Critical value = 2.79

Control = level (0) of contamination
```

```
Intervals for treatment mean minus control mean

Level    Lower  Center   Upper     -+---------+---------+---------+--------
 0.5   -1059.2  -469.4   120.4               (-----------*----------)
 1.0    -910.2  -320.4   269.4                  (-----------*----------)
 2.5   -1396.6  -806.8  -217.0        (-----------*-----------)
 5.0   -1452.4  -862.6  -272.8       (-----------*-----------)
10.0   -1443.0  -853.2  -263.4       (-----------*-----------)
15.0   -1360.8  -771.0  -181.2         (-----------*----------)
20.0   -1545.2  -955.4  -365.6     (-----------*-----------)
30.0   -1426.4  -836.6  -246.8       (-----------*-----------)
                                   -+---------+---------+---------+--------
                                 -1500     -1000      -500         0
```

One-way ANOVA: OSD size versus contamination:

```
Source         DF       SS      MS     F      P
contamination   8  3786045  473256  5.67  0.000
Error          36  3005050   83474
Total          44  6791094

S = 288.9   R-Sq = 55.75%   R-Sq(adj) = 45.92%

                         Individual 95% CIs For Mean Based on
                         Pooled StDev
Level  N    Mean  StDev  ---+---------+---------+---------+------
 0.0   5  3223.6  645.7                              (------*-----)
 0.5   5  2337.0  181.5       (-----*------)
 1.0   5  2446.6  284.2          (-----*------)
 2.5   5  2667.6  210.3               (------*-----)
 5.0   5  2439.2  276.9         (------*------)
10.0   5  2155.4  138.6  (------*-----)
15.0   5  2355.2  150.5       (------*-----)
20.0   5  2564.6  136.4             (-----*------)
30.0   5  2331.0  198.1       (-----*------)
                         ---+---------+---------+---------+------
                         2000      2400      2800      3200
Pooled StDev = 288.9

Grouping Information Using Dunnett Method

Level           N    Mean  Grouping
 0.0 (control)  5  3223.6  A
 2.5            5  2667.6
20.0            5  2564.6
 1.0            5  2446.6
 5.0            5  2439.2
15.0            5  2355.2
 0.5            5  2337.0
30.0            5  2331.0
10.0            5  2155.4

Means not labeled with letter A are significantly different from control
level mean.
```

```
Dunnett's comparisons with a control

Family error rate = 0.05
Individual error rate = 0.0084

Critical value = 2.79

Control = level (0) of contamination

Intervals for treatment mean minus control mean

Level    Lower   Center   Upper  ---------+---------+---------+---------+
 0.5   -1396.1   -886.6  -377.1      (------------*------------)
 1.0   -1286.5   -777.0  -267.5         (------------*-----------)
 2.5   -1065.5   -556.0   -46.5              (------------*------------)
 5.0   -1293.9   -784.4  -274.9         (-----------*------------)
10.0   -1577.7  -1068.2  -558.7  (-----------*------------)
15.0   -1377.9   -868.4  -358.9       (-----------*------------)
20.0   -1168.5   -659.0  -149.5            (------------*-----------)
30.0   -1402.1   -892.6  -383.1      (------------*-----------)
                                  ---------+---------+---------+---------+
                                       -1200      -800      -400         0
```

One-way ANOVA: OSCS zeta versus contamination:

```
Source         DF      SS     MS      F      P
contamination   8  426.64  53.33  31.69  0.000
Error          36   60.59   1.68
Total          44  487.24

S = 1.297   R-Sq = 87.56%   R-Sq(adj) = 84.80%

                        Individual 95% CIs For Mean Based on
                        Pooled StDev
Level  N    Mean  StDev  ---+---------+---------+---------+------
 0.0   5   3.480  1.185                                  (---*---)
 0.5   5   2.140  1.613                              (---*---)
 1.0   5   1.155  1.198                          (---*---)
 2.5   5  -0.030  1.357                      (---*---)
 5.0   5  -0.990  1.348                   (---*---)
10.0   5  -2.508  1.327              (---*---)
15.0   5  -3.614  1.205         (---*---)
20.0   5  -5.208  1.149    (---*---)
30.0   5  -5.864  1.231  (--*---)
                        ---+---------+---------+---------+------
                        -6.0      -3.0       0.0       3.0

Pooled StDev = 1.297
```

```
Grouping Information Using Dunnett Method

Level           N    Mean  Grouping
 0.0 (control)  5   3.480  A
 0.5            5   2.140  A
 1.0            5   1.155
 2.5            5  -0.030
 5.0            5  -0.990
10.0            5  -2.508
15.0            5  -3.614
20.0            5  -5.208
30.0            5  -5.864

Means not labeled with letter A are significantly different from control
level mean.


Dunnett's comparisons with a control

Family error rate = 0.05
Individual error rate = 0.0084

Critical value = 2.79

Control = level (0) of contamination

Intervals for treatment mean minus control mean

Level    Lower  Center   Upper   ---+---------+---------+---------+------
 0.5    -3.627  -1.340   0.948                        (-----*------)
 1.0    -4.613  -2.325  -0.037                    (-----*------)
 2.5    -5.798  -3.510  -1.222                (------*------)
 5.0    -6.758  -4.470  -2.182            (-----*------)
10.0    -8.276  -5.988  -3.700        (------*-----)
15.0    -9.382  -7.094  -4.806     (------*-----)
20.0   -10.976  -8.688  -6.400   (-----*------)
30.0   -11.632  -9.344  -7.056  (-----*------)
                            ---+---------+---------+---------+------
                          -10.5      -7.0      -3.5       0.0
```

One-way ANOVA: OSD zeta versus contamination:

```
Source         DF      SS     MS      F      P
contamination   8  432.89  54.11  21.55  0.000
Error          36   90.40   2.51
Total          44  523.28

S = 1.585   R-Sq = 82.73%   R-Sq(adj) = 78.89%
```

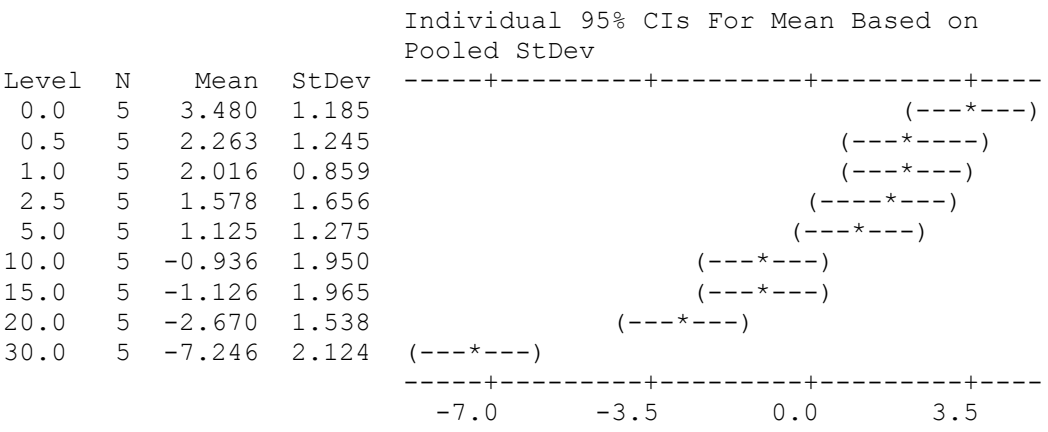

Pooled StDev = 1.585

Grouping Information Using Dunnett Method

Level	N	Mean	Grouping
0.0 (control)	5	3.480	A
0.5	5	2.263	A
1.0	5	2.016	A
2.5	5	1.578	A
5.0	5	1.125	A
10.0	5	-0.936	
15.0	5	-1.126	
20.0	5	-2.670	
30.0	5	-7.246	

Means not labeled with letter A are significantly different from control level mean.
Dunnett's comparisons with a control

Family error rate = 0.05
Individual error rate = 0.0084

Critical value = 2.79

Control = level (0) of contamination

Intervals for treatment mean minus control mean